

**GENERATION AND USE OF HLA-A2-RESTRICTED, PEPTIDE-  
SPECIFIC MONOCLONAL ANTIBODIES AND CHIMERIC  
ANTIGEN RECEPTORS**

by

Dimiter Velitchkov Tassev

A Dissertation

Presented to the Faculty of the Louis V. Gerstner, Jr

Graduate School of Biomedical Sciences,

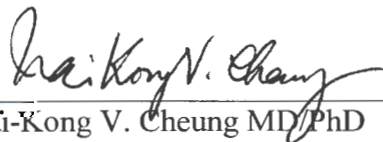
Memorial Sloan-Kettering Cancer Center

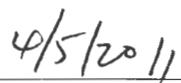
in Partial Fulfillment of the Requirements for the Degree of

Doctor of Philosophy

New York, NY

May, 2011

  
Nai-Kong V. Cheung MD/PhD  
Dissertation Mentor

  
Date

Copyright by Dimitar V. Tassev 2011

## DEDICATION

I would like to dedicate this thesis to my parents, Elena and Velitchko Tassev. Of all the great people whom I have met over my lifetime, these two individuals have always stood by me. If it wasn't for their bravery, sacrifice and perseverance, none of this work would have been possible.

## ABSTRACT

Advances in adoptive T cell immunotherapy have led to several promising options for cancer patients in the past decade. These advances have been made possible by targeting tumor-derived T cell epitopes (TCEs) on the surface of cancer cells. We sought to generate MHC-restricted, peptide-specific monoclonal antibodies in order to study antigen presentation and retarget immune cells towards specific TCEs of interest. High affinity single-chain variable fragments (scFv) were selected for using a human phage display library on recombinant HLA-A2-peptide complexes. Two antibodies (EBNA Clone 315 and WT1 Clone 45) specific for HLA-A2-LLDFVRFMGV (derived from the Epstein-Barr virus latent protein EBNA3C) and HLA-A2-RMFPNAPYL (derived from the transcription factor WT1) were shown to possess TCR-like specificity as both scFvs and scFv-Fc fusion proteins (scFv fused to CH<sub>2</sub> and CH<sub>3</sub> immunoglobulin Fc domains of a human IgG<sub>1</sub> antibody). In addition, these antibodies allowed us to demonstrate a 10-100 fold increase in affinity over a typical T cell receptor (TCR) and the ability to quantitate antigen density on the surface of cells.

Subsequently, chimeric antigen receptor (CAR) versions of these antibodies, consisting of the 4-1BB and CD3 $\zeta$  effector-cell activation signaling domains, were generated and retrovirally transduced into NK92MI cells. Using membrane CD107a expression and <sup>51</sup>Cr target cell release as markers of effector cell activation and target cell killing, CAR-equipped NK92MI showed highly specific cytotoxicity towards cells bearing their targeted HLA-A2-peptide complex, but not those carrying irrelevant complexes or those blocked by their respective scFv-Fc antibodies. The CAR-mediated approach of recognizing antigen was also shown to be far more sensitive at detecting low

levels of antigen and far superior at killing target cells versus scFv-Fc-mediated flow cytometric staining or antibody dependent cellular cytotoxicity (ADCC). We conclude that TCR-like antibodies can be obtained from naïve human phage display libraries and have utility in redirecting immune effector cells towards tumor-derived TCEs.

## BIOGRAPHICAL SKETCH

Dimiter was born to Elena and Velitchko Tassev on May 15<sup>th</sup> 1984 in Plovdiv, Bulgaria. At the age of five, Dimiter and his parents immigrated to Hamburg, West Germany, where he attended his first year of elementary school. Subsequently, his family immigrated to San Francisco, California, where they lived for one year before temporarily moving to Harrisonburg, Virginia, and eventually settling in Harrisburg, Pennsylvania. Dimiter graduated from Central Dauphin East High School in 2002, and began college at the University of the Sciences in Philadelphia that same year. After the completion of his first year, Dimiter transferred to The Ohio State University (OSU) where he eventually graduated with a Bachelor in Science (BS) in Microbiology in 2006. During his time at OSU, Dimiter was employed part-time at the OSU Medical Center, as an Admissions Representative in the hospital's emergency room, while completing an undergraduate senior thesis project in the Department of Biochemistry under the mentorship of Dr. Peng (George) Wang. In July 22<sup>nd</sup>, 2006, Dimiter moved to New York, New York, where he began the first year of his PhD at the inaugural Louis V. Gerstner Jr. Graduate School of Biomedical Sciences at Memorial Sloan-Kettering Cancer Center.

## ACKNOWLEDGMENTS

I would like to thank my mentor, Dr. Nai-Kong Cheung, for providing me with the training, support and independence needed to complete this work, Drs. Mahiuddin Ahmed and Sarang Puranik for providing me with the sanity needed to complete my dissertation, Dr. David Cobrinik for critically reviewing this thesis, Hong-fen Guo for help regarding antibody purifications, Dr. Hong Xu for help regarding the scFv-Fc expression vector, Dr. Ming Cheng for technical advice related to  $^{51}\text{Cr}$  cytotoxicity assays, and Dr. Dario Campaña for providing us with the CAR vector used in my studies.

I would like to thank my thesis committee members, Drs. David Scheinberg, Eric Pamer and Michael Glickman. In particular, I would like to thank Dr. Pamer and Ingrid Leiner for providing me with the MHC-peptide complexes used in this work, and Dr. Scheinberg and Dr. Tao Dao for providing me with reagents and helpful advice throughout the years. I would also like to thank my clinical mentor, Dr. Ronald DeMatteo, for exposing me to clinical trials and surgical oncology.

I would like to thank Dr. Richard O'Reilly for showing his support and sharing his thoughts and ideas with me regarding my work. I would also like to thank several members of his laboratory, including Dr. Aisha Hasan, Dr. Annamalai Selvakumar, Dr. Ekaterina Doubrovina, Dr. Guenther Koehne, Lorna Barnett, and Eleanor Tyler for providing me with technical advice throughout the years.

Lastly, I would like to thank our graduate school, particularly Drs. Ken Marians, Tom Kelly, Harold Varmus, and our benefactor Louis V. Gerstner. If it wasn't for their vision, initiative and generosity, our graduate program would not exist today. Additionally, I would like to thank Iwona Abramek for helping format this dissertation.

## TABLE OF CONTENTS

LIST OF TABLES .....	xi
LIST OF FIGURES .....	xii
LIST OF ABBREVIATIONS.....	xv
INTRODUCTION .....	1
Monoclonal antibodies.....	1
Class I major histocompatibility complex (MHC) and antigen presentation .....	13
Phage display .....	17
T cell signaling and activation .....	22
Adoptive T cell therapy .....	27
Introduction to the thesis.....	32
MATERIALS AND METHODS.....	37
Production of biotinylated MHC-peptide complexes .....	37
Selection of phage on HLA-A2-LLDFVRFMGV (EBNA3C) complex .....	38
Selection of phage on HLA-A2-RMFPNAPYL (WT1) complex .....	40
Expression and purification of soluble scFv from HB2151.....	41
Construction of scFv-Fc fusion protein and expression in DG44 CHO cells.....	43
Expression and purification of soluble scFv-Fc.....	48
Monoclonal ELISA with bacterial phage clones, purified scFv and scFv-Fc .....	49
Cell lines and peptides .....	50
Binding kinetics using surface plasmon resonance .....	51
Flow cytometry .....	52
Quantitation of HLA-A2-LLDFVRFMGV complexes on peptide-pulsed T2 cells.....	53



Construction of the WT1 Clone 45 chimeric antigen receptor .....	54
Construction of the EBNA Clone 315 chimeric antigen receptor .....	59
Retroviral production, DNA packaging, and infection of NK92MI cells.....	66
<sup>51</sup> Cr release cytotoxicity assay .....	67
CHAPTER 1 .....	68
SELECTING HLA-A2-RESTRICTED, PEPTIDE-SPECIFIC MONOCLONAL ANTIBODIES USING PHAGE DISPLAY TECHNOLOGY .....	68
<i>1.1 Introduction</i> .....	68
<i>1.2 Affinity selection of phage on virally-derived recombinant HLA-A2-peptide         complexes</i> .....	70
<i>1.3 Affinity selection of phage on WT1-derived recombinant HLA-A2-peptide         complex</i> .....	74
<i>1.4 Binding kinetics and specificity of purified scFv (EBNA Clone 315 and WT1         Clone 45) on peptide-pulsed T2 cells</i> .....	78
<i>1.5 Demonstrating HLA restriction of the LLDFVRFMGV peptide and EBNA Clone         315 using peptide-pulsed BLCLs</i> .....	82
<i>1.6 Conclusions</i> .....	86
CHAPTER 2 .....	87
GENERATING SCFV-FC FUSION PROTEINS FOR ANTIGEN QUANTITATION, AFFINITY DETERMINATION AND ANTIBODY-DEPENDENT CELL CYTOTOXICITY .....	87
<i>2.1 Introduction</i> .....	87

2.2 Binding kinetics and sensitivity of EBNA Clone 315 scFv-Fc on recombinant HLA-A2-peptide complex and peptide-pulsed T2 cells.....	89
2.3 Binding and specificity studies of WT1 Clone 45 scFv-Fc on recombinant HLA-A2-peptide complex and peptide-pulsed cells.....	94
2.4 Antibody-dependent cellular cytotoxicity (ADCC) of EBNA Clone 315 scFv-Fc on peptide-pulsed cells.....	97
2.5 Conclusions.....	99
CHAPTER 3 .....	100
ENGINEERING AND USE OF HLA-A2-RESTRICTED, PEPTIDE-SPECIFIC CHIMERIC ANTIGEN RECEPTORS.....	100
3.1 Introduction.....	100
3.2 EBNA Clone 315 CAR-equipped NK92MI cells can detect cells bearing the specific HLA-A2-LLDFVRFMGV complex via CD107a expression .....	102
3.3 EBNA Clone 315 CAR-equipped NK92MI cells can destroy cells bearing the specific HLA-A2-LLDFVRFMGV complex via <sup>51</sup> Cr release .....	108
3.4 WT1 Clone 45 CAR-equipped NK92MI cells can destroy cells bearing the specific HLA-A2-RMFPNAPYL complex via <sup>51</sup> Cr release .....	116
3.5 Conclusions.....	123
DISCUSSION .....	125
BIBLIOGRAPHY .....	137

## LIST OF TABLES

Table 1. Persistence and immune-mediated functions of IgG. ....	10
Table 2. Properties of the major classes of antibodies in humans. ....	11
Table 3. General binding characteristics of human Fc receptors. ....	12
Table 4. Phage display selection results on recombinant HLA-A2-LLDFVRFMGV and HLA-A2-NLVPMVATV complexes. ....	72
Table 5. Phage display selection results on recombinant HLA-A2-RMFPNAPYL complex. ....	76

## LIST OF FIGURES

Figure 1. Immunoglobulin structure. ....	6
Figure 2. Immunoglobulin isotypes. ....	7
Figure 3. Hybridoma technology for making murine monoclonal antibodies.....	8
Figure 4. Antibody structure and derived fragments. ....	9
Figure 5. Structure of the MHC Class I molecule. ....	15
Figure 6. MHC class I assembly. ....	16
Figure 7. Display of proteins on filamentous bacteriophage .....	20
Figure 8. Biopanning using a phage display library .....	21
Figure 9. Structure of the T cell receptor complex .....	25
Figure 10. TCR intracellular signaling pathways .....	26
Figure 11. Chimeric antigen receptor (CAR) architecture.....	31
Figure 12. Structure of a full immunoglobulin and scFv-Fc fusion protein .....	36
Figure 13. Tomlinson library vector, PCR reaction and NheI/ApaI digestion .....	45
Figure 14. Full IgG expression vector and proposed scFv-Fc vector .....	46
Figure 15. Validation and HindIII digestion of scFv-Fc fusion constructs .....	47
Figure 16. WT1 pUC57 and St. Jude CAR vectors .....	56
Figure 17. EcoRI and XhoI digestion of the WT1 pUC57 and St. Jude CAR vectors .....	57
Figure 18. EcoRI and XhoI digestion validation of the WT1 Clone 45 CAR vector .....	58
Figure 19. Tomlinson and WT1 pUC57 vectors.....	61
Figure 20. SfiI and NotI digestion of the WT1 pUC57 and Tomlinson vectors.....	62
Figure 21. EcoRI and XhoI digestion validation of the EBNA pUC57 vector.....	63
Figure 22. XhoI partial and EcoRI complete digestion of the EBNA pUC57 vector.....	64

Figure 23. EcoRI digestion validation of the EBNA Clone 315 CAR vector .....	65
Figure 24. EBNA Clone 315 scFv is highly specific for the recombinant HLA-A2-LLDFVRFMGV complex.....	73
Figure 25. WT1 Clone 45 scFv is highly specific for the recombinant HLA-A2-RMFPNAPYL complex.....	77
Figure 26. EBNA Clone 315 can recognize HLA-A2-LLDFVRFMGV on peptide-pulsed T2 cells.....	80
Figure 27. WT1 Clone 45 can recognize HLA-A2-RMFPNAPYL on peptide-pulsed T2 cells .....	81
Figure 28. EBNA Clone 315 is LLDFVRFMGV peptide specific and HLA-A2-restricted .....	84
Figure 29. The HLA-A2-LLDFVRFMGV complex is stable on the cell surface .....	85
Figure 30. Binding studies using EBNA Clone 315 scFv-Fc .....	91
Figure 31. Kinetics determination of EBNA Clone 315 to HLA-A2-LLDFVRFMGV... ..	92
Figure 32. Quantitation of HLA-A2-LLDFVRFMGV complex on T2 cells .....	93
Figure 33. Binding and specificity studies of WT1 Clone 45 scFv-Fc.....	95
Figure 34. WT1 Clone 45 is RMFPNAPYL peptide specific and HLA-A2-restricted ....	96
Figure 35. EBNA Clone 315 scFv-Fc mediates ADCC of peptide-pulsed cells .....	98
Figure 36. Retroviral transduction of EBNA Clone 315 CAR into NK92MI cells .....	105
Figure 37. EBNA Clone 315 CAR-expressing NK92MI cells can specifically detect the HLA-A2-EBNA3C complex on peptide-pulsed T2 cells via CD107a expression.....	106
Figure 38. EBNA Clone 315 CAR-expressing NK92MI cells can specifically detect the HLA-A2-EBNA3C complex on peptide-pulsed BLCLs via CD107a expression.....	107

Figure 39. EBNA Clone 315 CAR-expressing NK92MI cells can specifically detect the HLA-A2-EBNA3C complex on peptide-pulsed T2 cells via <sup>51</sup> Cr release .....	111
Figure 40. EBNA Clone 315 CAR-expressing NK92MI cells can specifically detect the HLA-A2-EBNA3C complex on peptide-pulsed BLCLs via <sup>51</sup> Cr release .....	112
Figure 41. EBNA Clone 315 CAR-mediated cytotoxicity can be blocked using scFv-Fc fusion protein and anti-HLA-A2 full immunoglobulin .....	113
Figure 42. EBNA Clone 315 CAR-expressing NK92MI cells can specifically detect the HLA-A2-EBNA3C complex on HLA-A2 <sup>+</sup> BLCLs via <sup>51</sup> Cr release .....	114
Figure 43. CAR-mediated killing is more potent than scFv-Fc-mediated ADCC on peptide-pulsed DIMT BLCL.....	115
Figure 44. Retroviral transduction of WT1 Clone 45 CAR in NK92MI cells.....	119
Figure 45. WT1 Clone 45 CAR expressing NK92MI cells can specifically detect the HLA-A2-RMFPNAPYL complex on peptide-pulsed BLCLs via <sup>51</sup> Cr release .....	120
Figure 46. WT1 Clone 45 CAR expressing NK92MI cells can specifically detect the HLA-A2-RMFPNAPYL complex on unpulsed DIMT BLCL via <sup>51</sup> Cr release .....	121
Figure 47. WT1 Clone 45 CAR expressing NK92MI cells can specifically detect the HLA-A2-RMFPNAPYL complex on 697 and OVCAR-3 cells via <sup>51</sup> Cr release.....	122

## LIST OF ABBREVIATIONS

- ABC transporters:** ATP binding cassette transporter
- ADCC:** Antibody-dependent cellular cytotoxicity
- ALL:** Acute lymphocytic leukemia
- AML:** Acute myeloid leukemia
- APC:** Antigen presenting cell
- $\beta$ 2M:** Beta-2-microglobulin
- BiTE:** Bi-specific T cell engaging antibody
- BLCL:** EBV-transformed B-cell lymphoblastic cell line
- CAR:** Chimeric antigen receptor
- CDC:** Complement dependent cytotoxicity
- CMC:** Complement mediated cytotoxicity
- CMV:** Cytomegalovirus
- CDR:** Complementarity determining region
- C<sub>L</sub>:** Constant domain of the light chain
- CH<sub>1</sub>:** 1<sup>st</sup> constant domain of the heavy chain
- CH<sub>1,2,3</sub>:** 1<sup>st</sup>, 2<sup>nd</sup> and 3<sup>rd</sup> constant domains of the heavy chain
- CH<sub>2,3</sub>:** 2<sup>nd</sup> and 3<sup>rd</sup> constant domains of the heavy chain
- CHO:** Chinese hamster ovary
- CTL:** Cytotoxic T cell
- EBNA3C:** Epstein-Barr nuclear antigen 3C
- EBV:** Epstein-Barr virus
- ECMV:** Encephalomyocarditis virus

**ER:** Endoplasmic reticulum

**ERAP1:** Endoplasmic reticulum aminopeptidase 1

**ERK:** Extracellular signal regulated kinase

**E:T Ratio:** Effector:Target ratio

**Fab:** Antibody binding fragment

**FACS:** Flow assisted cytometric cell sorting

**FBS:** Fetal bovine serum

**FDA:** Food and Drug Administration

**GFP:** Green fluorescence protein

**GM-CSF:** Granulocyte-macrophage colony stimulating factor

**HC:** Heavy chain

**HEL:** Hen egg lysozyme

**HLA:** Human leukocyte antigen

**HPV:** Human papillomavirus

**HSP90:** Heat shock protein 90

**IFN- $\gamma$ :** Interferon gamma

**Ig:** Immunoglobulin

**IPTG:** isopropyl-1-thio- $\beta$ -D-galactopyranoside

**IRES:** Internal ribosome entry site

**ITAM:** Immunoreceptor tyrosine-based activation motifs

**JNK:** c-Jun N-terminal kinase

**$K_D$ :** Dissociation constant

**$k_{off}$ :** Dissociation rate



**$k_{on}$** : Association rate

**LAT**: Linker of activation in T cells

**MAP kinase**: p38 mitogen-associated protein kinase

**MEK**: MAP kinase/ERK kinase kinase

**MHC**: Major histocompatibility complex

**OPD**: O-phenylenediamine

**PEG**: Polyethylene glycol

**RAS**: RAt Sarcoma

**SCID**: Severe combined immunodeficiency

**scFv**: Single-chain variable fragment

**SLP-76**: SH2-domain-containing leukocyte protein of 76 kDa

**SPR**: Surface plasmon resonance

**TAP**: Transporter associated with antigen processing

**TB**: Terrific Broth

**TCE**: T cell epitope

**TCR**: T cell receptor

**TIL**: Tumor infiltrating lymphocyte

**V<sub>H</sub>**: Variable heavy chain

**V<sub>L</sub>**: Variable light chain

**TNFR**: Tumor necrosis factor receptor

**TRAF**: TNFR-associated factors

**WT1**: Wilms tumor protein 1

**ZAP-70**: Zeta-chain associated protein of 70 kDa

## INTRODUCTION

### *Monoclonal antibodies*

The initial discovery and characterization of antibodies first began in the 1890s by Paul Ehrlich, Emil von Behring and Kitasato Shibasaburo. These three scientists described antibodies as agents which had activity against diphtheria and tetanus toxins (1). Subsequently, several other researchers such as Michael Heidelberger and Oswald Avery showed that antibodies were made up of protein (2), and in the 1940s Linus Pauling further confirmed Ehrlich's "lock-and-key" theory which showed that the antibody-antigen interaction was dependent on the shape of both proteins. The next major discovery came from Astrid Fagraeus, who discovered that B plasma cells were the source of these proteins; this was followed by work from Gerald Edelman and Rodney Porter, which led to the 1972 Nobel Prize for the structure and complete amino acid sequence of immunoglobulins.

The full length immunoglobulin antibody molecule (~150 kDa) is based on a 4-chain structure consisting of two identical heavy chains and two identical light chains (Fig. 1). The light chain consists of a single constant and single variable domain, while the heavy chain consists of several constant domains (depending on the isotype) and a single variable domain. The variable domains of an antibody are responsible for antigen recognition. Antigen recognition is mediated by a combining site in the variable fragments (Fab) that requires contributions from both the variable heavy chain ( $V_H$ ) and variable light chain ( $V_L$ ). Within these two domains are three hypervariable regions termed complementarity determining regions (CDRs). Separating the CDRs from one another within each chain is a framework region that is more highly conserved.

While the Fab portion of the IgG binds to the antigen, most of the effector functions and metabolic fate are derived from the Fc fragment. Depending on the specific antibody class, the Fc region of full length immunoglobulin is typically involved in Fc receptor and complement binding, inducing antibody dependent cellular cytotoxicity (ADCC) and complement dependent cytotoxicity (CDC), respectively (Table 1) (3). In mammals, there are five main classes of antibodies, IgA, IgD, IgE, IgG, and IgM (Fig. 2). These vary based on their valency, number of heavy chains, and biological properties (Table 2). IgM is not only the first class of antibody to be presented on the surface of a developing B cell, but it's also the predominant class to be secreted into the blood (as a pentameric molecule) during a primary antibody response. In combination with cell surface IgD, both are co-expressed on the surface of mature naïve B cells, with both molecules having the same specificity (4). IgG on the other hand is a monomer typically produced in large quantities during a secondary immune response. Depending on the specific subclass, its Fc domain binds to Fc receptors on immune cells as well as complement proteins with varying affinities. IgG are the only antibodies which can pass from the mother to the fetus via the placenta, and IgG<sub>1</sub> is the most common subclass of IgG used for immunotherapy (3). IgA is either a monomer in the blood or a dimer in saliva, tear, milk, respiratory and intestinal secretions. It is synthesized by plasma cells in subepithelial regions of the gastrointestinal and respiratory tracts. Lastly, IgE is a monomer which binds to an Fc receptor located on mast cells and basophils in the blood. Once bound, the cells use IgE as a passively acquired receptor, which can trigger secretion of a variety of molecules involved in allergic reactions.

The original method by which Köhler and Milstein began to produce monoclonal antibodies came about in 1975, with the advent of hybridoma technology (5). This technique worked by first immunizing mice against a variety of antigens, isolating their spleens, and then fusing their splenocytes with a drug-sensitive multiple myeloma cell line. The resulting hybridomas (fused cells) were then cloned into individual microwell plates and selected based on their production of a desired antibody in the culture supernatant (Fig. 3). Since then, researchers have applied hybridoma technology for the generation of human monoclonal antibodies using human B cells, specifically those which bind to botulinum neurotoxin (6). In addition, with the advent of transgenic mice which have their heavy and light chains replaced with those of a human, these mice are able to produce fully human antibodies upon immunization and subsequent hybridoma generation (7-9). Lastly, with the development of a polymerase chain reaction (PCR)-based method for amplifying immunoglobulin genes, researchers began to generate libraries of plasmids which encode heavy chains and light chains, either in the form of a Fab or as a single-chain variable fragment (scFv) (Fig. 4). This led to the development and use of phage display technology, which is discussed in greater detail in subsequent sections of this thesis.

More than 25 years after the first patient was treated with the murine antibody AB 89, considerable progress has been made in the field of cancer immunotherapy (10). Since then several monoclonal antibodies have been approved by the Food and Drug Administration (FDA) for the treatment of patients with both liquid and solid tumors (3, 11, 12). Therapeutic antibodies have been exploited based on their mechanism of action, which include the following: 1) killing tumor cells directly by way of ADCC or CDC

(e.g. rituximab), 2) blocking or stimulating a cell membrane molecule to induce cell death (e.g. cetuximab and trastuzumab), 3) neutralizing a secreted moiety (e.g. bevacizumab), 4) killing via an attached moiety such as a drug, toxin, radioisotope and 5) modulating the immune system via T cell effector functions (e.g. ipilimumab). In almost all cases, to generate a therapeutic benefit, antibodies have to possess critical properties including high affinity for their targeted antigen, minimal acute and long-term side effects, minimal immunogenicity, and in specific applications, high affinity for human Fc receptors (Table 3) (13). In addition, the targeted antigen has to be expressed at high levels on tumors but not on normal tissues (specificity or selectivity), consistently expressed in the specific tumor among patients and within patients (low heterogeneity), and should either be essential for the survival of the cancer cell or unlikely to be down regulated. To achieve these attributes, researchers are now reengineer existing antibodies to make them less immunogenic (14), modifying both protein and carbohydrate residues in the Fc regions to enhance ADCC and CDC (15), shrinking their sizes for potentially greater tumor penetration (16), modifying the variable regions to improve affinity (17), increasing avidity by changing antibody valency (18), and constructing novel antibody-fusion proteins such as those for multi-step targeting (19, 20).

Beginning in the mid 1990s, several groups became interested in creating monoclonal antibodies which would be specific for an MHC-peptide complex in order to study antigen presentation (21-24). These antibodies were initially obtained using standard hybridoma technology involving mouse immunization with recombinant, mouse-derived, MHC-peptide complexes (Class I and II). Some of the early targets included the K<sup>k</sup>-restricted influenza virus-derived peptide Ha<sub>255-262</sub>, a hen egg lysozyme

(HEL) peptide bound to the MHC Class II molecule I-A<sup>k</sup>, and the ovalbumin peptide SIINFEKL bound to H-2K<sup>b</sup>. While this work did lead to the discovery of several epitope-specific antibodies, subsequent work began to focus on the selection of these antibodies using phage display technology (25-35). This resulted in several scFvs and Fabs which bound to human HLA-A1 and HLA-A2-peptide complexes containing peptides derived from HER2, Tax, NY-ESO-1, SSX2, MAGE, Melan-A, MUC1, telomerase, gp100, TARP and pp65. Subsequent studies with these antibodies have led to several discoveries regarding the differential presentation of T cell epitopes from melanoma differentiation antigens (36), quantitation studies looking at the number of MHC-peptide complexes on the surface of cells (22, 29, 31, 37), and cytotoxicity studies involving full Ig (38-40), antibody-toxin fusion proteins (27, 30, 33, 41), and chimeric antigen receptors (42-45). Furthermore, several crystal structures which show the antibodies bound to their targeted complex demonstrate how their interactions are quite similar to that of a TCR-MHC-peptide (42, 46).

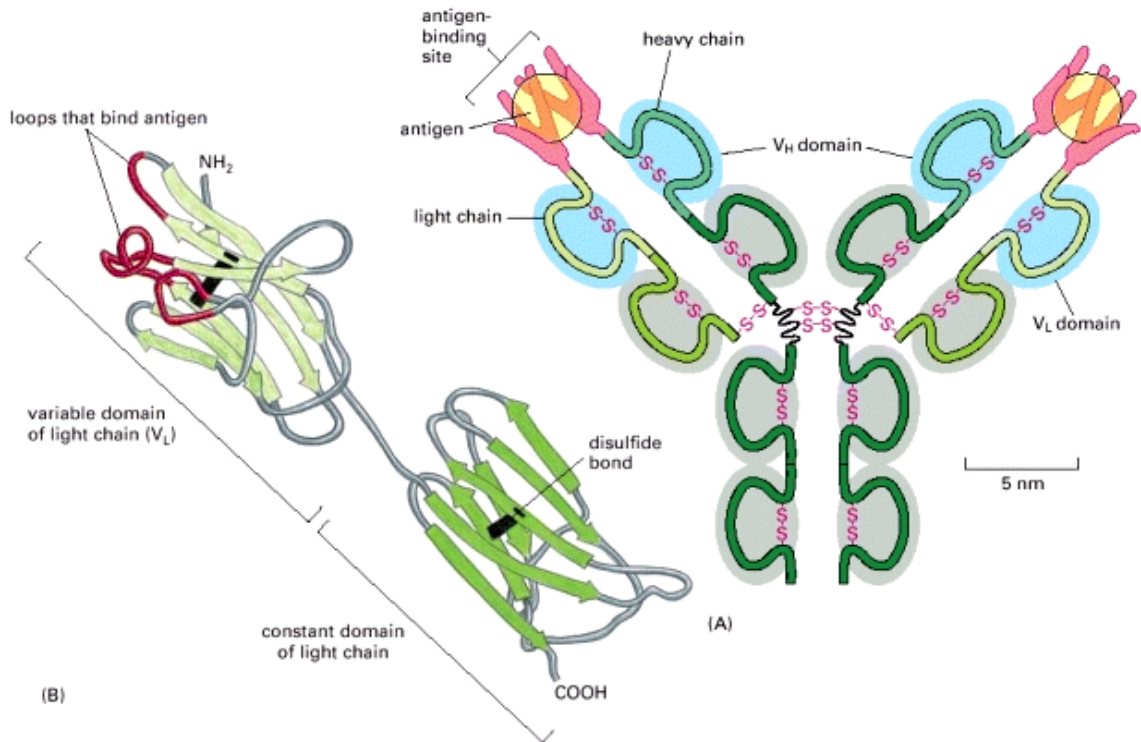


**Figure 1.** Immunoglobulin structure.

A. Depicted is the typical structure of a monoclonal antibody, composed of the antibody binding fragment (Fab) along with the Fc region which carries out effector mediated (biological) functions. The light chains are linked to the heavy chains via disulfide bonds, which are also used for dimerization. B. A close-up view of the variable light chain and constant light chain. The CDRs are highlighted in red and are exposed so that they can interact with antigen. The figure was obtained from Figure 3-42 in the text book *Molecular Biology of the Cell*, 4<sup>th</sup> Edition.

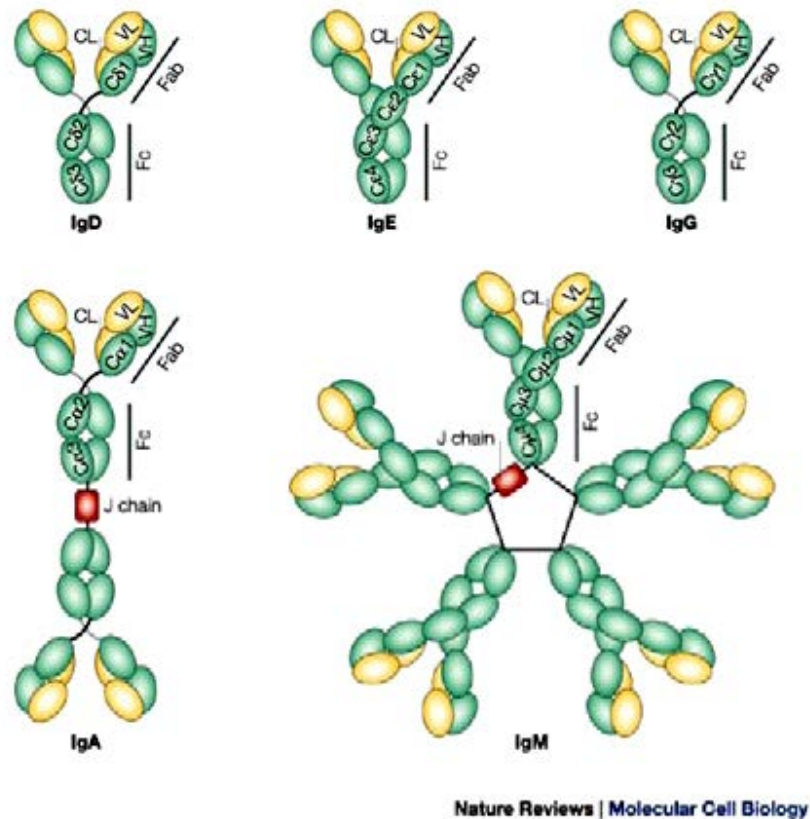


**Figure 2.** Immunoglobulin isotypes.

In mammals, antibodies come in five different varieties (isotypes or classes). These vary in their valency (number of Y units) and type of heavy chains. Heavy chains of IgG, IgM, IgA, IgD, and IgE are known as gamma, mu, alpha, delta, and epsilon, respectively. This figure was obtained from a Nature Reviews article (47).



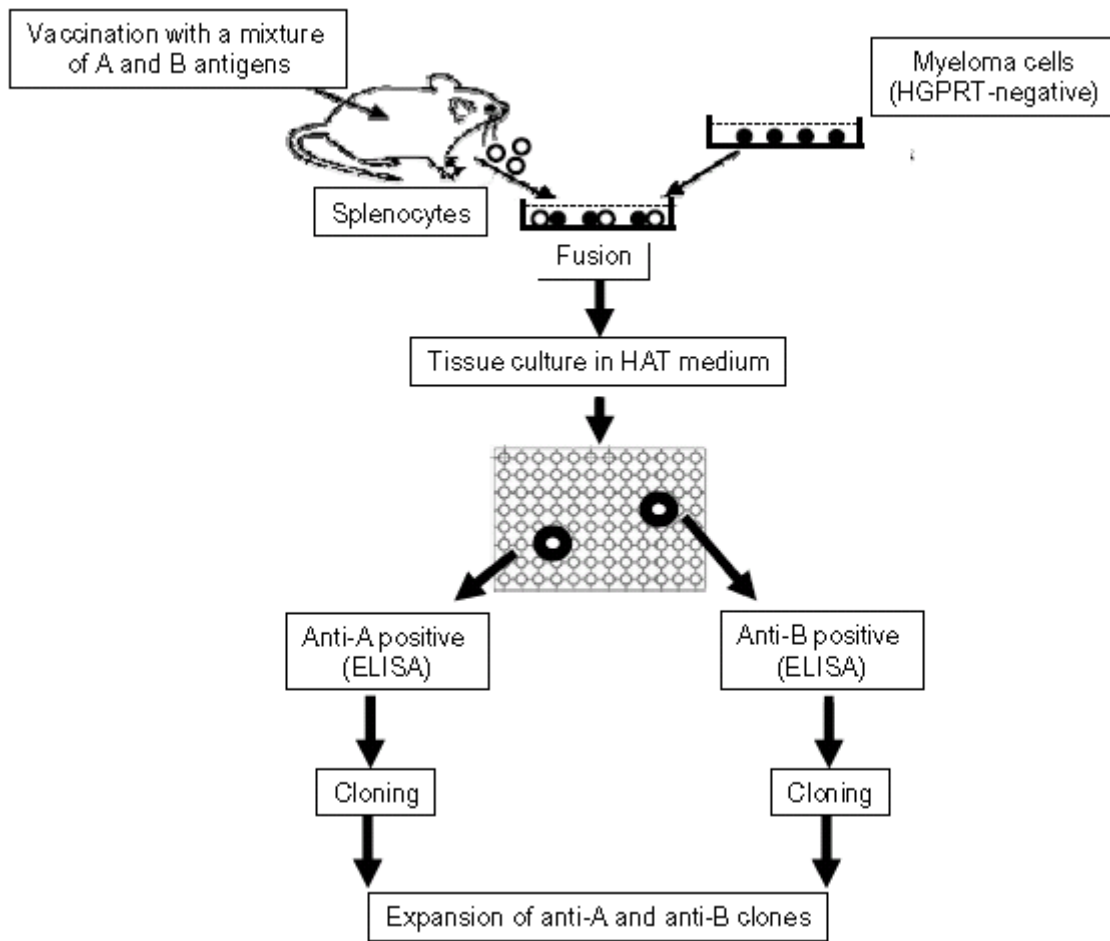


**Figure 3.** Hybridoma technology for making murine monoclonal antibodies.

Mice are immunized against an antigen of interest, its splenocytes are fused to a myeloma cell line, the fused cells are cultured in selective media, and individual clones are tested for the production of the desired antibodies. This figure was obtained from a Human Antibodies article (48).

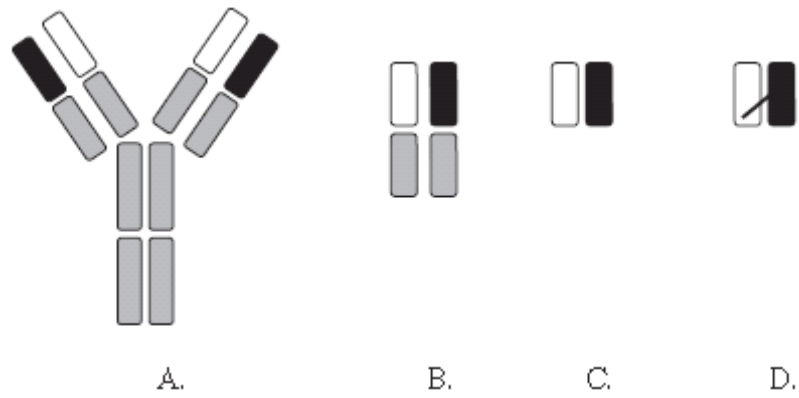


**Figure 4.** Antibody structure and derived fragments.  
A. Full length IgG (~150 kDa). B. Fab fragment (~50 kDa). C. Fv fragment (~30 kDa).  
D. scFv fragment (~30 kDa). This figure was obtained from a Briefings in Functional Genomics and Proteomics article (49).

**Table 1.** Persistence and immune-mediated functions of IgG.

<b>Antibody isotype</b>	<b>Human serum half-life</b>	<b>ADCC</b>	<b>CDC</b>
Human IgG <sub>1</sub>	3 Weeks	+++	+++
Human IgG <sub>2</sub>	3 Weeks	++	+
Human IgG <sub>3</sub>	1 Week	+++	+++++
Human IgG <sub>4</sub>	3 Weeks	±	±
Mouse IgG <sub>1</sub>	2 Days	–	±
Mouse IgG <sub>2a</sub>	2 Days	+++	+++
Mouse IgG <sub>3</sub>	2 Days	+++	+++

ADCC: Antibody-dependent cellular cytotoxicity; CDC: Complement-dependent cytotoxicity

This table was obtained from a Expert Opinions in Biological Therapy article (3).

**Table 2.** Properties of the major classes of antibodies in humans.

PROPERTIES	CLASS OF ANTIBODY				
	IgM	IgD	IgG	IgA	IgE
Heavy chains	$\mu$	$\delta$	$\gamma$	$\alpha$	$\epsilon$
Light chains	$\kappa$ or $\lambda$	$\kappa$ or $\lambda$	$\kappa$ or $\lambda$	$\kappa$ or $\lambda$	$\kappa$ or $\lambda$
Number of four-chain units	5	1	1	1 or 2	1
Percentage of total Ig in blood	10	<1	75	15	<1
Activates complement	++++	-	++	-	-
Crosses placenta	-	-	+	-	-
Binds to macrophages and neutrophils	-	-	+	-	-
Binds to mast cells and basophils	-	-	-	-	+

This table was obtained from Table 24-1 in the text book Molecule Biology of the Cell. 4<sup>th</sup> Edition.

**Table 3.** General binding characteristics of human Fc receptors.

<b>Human Fc<math>\gamma</math> receptor</b>	<b>Cell types</b>	<b>Fc affinity (K<sub>D</sub>)</b>	<b>Antibody isotype binding (Human)*</b>
I	Macrophages	10 <sup>-8</sup>	IgG <sub>3</sub> > IgG <sub>1</sub> > IgG <sub>4</sub> >>> IgG <sub>2</sub>
II	Monocytes Neutrophils Eosinophils B lymphocytes	10 <sup>-5</sup> – 10 <sup>-6</sup>	IgG <sub>3</sub> > IgG <sub>1</sub> , IgG <sub>2</sub> >>> IgG <sub>4</sub>
III	Macrophages Neutrophils Eosinophils NK cells T lymphocytes	10 <sup>-5</sup> – 10 <sup>-7</sup>	IgG <sub>3</sub> , IgG <sub>1</sub> >>> IgG <sub>4</sub> , IgG <sub>2</sub>

\*Hierarchy based on studies with some, but not all, cell types

This table was obtained from a Expert Opinions in Biological Therapy article (3).

### *Class I major histocompatibility complex (MHC) and antigen presentation*

Unlike immunoglobulins on the surface of B cells, which typically recognize soluble antigens derived from pathogens, T cells only recognize foreign or modified antigens which are displayed on the surface of the body's own cells. These antigens, or T cell epitopes (TCE), are presented in the context of the major histocompatibility complex (MHC), of which there is a class I (recognized by CD8<sup>+</sup> T cells) and a class II (recognized by CD4<sup>+</sup> T cells). Unlike the class II MHC, class I is presented on all nucleated cells; this allows for CD8<sup>+</sup> T cells to survey the body for any modifications to its normal protein repertoire.

In humans, the MHC is termed the human leukocyte antigen (HLA), of which there are many polymorphisms with amino acid modifications. These polymorphisms create different haplotypes, which are determined by the various HLA-A, B, C, DR, DP and DQ genes, with HLA-A2 being the most common class I MHC in the human population (50). The structure of the MHC class I molecule (HLA-A2) was determined in 1987 (51) and consists of two polypeptides: The first is composed of three alpha domains and the second is a noncovalently associated chain termed  $\beta_2$ -microglobulin ( $\beta_2$ M) (Fig. 5). Peptides which bind to class I MHC are usually derived from intracellular breakdown and processing of the cell's own proteins. Early studies using viral peptides demonstrated that MHC Class I assembly and stability depend on peptide binding (52, 53). Peptides with correct lengths (8-10 amino acids) and sequences bind to MHC class I with slower off rates relative to longer peptides (54, 55). These peptides are products of the proteasome (56), which degrade polyubiquitylated proteins via the C-terminus, along with a variety of aminopeptidases both in the ER (ERAP1) and the cytosol (57-61).

The assembly of the MHC class I molecule involves a variety of proteins and cofactors including transporter associated with antigen processing (TAP), tapasin, ERp57, calnexin and calreticulin. TAP is part of a family of ATP binding cassette transporter proteins (ABC transporters) and is assembled as a heterodimer of TAP1 and TAP2. The protein transports peptides from the cytosol to the ER in an ATP-dependent manner, with some degree of peptide size and sequence specificity (62). Tapasin on the other hand is a protein which stabilizes the MHC class I/  $\beta_2M$  complex until TAP arrives (63). In addition, this protein has also been shown to increase TAP levels and promote peptide binding to TAP (64, 65). ERp57, identified in 1998, is a thiol-dependent oxidoreductase (66-68). Its exact function in the ER during the formation of the MHC class I complex is unknown; however it has been hypothesized to potentially play a role in the formation of disulfide bonds. Calnexin and calreticulin are chaperone proteins; they have been shown to assist in the folding of newly synthesized glycoproteins in the ER. The role of these proteins in the assembly of the MHC class I molecule is also illustrated in Figure 6.

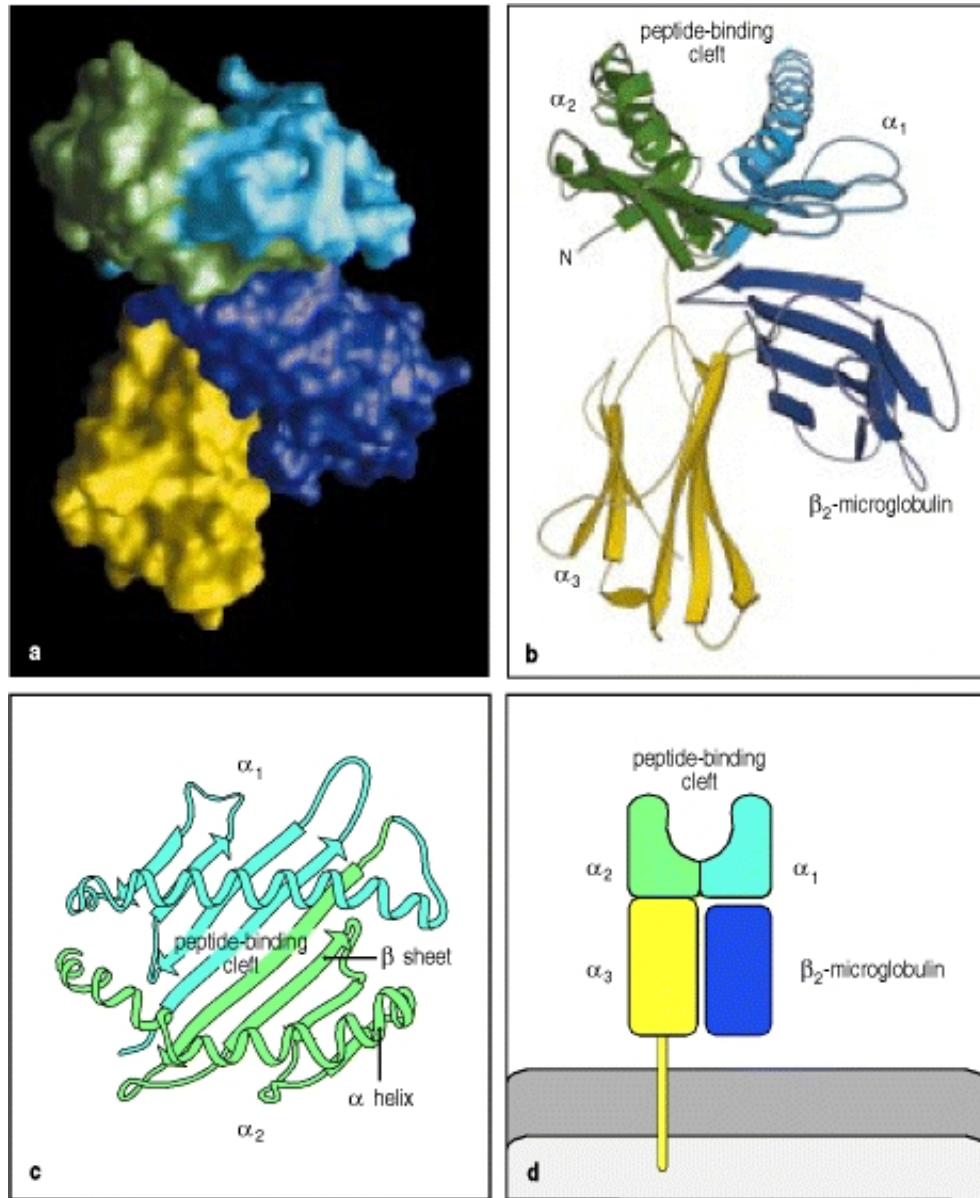


**Figure 5.** Structure of the MHC Class I molecule.

*A, B* and *C*. Shown are computer graphical representations of the structure of the human HLA-A2 molecule, with *B* and *C* being ribbon diagrams. *C*. A top-down view of the peptide binding region. *D*. A schematic view of the three alpha chains and the  $\beta_2$ M, which form a heterodimer with an approximate molecular weight of 43 kDa. The figure was obtained from Figure 3.20 in the text book Immunobiology, 5<sup>th</sup> Edition.



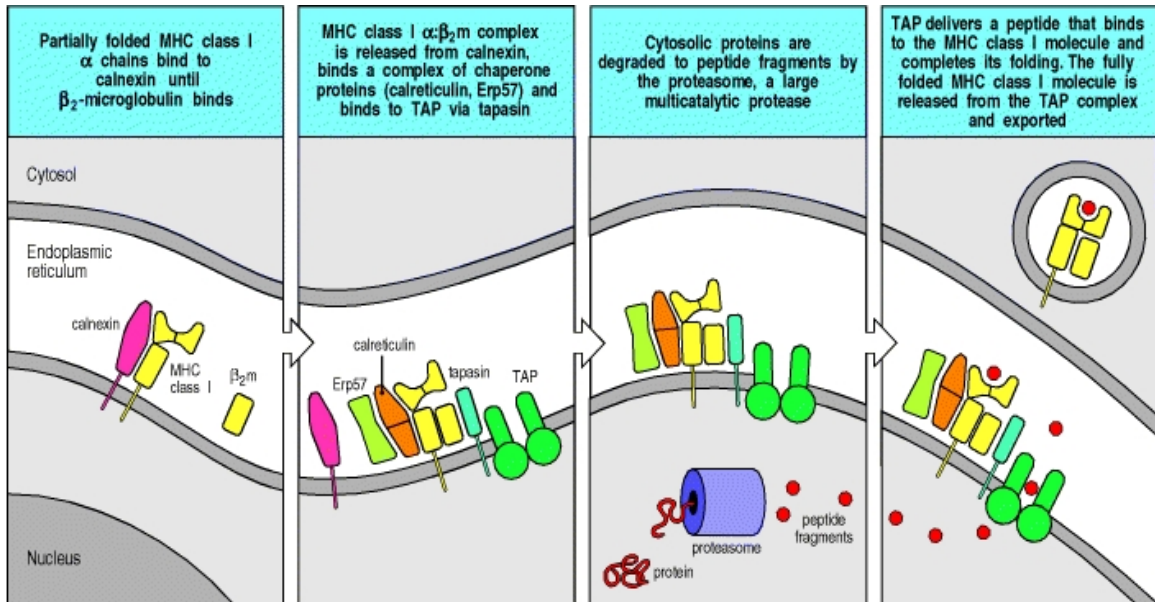


**Figure 6.** MHC class I assembly.

Newly synthesized MHC Class I alpha chain assembles in the ER with calnexin. Once  $\beta_2$ M binds to the alpha chain, calnexin dissociates and the MHC class I molecule binds to Erp57, calreticulin, tapasin and TAP. Once a peptide (8-10 amino acids) has been transported to the surface of the MHC via TAP and completes the folding process, the final complex is transported to the Golgi apparatus and then the cell membrane. The figure was obtained from Figure 5.5 in the text book Immunobiology, 5<sup>th</sup> Edition.

### *Phage display*

Over the past 26 years, beginning with the first report describing the display of polypeptides on the surface of bacteriophage particles (69), phage display has evolved to help scientists rapidly select for, identify, and optimize proteins based on their structural and functional properties. Conventional phage vectors usually fuse the gene of interest (which typically codes for a polypeptide) with a minor capsid protein of a filamentous phage (Fig. 7). When transcribed and translated, the resulting fusion protein will be expressed on the phage surface, allowing the phage to act as a vehicle for polypeptide transport and a carrier of the polypeptide gene sequence. In the setting of monoclonal antibodies, the polypeptide is usually in the form of a scFv or Fab. Once a library has been created, using PCR-based gene amplification of immunoglobulin variable genes ( $V_H$  and  $V_L$ ), the phage can then be used for screening against antigens of interest. Phage display libraries come in three main varieties, immune, naïve, and semi-synthetic. Immunized libraries are those which are derived from the immunoglobulin genes of an immunized organism (e.g. mouse, chicken, human, etc.) while naïve libraries are those which are derived from organisms which have not been exposed to the target antigen of interest (17, 70-72). Semi-synthetic libraries are those which take on the framework from known antibodies, but have their CDRs randomized using overlap extension PCR (73, 74). Regardless of the approach, the ultimate goal is to select for highly specific, high affinity antibodies against an antigen of interest.

There are several advantages in using phage display over standard hybridoma technology for obtaining monoclonal antibodies of interest (49). First, isolation of scFv/Fab fragments can be performed within a week if a library is already available. This

is compared to several months after initial immunization of a mouse or rabbit using standard hybridoma technology. Second, antibody sequences can be derived from almost any animal species, which allows for the selection of fully human antibodies using RNA from human B lymphocytes. This is in contrast to antibodies typically isolated from hybridoma technology since it usually requires immunization and subsequent harvest of splenic lymphocytes. Third, once a candidate scFv or Fab has been discovered, the variable regions can easily be cloned into an expression plasmid for the production of full Ig or fusion proteins such as bi-specific T cell engaging antibodies (BiTEs) (75). While class switching of Ig using hybridoma technology is possible, the only way to switch the variable regions from one species to another (e.g. mice to man) is by genetic engineering.

The most important factor in isolating an antibody using phage display technology is library diversity (76). In general, greater library diversity (i.e., the more differences in polypeptide sequence) translates to a higher success rate in selecting for high affinity antibodies. Normally, antibody phage display libraries have in the order of  $10^9 - 10^{11}$  unique antibody species. Typical phage display library screening (biopanning) is done either in solution or on a solid surface. Conventional biopanning on a solid surface usually begins with non-specific immobilization of the target antigen (usually a purified protein or peptide). Subsequently, the phage display library is incubated with the antigen, the unbound phage are washed off, and the bound phage are eluted from the solid support. This single round of biopanning is then repeated two or three more times (after amplification following *E. coli* infection) to further enrich for phage which present the antibody of interest; this entire process is illustrated in Figure 8. While this selection approach is very common and basic, issues regarding epitope accessibility and protein

folding after immobilization can arise (77). Alternatively, solution phase biopanning is similar in most respects except that the target antigen is first site-specifically conjugated to a tag (e.g. biotin) which can be captured using magnetic beads (78); this allows for the target epitope to be fully exposed during biopanning and the protein folded properly in the correct buffer. To prevent nonspecific binding, an irrelevant control antigen (without a tag) can be added to the solution of specific antigen and library. Once captured by a magnet, the non-specific binding phages can be washed off and discarded. In addition to purified polypeptides, this strategy has also been applied to whole cells using a cell-based panning approach (79). In many cases, a negative selection step is also incorporated so that the antibodies which are recovered do not bind to normal cell surface proteins (80). This allows for both the identification of new antibodies as well as potentially new antibody targets.

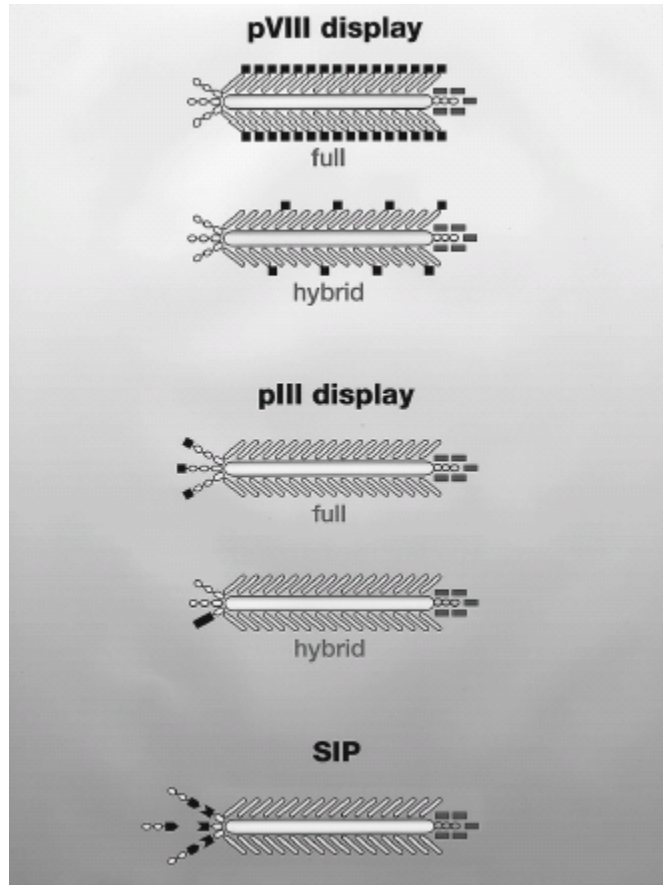


**Figure 7.** Display of proteins on filamentous bacteriophage.

Three different methods by which polypeptides (dark solid symbols) are presented on the surface of bacteriophage based on their coat proteins (pVIII versus pIII). Selectively infective phage (SIP) is a phage “two-hybrid system” based presentation and selection method. The figure was obtained from Figure 1.6 in the text book Phage Display: A Laboratory Manual, 1st Edition.

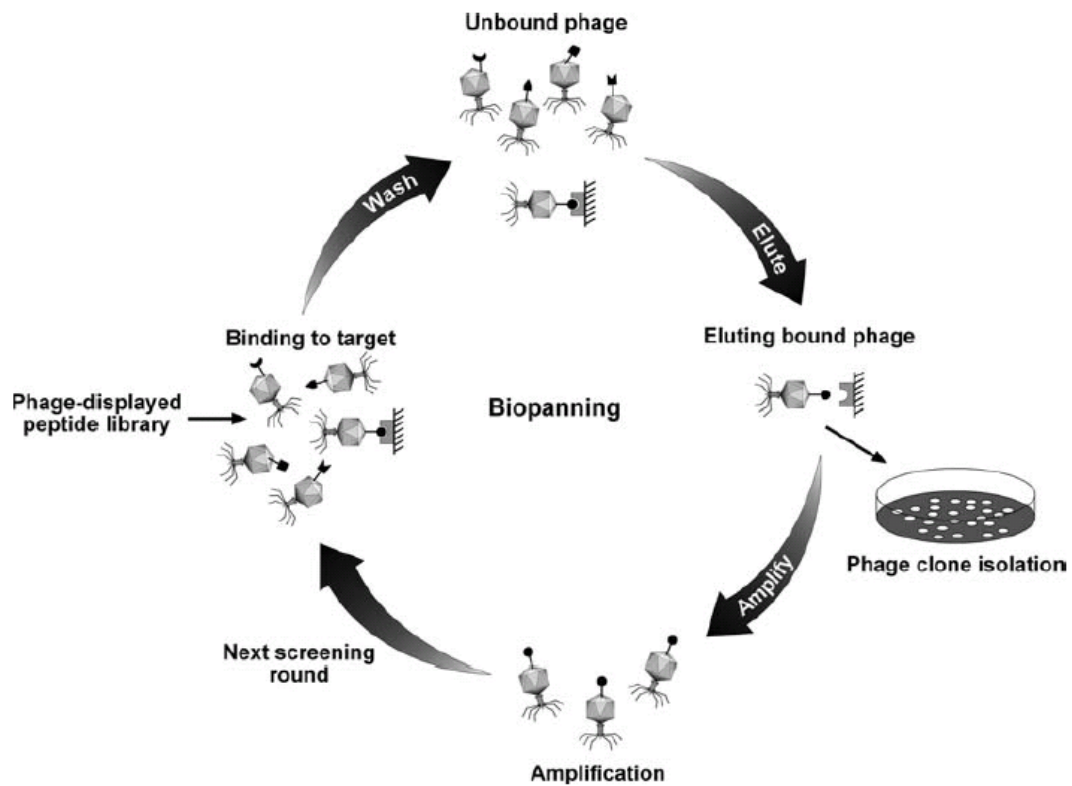


**Figure 8.** Biopanning using a phage display library.

A phage display library is first allowed to bind to a target antigen, unbound phage are washed away, bound phage are eluted off of the antigen/solid support, and eluted phage are amplified overnight in *E.coli* for a subsequent round of selection. The figure was obtained from a International Journal of Peptide Research and Therapeutics article (81).

### *T cell signaling and activation*

One of the major cell types of the adaptive immune system are T cells. These cells arise from hematopoietic progenitors in the bone marrow and mature within the thymus, where a series of positive and negative selection steps result in single-positive CD4 and CD8 naïve T cells. In order to be activated, naïve T cells have to recognize antigen as a linear peptide in the context of the major histocompatibility complex (MHC). This T cell receptor (TCR) recognition event is not typically sufficient for activation, and requires the simultaneous delivery of a co-stimulatory signal. Once these receptors and antigens come in contact with each other on the T cell surface, several intracellular phosphorylation signaling events occur, along with phospholipid metabolism, cytoskeleton rearrangements, and an increase in intracellular calcium levels, which eventually regulate genes involved in proliferation, differentiation, survival and apoptosis (82-85).

In  $\alpha\beta$  T cells, the 39-46 kDa  $\alpha$  and 40-44 kDa  $\beta$  chains of a TCR form a heterodimer (86, 87) which has dual specificity for both a peptide antigen as well as polymorphic determinants of the MHC molecule (88, 89). In addition, several non-polymorphic proteins have been found to interact with the  $\alpha$  and  $\beta$  chains, which constitute the CD3 complex ( $\gamma$ ,  $\delta$ ,  $\epsilon$ , and  $\zeta$ ) (90, 91) (Fig. 9). Along with the TCR and CD3 complex, the CD8 and CD4 membrane glycoprotein co-receptors also play a functionally significant role in signaling. These co-receptors bind MHC class I (CD8) and MHC class II (CD4) molecules (92), and function synergistically with the TCR to increase response sensitivity and phosphorylate immunoreceptor tyrosine-based activation motifs (ITAMs) on the CD3 complex. Aggregation of the TCR with its

corresponding CD4 or CD8 co-receptor leads to T cell activation by bringing the Lck and Fyn tyrosine kinases together with the ITAMs on the cytoplasmic domains of the CD3 complex (93, 94). Once the ITAMs have been phosphorylated, the zeta-chain associated protein of 70 kDa (ZAP-70) can bind to phosphotyrosines via its two SH2 domains; this allows ZAP-70 to further phosphorylate LAT (linker of activation in T cells) (95, 96) and the SH2-domain-containing leukocyte protein of 76 kDa (SLP-76) (97). The signal then propagates further by way of several protein tyrosine kinases such as MEK and its substrate ERK (extracellular-regulated kinase) along with G proteins such as Ras and Rac (98).

Along with kinase activity, phosphatase activity has also been demonstrated to play a role in T cell activation, with CD45 being the best characterized transmembrane phosphatase in lymphocytes (99). CD45 has been shown to be involved in dephosphorylating negative-regulatory residues on Lck, which results in enhanced kinase activity (100, 101). However, contradictory studies show that removal of a phosphate on a tyrosine residue inside the kinase domain of Lck can result in a decrease in kinase activity (102). This discrepancy was later explained using localization studies which demonstrate that CD45 functions by moving to different compartments of the cell during T cell engagement with an antigen presenting cell (103). These signaling events will ultimately lead to the activation of transcription factors such as NF $\kappa$ B, NFAT and AP-1 (Fig. 10).

Along with signals directly related to the TCR and CD3 complex, several other co-stimulatory molecules have been identified and implicated in T cell activation. CD28, initially identified by the monoclonal antibody MoAb 9.3, is the most well characterized



and shown to be responsible for T cell activation in the presence of the TCR/CD3 complex (104, 105). CD28 binds to B7.1 (CD80) and B7.2 (CD86) on antigen presenting cells (APCs) and carries out a necessary co-stimulatory signal (106); these B7 family of proteins are upregulated on APCs after stimulation of CD40 on APCs. TCR activation and CD28 engagement together synergize to induce high levels of Vav 1 and PLC $\gamma$  phosphorylation (107, 108), which amplifies TCR signaling. Thus, CD28 mediated signals essentially regulate the threshold of T cell activation and reduce the number of TCR engagements needed for activation. Additional co-stimulatory/ligand pairs have since been identified, including ICOS/ICOSL, OX40/OX40L, and 4-1BB/4-1BBL (109-111), which will be discussed in more detail later in this thesis.

On the other hand, there have been several molecules which have been shown to inhibit T cell signaling and protect against over stimulation. The most studied of these is the inhibitory receptor cytotoxic T lymphocyte associated antigen 4 (CTLA-4). While it is about 30% similar to CD28, CTLA-4 has a much higher affinity to the B7 ligands (112). Its expression is upregulated during CD28 engagement, and once expressed on the cell surface, it out competes CD28 for ligand binding (113, 114). CTLA-4 inhibits IL-2 production and halts the T cell at the G1 phase of the cell cycle, effectively terminating the T cell immune response (115, 116). Other inhibitory molecules include PD-L1 and PD-L2, which bind to PD-1 on activated T cells. These members of the programmed death (PD) family of receptors and ligands have been shown to inhibit T cell activation and induce tolerance in mice (117), with PD-1 knockout mice developing spontaneous autoimmune diseases (118, 119).

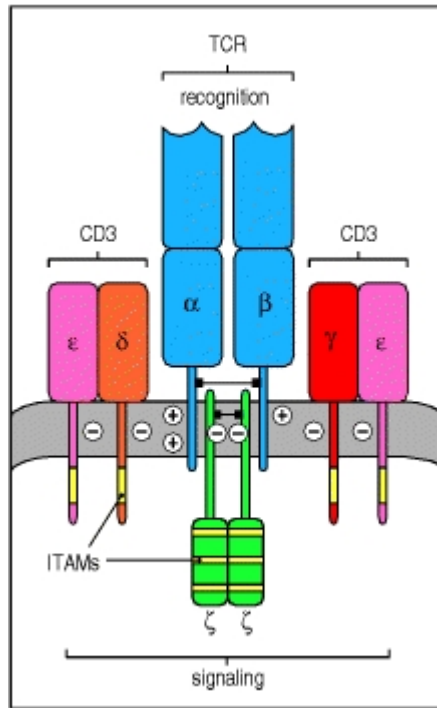


**Figure 9.** Structure of the T cell receptor complex.

Shown is a schematic view of the TCR  $\alpha$  and  $\beta$  chains along with the four invariant signaling domains ( $\gamma$ ,  $\delta$ ,  $\epsilon$ , and  $\zeta$ ) which are collectively referred to as CD3. The figure was obtained from Figure 6.8 in the text book Immunobiology, 5<sup>th</sup> Edition.

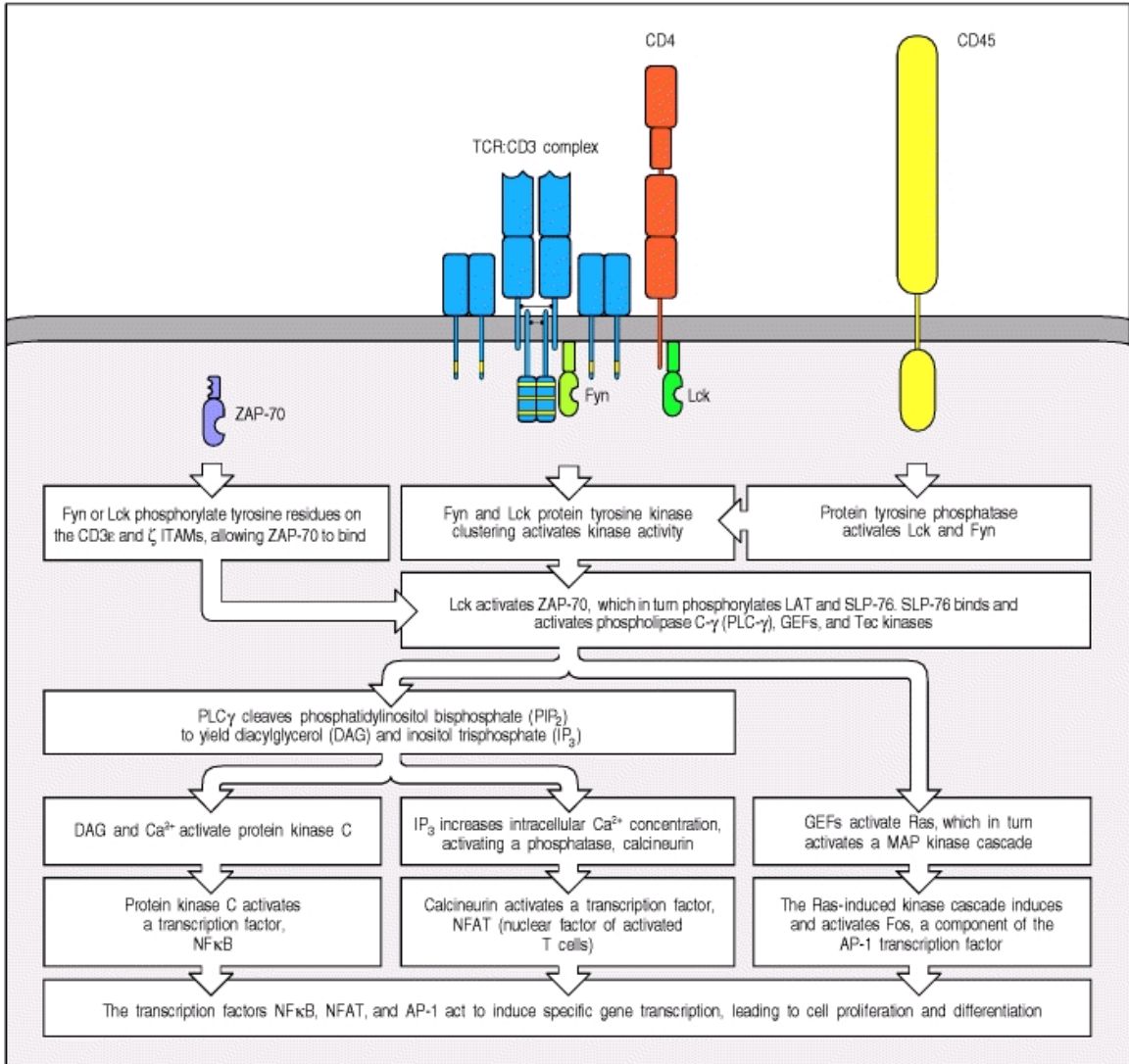


**Figure 10.** TCR intracellular signaling pathways.

Shown is a simplified view of the TCR and co-receptor signaling inside of T cells. The figure was obtained from Figure 6.15 in the text book Immunobiology, 5<sup>th</sup> Edition.

### *Adoptive T cell therapy*

Over the past several decades, the adoptive transfer of antigen-specific T cells for the treatment of cancer has led researchers to further manipulate these cells using genetic engineering. Since the cloning of the first tumor-associated antigens in the early 1990s, tremendous attention has been focused on generating antigen specific T cells against viral antigens, differentiation antigens, cancer testis antigens, and other oncogenes. Currently, there are 2 major genetic strategies which redirect effector T cell specificity towards a target antigen of interest: T cell receptor (TCR) and chimeric antigen receptor (CAR) gene transfer.

The adoptive T cell therapy field first began using non-gene modified T cells for the treatment of viral and non-viral malignancies. In the early 1990s, researchers reported that it was possible to transfer antigen-specific T cell clones into a patient to prevent cytomegalovirus (CMV) reactivation after hematopoietic stem cell transplantation (120). This work was made possible by harvesting the donor's own peripheral blood lymphocytes, expanding them in the presence of CMV-infected autologous fibroblast, isolating CMV-specific T cell clones, and infusing them back into the patient. The approach was later applied to the prevention of latent Epstein-Barr virus (EBV) reactivation in patients who get post-transplant lymphoproliferative diseases (121) as well as a variety of other viral-related malignancies (122, 123). During the same time, several reports came out regarding the use of adoptive cell therapy in the non-viral cancer setting; this began after a study demonstrated that tumor infiltrating lymphocytes could mediate tumor regression in melanoma patients (124). Subsequently, successful adoptive T cell therapy was report for the treatment of chronic myelogenous leukemia in the

nonmyeloablative setting (125). While these initial studies did result in an overall response rate of about 30%, further improvements in host preconditioning using nonmyeloablative chemotherapy resulted in greater and more durable objective response rates (126, 127).

The first reported TCR gene transfer came in 1986 (128), and by 1989 the FDA approved a protocol for the use of TCR gene-modified lymphocytes for the treatment of malignant melanoma (129). One of the earliest reports involved the transfer of a tumor associated antigen-specific TCR using gamma retroviral vector transduction (130). Subsequently, other groups used a similar approach to target MDM2 (131) and WT1-derived T cell epitopes (132). The choice in gene transfer method has been shown to be crucial, and includes standard laboratory-based chemical approaches, electroporation/nucleofection, and the more widely used viral-based methods. Virtually all clinical trials which involve TCR gene transfer are based on gamma retroviral expression vectors such as MFG/SFG, MP71/SF91, and MSGV1 (133-135). However, more recent approaches using lentiviral vectors have improved transduction efficiency since T cell activation or proliferation is not absolutely required for genomic integration (136, 137).

While TCR gene transfer has been widely used, proper expression has been a major limitation. First, since the TCR is composed of two separate chains which come together via disulfide bonds on the extracellular surface, the TCR genes were initially expressed using two individual vectors, or one vector with two separate promoters. This issue was address by incorporating picornavirus ribosomal skip peptides to link both chains (138, 139). In addition, since the transduced TCR molecule has the same structure

as that of the T cells endogenous TCR, mispairing between the  $\alpha$  and  $\beta$  chains became very common. Currently, one of the most successful approaches to overcome the mispairing has been the use of chimeric TCRs, in which the constant regions are mouse-derived while the antigen binding domains are still human (140-142).

The chimeric antigen receptor (CAR) strategy of retargeting immune effector cells is independent of the MHC-peptide-TCR interaction and allows cells to react against a large variety of cell surface antigens (143). Several methods have been used in the design of CARs, with most of them employing the antigen binding domain of a monoclonal antibody in the form of a single-chain variable fragment (scFv) for antigen recognition. The initial T cell activating receptors originated from studies which allowed researchers to elucidate the role of the CD3 $\zeta$  chain (144, 145). In subsequent studies, scFvs of interest were fused to the CD3 $\zeta$  chain (146) or Fc $\epsilon$ RI $\gamma$  (147), and both were found to be sufficient for T cell activation (Fig. 11). While this laid the blueprint for CAR construction, the incorporation of costimulatory molecules came about after it was found that first generation CARs were able to induce T cell proliferation for only up to 2-3 cell divisions, followed rapidly by cell death (148). By expressing CD80 on the target tumor cell, researchers were able to show that CAR expressing cells could be restimulated, leading to further increases in T cell numbers. The first CARs which incorporated the CD28 costimulatory molecule alongside the CD3 $\zeta$  chain showed vast improvements over those which expressed the CD3 $\zeta$  chain alone (149-151); this included an absolute increase in T cell numbers as well as an increase in IL-2 production. Since then, several other groups began to use other costimulatory molecules, either in combination with CD3 $\zeta$  alone or with both CD3 $\zeta$  and CD28. These additional signaling

molecules include 4-1BB (152-155), DAP10 (153), OX40 (153, 155-158) and ICOS (155), and have been applied in the context of T cells as well as NK cells (159-163). While first generation CARs are the only ones which have been tested in the clinic up to this point, both *in vitro* and *in vivo* comparisons have demonstrated a clear superiority with second and third generation CARs (150, 153, 164-169).

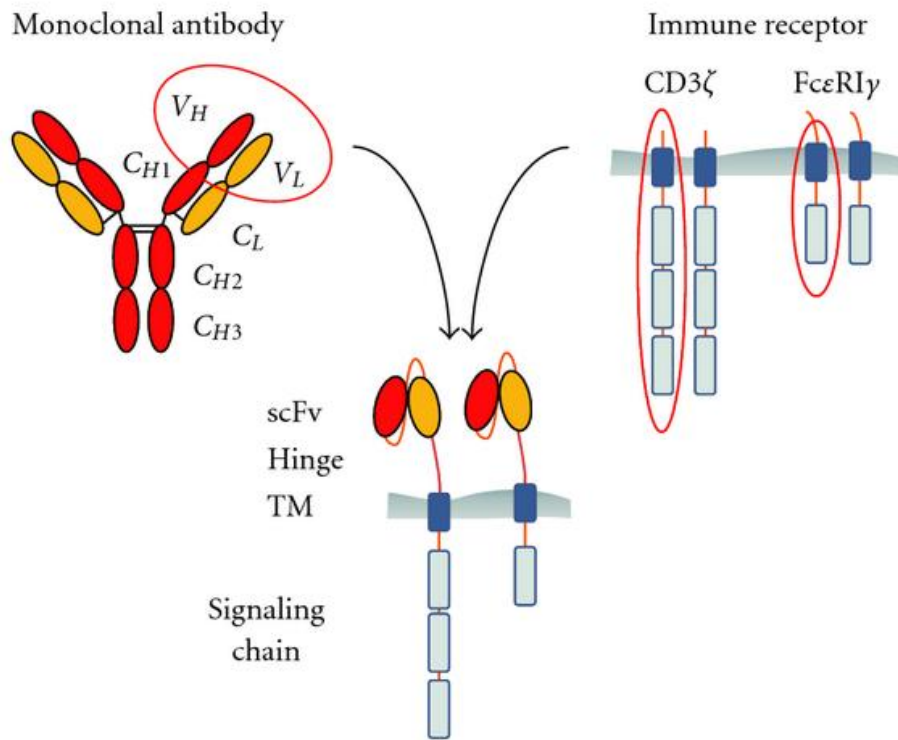


**Figure 11.** Chimeric antigen receptor (CAR) architecture.

A typical CAR is composed of the variable domains of a monoclonal antibody (in the form of a scFv) in combination with an intracellular signaling ectodomain. The figure was obtained from a Journal of Biomedicine and Biotechnology article (170).



## *Introduction to the thesis*

As a proof of principle in determining whether we were able to obtain MHC-restricted, peptide-specific monoclonal antibodies using phage display, we first selected against viral-derived TCEs using a human phage display library with diversity in the order of  $10^8$ . Our initial screen allowed us to recover a scFv which we termed EBNA Clone 315. This antibody was specific for an EBNA3C-derived peptide (LLDFVRFMGV) in the context of HLA-A2. EBNA3C is an Epstein-Barr virus (EBV)-encoded nuclear protein demonstrated to interact with the p300 transcriptional coactivator, in combination with prothymosin alpha, to regulate transcription and histone acetylation (171). In addition, recent studies have found that EBNA3C is also able to repress p16(INK4A) and p14(ARF), crucial cell cycle tumor suppressor proteins (172). The virus was discovered using electron microscopy over 40 years ago on cells obtained from Burkitt's lymphoma tissue (173). As one of the most prevalent viruses in the human species (over 90%), EBV-associated diseases range from infectious mononucleosis (174) to cancers such as nasopharyngeal carcinoma (175), non-Hodgkin's lymphoma (176) and Hodgkin's disease (177). EBNA3C has also been shown to be essential for initiation of B-cell growth and conversion of B-cells to immortalized lymphoblasts (178). Furthermore, previous studies using cytotoxic T lymphocytes which target EBV-infected cells showed that the peptide LLDFVRFMGV displayed on HLA-A2 was immunogenic (179). This allows for EBV-transformed B cell lymphoblastoid cell lines (BLCLs) to be useful targets for pre-clinical testing of EBNA3C-directed immunotherapies (180).

Subsequent screens using the same phage display library against a variety of tumor associated HLA-A2-peptide complexes led to the discovery of a scFv which we termed WT1 Clone 45. This antibody targeted the Wilms tumor protein 1 (WT1)-derived RMFPNAPYL peptide on HLA-A2. Wilms tumor protein 1 (WT1) is a zinc-finger transcription factor found to play an important role in cell growth and differentiation. WT1 is normally expressed in a tissue-specific manner, found mainly in the urogenital system of a developing embryo as well as the central nervous and hematopoietic systems in adults (181). In its aberrant state, WT1 expression has been linked to a variety of leukemias, lymphomas and solid tumors including astrocytic tumors, head and neck tumors, thyroid cancer, esophageal cancer, sarcomas, breast, lung, pancreatic and colorectal cancer, mesothelioma, and neuroblastoma (181, 182). While it was initially characterized as a tumor suppressor from studies with osteosarcoma and Wilms tumor (a rare pediatric kidney malignancy) (183, 184), recent studies on WT1 in malignant cells has led researchers to believe that it acts more as an oncogene (185). There are currently four HLA-A2-restricted WT1 TCEs used for peptide vaccination in humans (VLDFAPPGA, RMFPNAPYL, SLGEQQYSV and CMTWNQMNL) (186), of which RMFPNAPYL is the most extensively studied. In fact, the crystal structure of the RMFPNAPYL peptide in complex with HLA-A2 has recently been solved (187), further demonstrating this epitope's interest in the field of cancer immunotherapy. In preclinical studies, HLA-A2-RMFPNAPYL-specific T cells could be generated using HLA-A2-positive donor cells, which could subsequently lyse HLA-A2<sup>+</sup>, WT1<sup>+</sup>, CD34<sup>+</sup> myeloid leukemia blasts *in vitro* and deplete clonogenic cells capable of transferring leukemia in NOD/SCID mice, *in vivo* (188). Furthermore, clinical studies involving the

RMFPNAPYL peptide have led to durable responses in cancers such as acute myeloid leukemia (AML) (189, 190).

Once both scFvs were demonstrated to bind well to their target antigens, they were reengineered to act as scFv-Fc fusion proteins, in which the scFvs were fused to the 2<sup>nd</sup> and 3<sup>rd</sup> constant domains of a human IgG<sub>1</sub> Fc (Fig. 12). These proteins effectively recreate a smaller intact immunoglobulin at approximately 100 kD. They assembled into bivalent molecules and have previously been shown to retain antigen binding, Fc-mediated cytotoxicity and localization to tumor xenografts (50, 191). In addition, while their serum half-life is shorter than full length immunoglobulins, it is longer than a scFv (50, 192) and their larger size allows for chemical conjugation of cargo such as drugs, toxins or fluorescent labels.

Furthermore, after the scFvs were engineered to act as CARs, they were then tested in the setting of NK92MI cells, a highly cytotoxic natural killer-derived cell line which has been genetically modified to produce high levels of IL-2. This allowed us to take advantage of some of the attributes that CARs can afford us, in regards to independence from separate costimulatory molecules, while allowing us to target a TCE of interest. To some respect, these types of CARs have already been generated and shown to cause target specific killing (42-45); however these constructs were only expressed on T cells and not any other cell type. We on the other hand were able to demonstrate that these CARs were useful in redirecting NK92MI cells towards HLA-A2-restricted peptide complexes. In addition, we could also demonstrate that these CARs were a very sensitive means of detecting their target complexes under very low antigen density settings.

We believe the work presented here outlines a systematic approach towards isolation of MHC-restricted, peptide-specific monoclonal antibodies, subsequent engineering into proteins with Fc effector functions (scFv-Fc), and use as CARs for retargeting immune effector cells. We conclude that MHC-restricted, peptide-specific CARs are a highly-specific, highly sensitive approach for retargeting NK92MI cells towards tumor associated antigens of interest.

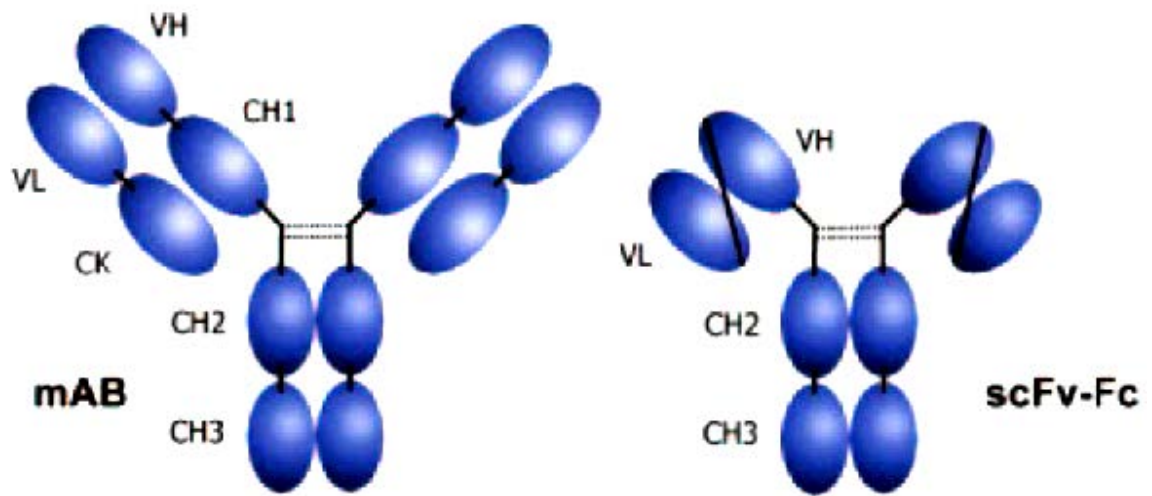


**Figure 12.** Structure of a full immunoglobulin and scFv-Fc fusion protein. The scFv-Fc fusion protein consists of the 2<sup>nd</sup> and 3<sup>rd</sup> constant domains of an immunoglobulin Fc fragment in tandem with the scFv sequence. The figure was obtained from a Proceedings of the National Academy of Sciences article (193).

## MATERIALS AND METHODS

### *Production of biotinylated MHC-peptide complexes*

Soluble MHC class I/peptide complexes were generated by overexpression of the HLA-A2 heavy chain (HC) and  $\beta_2M$  as recombinant proteins in *E. coli* and subsequent *in vitro* refolding and assembly in the presence of high concentrations of specific peptide (194, 195). To obtain soluble MHC/peptide complexes the HC sequence was mutagenized to remove the cytosolic and transmembrane regions. In order to specifically biotinylate refolded, monomeric MHC/peptide complexes, the HC was expressed as a fusion protein containing a specific biotinylation site at the C-terminus (196, 197). These short sequences are sufficient for enzymatic *in vitro* biotinylation of a single lysine residue within this sequence using the biotin protein ligase BirA (198). This procedure was carried out by, and purchased from, the MSKCC Tetramer Core Facility, under the direction of Ingrid Leiner and Dr. Eric Pamer.

*Selection of phage on HLA-A2-LLDFVRFMGV (EBNA3C) complex*

The Tomlinson I + J human scFv phage display libraries (199) containing approximately  $2.85 \times 10^8$  independent scFv clones, were used for selection according to previously published methods (25) with modifications.  $7.5 \times 10^{12}$  Phage, from the combination of both libraries, were first preincubated with streptavidin paramagnetic Dynabeads (30  $\mu$ l; Dynal, Oslo, Norway) and 150  $\mu$ g unbiotinylated HLA-A2-YVDPVITSI (irrelevant complex) in 1 ml of PBS to deplete the streptavidin and HLA-A2 binders. The dynabeads were subsequently captured using a magnet and the supernatant (phage and irrelevant complex mixture) transferred to a separate tube containing 7.5  $\mu$ g of biotinylated HLA-A2-LLDFVRFMGV (Epstein-Barr virus EBNA3C-derived) and 7.5  $\mu$ g of biotinylated HLA-A2-NLVPMVATV (Cytomegalovirus pp65-derived) and incubated at RT for 1 hour. The final mixture (1 ml) was then added to 200  $\mu$ l of Dynabeads (preincubated with 2% Milk and washed with PBS) and the contents were mixed for 15 min. at RT with continuous rotation. The beads were then washed 10 times with PBS/0.1% Tween and 3 times with PBS and the bound phage were eluted from the Dynabeads using 1 mg/ml trypsin in PBS (0.5 ml) for 15 min. at RT. The phage were then used to infect TG1 *E. coli* (growing in log phase) at 37°C in 20 ml of LB for 1 hour.  $10^{12}$  KM13 helper phage was subsequently added to the mixture, further incubated for an additional 30 minutes, and the cells pelleted using centrifugation (3000 rpm for 10 min.). The resulting cell pellet was resuspended in 200 ml LB + Ampicillin (100  $\mu$ g/ml) + Kanamycin (50  $\mu$ g/ml) and incubated overnight at 30°C. On the following morning, the overnight cultures were harvested and centrifuged at 3000 rpm for 15 min. and the supernatant (180 ml) was mixed with polyethylene glycol (PEG)

on ice for 1 hour so as to precipitate the amplified phage from the previous round of selection. The PEG/phage mixture was then centrifuged at 3000 rpm for 20 min., and some of the resulting phage pellet used for subsequent rounds of panning while the rest was frozen down in 15% glycerol at -80°C. Subsequent rounds of panning were done using the same protocol as above with an increase in Dynabead washing steps and a decrease in the amount of biotinylated complexes used for selection.

After the final round of antibody selection (3<sup>rd</sup> or 4<sup>th</sup>), the eluted phage were used to infect both TG1 and HB2151 *E. coli*. TG1 is able to suppress termination and introduce a glutamate residue at the TAG stop codon position at the end of the scFv sequence and before the gIII sequence. Unfortunately, since the TAG stop codon between the scFv and the gIII gene is also suppressed this leads to co-expression of the scFv-pIII fusion protein which tends to lower the overall levels of the scFv expression, even in clones where there are no TAG stop codons. To circumvent this problem, the selected phage can be used to infect HB2151 (a non-suppressor strain) which is then induced to give soluble expression of antibody fragments. TG1 cells were cultured overnight as mentioned above while the HB2151 cells were plated on TYE + Ampicillin (100 µg/ml) agar plates. The next morning, individual colonies from the agar plate were picked and used to inoculate individual wells of a 48-well plate containing 400 µl LB + Ampicillin (100 µg/ml)/well. After incubation for 3-6 hours at 37°C, 200 µl of 50% glycerol solution was added to each well and the plates stored at -80°C as monoclonal stock cultures.



*Selection of phage on HLA-A2-RMFPNAPYL (WT1) complex*

Selection was done similarly to the method above with slight modifications.  $3.7 \times 10^{12}$  phage, from the combination of both libraries, were first preincubated with streptavidin paramagnetic Dynabeads (50  $\mu$ l; Dynal, Oslo, Norway) and 20  $\mu$ g unbiotinylated HLA-A2-NLVPMVATV (irrelevant complex) in 1 ml of PBS to deplete the streptavidin and HLA-A2 binders. The dynabeads were subsequently captured using a magnet and the supernatant (phage and irrelevant complex mixture) transferred to a separate tube containing 5  $\mu$ g of biotinylated HLA-A2-RMFPNAPYL (WT1-derived) and incubated at RT for 1 hour. The final mixture (1 ml) was then added to 100  $\mu$ l of Dynabeads (preincubated with 2% Milk and washed with PBS) and the contents were mixed for 30 min. at RT with continuous rotation. The beads were then washed 10 times with PBS/0.1% Tween and 3 times with PBS and the bound phage were eluted from the Dynabeads using 1 mg/ml trypsin in PBS (0.5 ml) for 20 min. at RT. All subsequent steps were performed as above.

### *Expression and purification of soluble scFv from HB2151*

Using the monoclonal glycerol stocks containing individual HB2151 clones, separate 48-well plates containing 400  $\mu$ l LB + Ampicillin (100  $\mu$ g/ml)/well were inoculated in a replica-plate type format using sterile pipette tips. The 48-well culture plates were subsequently incubated at 37°C until the majority of the wells reached an OD600 of 0.4. 200  $\mu$ l LB + Ampicillin (100  $\mu$ g/ml) + isopropyl-1-thio- $\beta$ -D-galactopyranoside (IPTG; 1mM final concentration) was subsequently added to each well to induce scFv production and the plates were further incubated overnight at 28°C. The next morning, the plates were centrifuged at 3000 rpm for 15 min. and the supernatant used for scFv screening.

For large scale expression and purification, monoclonal glycerol stocks were used to inoculate 3 ml of Terrific Broth (TB) and incubated at 37°C until an OD600 of 0.8 was reached. Each 3 ml culture was subsequently divided amongst four flasks, each containing 250 ml TB + Ampicillin (100  $\mu$ g/ml). The cultures were then incubated at 37°C until an OD600 of 0.4-0.5 was reached, after which IPTG was added to a final concentration of 0.5 mM and the cultures incubated overnight at 30°C. The next morning, the overnight cultures were centrifuged at 4000 rpm for 25 min. The supernatant was discarded and the pellets dissolved in 50 ml PBS + 10 mM imidazole. The cell suspensions were passed through a cell homogenizer (5000 pounds per square inch) and the resulting cell lysates were centrifuged at 12,000 rpm for 15 min. The supernatants were then passed over a 0.22  $\mu$ m filter pre-layered with diatomaceous earth and the resulting filtrates loaded over Vivapure maxiprepMC Nickel affinity columns (Sartorius Stedim Biotech, Aubagne, France) using centrifugation (100 rpm for 5 min.).

The columns were then washed 4 times using 10ml PBS + 30 mM imidazole (500 rpm for 3 min.) and the scFvs eluted using 20 ml PBS + 300 mM imidazole (500 rpm for 3 min.). The eluted scFvs were concentrated using 10,000 molecular weight cut-off membrane Vivaspin centrifuge tubes at 3000 rpm for 30 min. (Sartorius Stedim Biotech) and dialyzed back into regular PBS. The final scFv products were subsequently stored at -80°C.

### *Construction of scFv-Fc fusion protein and expression in DG44 CHO cells*

Initially, we needed to make the scFv sequences compatible for cloning into a modified scFv-Fc expression vector. We did this by using PCR to add the desired restriction enzyme sites (NheI and ApaI) to either side of the EBNA Clone 315 and WT1 Clone 45 scFv sequences. The PCR reaction was done on the Tomlinson library vector which contained the WT1 Clone 45 and EBNA Clone 315 scFv sequences (Fig. 13A). After subsequent digestion using NheI and ApaI, the digested PCR products were removed from a 1% agarose gel and purified (Fig. 13B).

With regards to cloning and expression of the scFv-Fc fusion proteins, we decided to use a proprietary vector, similar to that of pFUSE—hIgG1-Fc1 (Invivogen; San Diego, California), that we obtained from Eureka therapeutics (IgG Vector; Fig. 14A). For our purpose, Hong Xu in our laboratory removed the first constant heavy chain (CH<sub>1</sub>) from this vector, something which is typically done when generating Fc fusion proteins (200). Once generated, the vector which Hong Xu made was digested with NheI and ApaI and then ligated to the predigested PCR products from Figure 13B. The ligated products yielded a vector which expressed the EBNA Clone 315 or WT1 Clone 45 scFv genes in tandem to the CH<sub>2,3</sub> domains of a human IgG<sub>1</sub> under a single CMV promoter (scFv-Fc Vector; Fig. 14B). They were then transformed into *E.coli*, plated on TYE + Ampicilin (100 µg/ml), colonies were picked and their plasmids sequenced at the MSKCC Sequencing Core Facility. After further validation using DNA sequencing, the two fusion constructs were linearized using HindIII and ran on a 1% agarose gel (Fig. 15). Digestion with HindIII also allowed us to block the expression of the light chain that is still present in the vector, which for all intensive purposes was undesired. As expected,

both digested plasmids ran at the anticipated size (~11,000 bp) based on their location relative to the lambda HindIII marker. Subsequently, the linearized DNA (5-6 µg) was electroporated (Amaxa Nucleofactor; Lonza, Switzerland) into  $5 \times 10^6$  DG44 Chinese Hamster Ovary (CHO) Cells (Invitrogen) using Program U-030 and 100 µl Solution V. The cells were then cultured in OptiCHO media (Invitrogen) containing G418 (500 µg/ml; added 7 days post-electroporation) at a cell density of  $1-5 \times 10^6$  DG44 per ml of media. The cells were then expanded to approximately 700 ml of culture media, which was centrifuged to remove the cells and supernatant used for antibody purification.

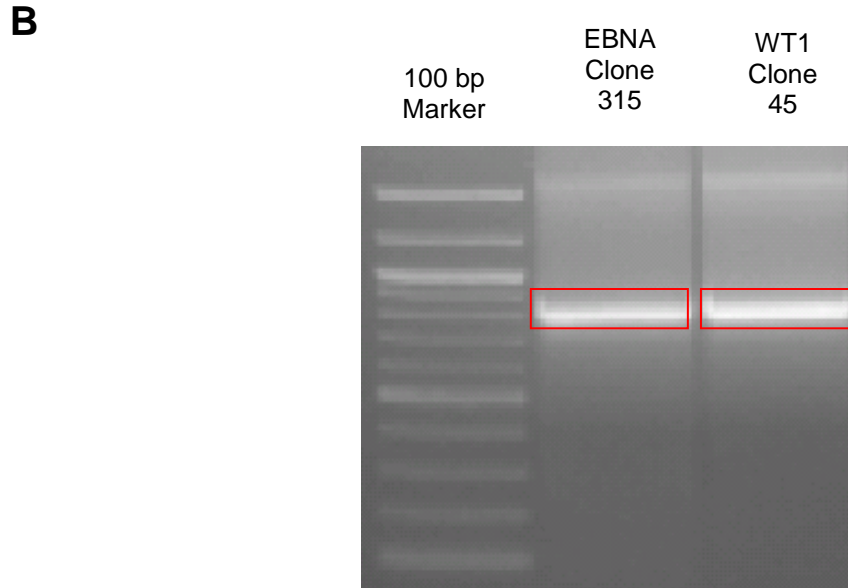
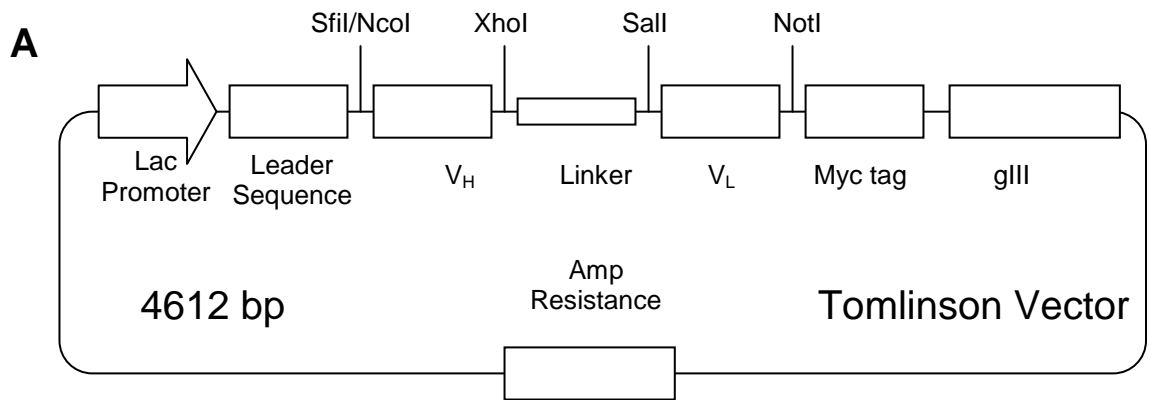


**Figure 13.** Tomlinson library vector, PCR reaction and NheI/ApaI digestion. *A.* The structure of the Tomlinson library vector (4612 bp). A beta-galactosidase promoter drives the expression of the scFv (V<sub>H</sub> – 15 amino acid Glycine/Serine Linker – V<sub>L</sub>) fused to a myc-tag and gIII by way of an amber codon. An ampicillin resistance gene is also present. *B.* After a PCR reaction was carried out on EBNA Clone 315 and WT1 Clone 45 containing plasmids, the PCR products were purified, digested with NheI and ApaI, and ran on a 1% agarose gel. The highlighted bands were determined to be the correct size (800 bp, based on the 100 bp marker), excised from the gel, and purified.

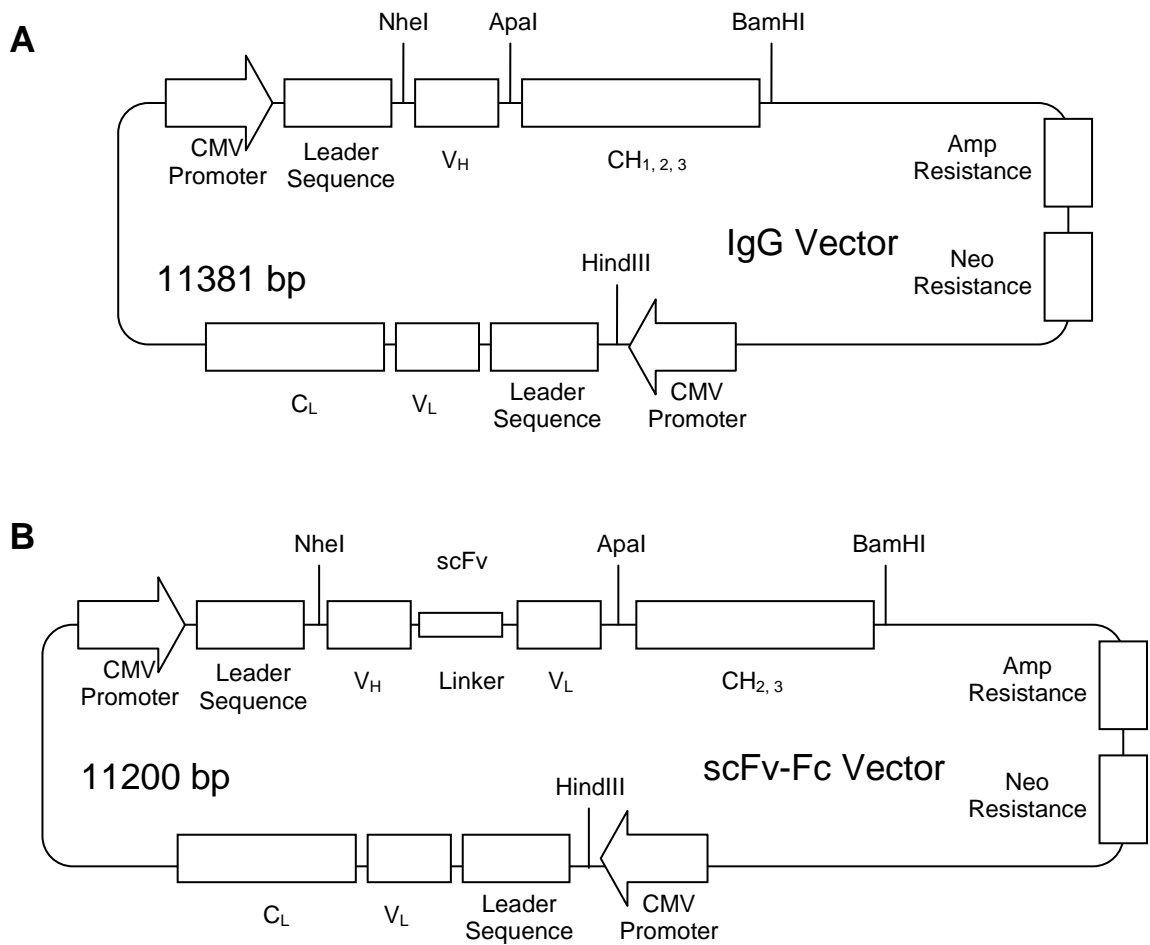


**Figure 14.** Full IgG expression vector and proposed scFv-Fc vector.

**A.** The structure of the proprietary IgG expression vector (11381 bp). The vector expresses the heavy and light chains under two separate CMV promoters. The variable heavy chain ( $V_H$ ) is fused to the first, second and third constant heavy chains ( $CH_{1,2,3}$ ) and expressed under one promoter while the variable light chain ( $V_L$ ) is fused to the constant light chain ( $C_L$ ) and expressed under a different promoter. This vector was further modified to lack the first constant region of the heavy chain ( $CH_1$ ), and this vector was used for the construction of scFv-Fc fusion proteins. **B.** After excision of the  $V_H$  from the IgG vector using NheI and ApaI, the pre-digested, purified scFv PCR products were ligated to the IgG vector to allow for the expression of the scFv fused to the  $CH_{2,3}$  domains (Fc).

Lambda	EBNA	WT1	EBNA	WT1
HindIII	Clone	Clone	Clone	Clone
Marker	315	45	315	45
	Uncut	Uncut	Cut	Cut

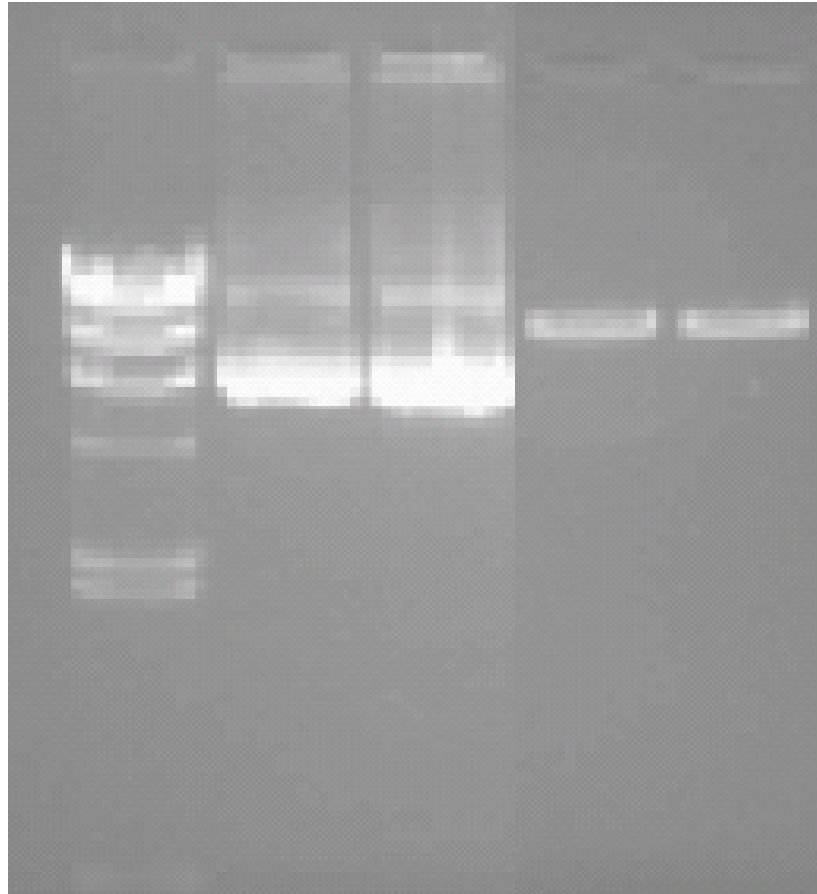


**Figure 15.** Validation and HindIII digestion of scFv-Fc fusion constructs. Along with sequence validation, the scFv-Fc plasmids were ran on a 1% agarose before (left) and after (right) HindIII digestion. Based on the lambda HindIII marker, it was determined that the bands after HindIII digestion were the correct sizes (~12,000 bp). HindIII digested DNA was subsequently used for electroporation into DG44 cells.



### *Expression and purification of soluble scFv-Fc*

DG44 supernatant containing the soluble scFv-Fc fusion protein was purified using the KappaSelect affinity chromatograph resin (GE Healthcare). First, 1.5 ml of KappaSelect resin was loaded onto a column and activated with 20 ml of PBS. The supernatant was loaded onto the column using a peristaltic pump at a flow rate of approximately 1 ml/min. The column was subsequently washed using 40 ml of PBS until the flow-thru registered an OD280 of less than 0.05. The scFv-Fc fusion protein was then eluted from the resin using 10 ml citrate buffer (pH 2.0) directly into 10 ml of 1 M Tris for neutralization. The eluted scFv-Fc was subsequently concentrated using a 50,000 MWCO Vivaspin centrifuge tube (Sartorius Stedim) and tested for its ability to bind to recombinant antigen using ELISA and the Biacore T100 (GE Healthcare) as well as natively presented peptide on the surface of T2 cells using flow cytometry.

*Monoclonal ELISA with bacterial phage clones, purified scFv and scFv-Fc*

Vinyl flat bottom microtiter plates (Thermo Fisher) were used for ELISA assays. Plates were initially coated overnight at 4°C with BSA-biotin (10 µg/ml; 50 µl/well). The next morning, the contents were discarded and the plates incubated at RT with streptavidin (10 µg/ml; 50 µl/well) for 1 hour. The contents were discarded and the plates incubated with recombinant biotinylated HLA-A2-peptide complexes (5 µg/ml; 50 µl/well) at RT for 1 hour. The plates were then incubated with 2% Milk (150 µl/well) at RT for 1 hour. After blocking, the plates were washed 2 times with PBS and then incubated with bacterial supernatant from their respective HB2151 culture plate wells, purified scFv, or purified scFv-Fc at RT for 1 hour. The contents were discarded, the plates washed 5 times with PBS, and then incubated at RT for 1 hour with either a mouse-anti-myc tag antibody (Clone 9E10; Sigma Aldrich. 0.5 µg/ml; 100 µl/well in 0.5% Milk) to detect the scFv or a goat-anti-human-HRP (Jackson Immunoresearch Laboratories. 0.5 µg/ml; 100 µl/well in 0.5% Milk) to detect the scFv-Fc. The contents were discarded, the plates washed 5 times with PBS, and those receiving the scFv were further incubated with a goat-anti-mouse-HRP (Jackson Immunoresearch Laboratories. 0.5 µg/ml; 100 µl/well in 0.5% Milk) at RT for 1 hour while the plates receiving the scFv-Fc were developed using o-phenylenediamine (OPD) buffer (150 µl/well), which was made by combining 20 mg of OPD tablets in 40 ml of citrate phosphate buffer with 40 µl 30% hydrogen peroxide. The color reaction was stopped by adding 30 µl of 5N sulfuric acid to each well and the plates read using the Dynex MRX ELISA plate reader at 490 nm. Lastly, the contents of the scFv plates were discarded, the plates washed 5 times with PBS, and developed according to the method above.

### *Cell lines and peptides*

Tap-deficient HLA-A2<sup>+</sup> T2 cells, 6268A, GKO, (both HLA-A2<sup>-</sup>), DIMT, LUY and JG19 (all three are HLA-A2<sup>+</sup>) B-cell lymphoblastic cell lines (BLCLs) were used for antigen presentation studies. 697 and OVCAR-3 cells were also used for WT1-related killing studies. Cells were normally cultured in RPMI 1640 + 10% Fetal Bovine Serum (FBS). For antigen presentation, T2 cells were harvested and transferred to serum-free IMDM + 10-20  $\mu\text{g/ml}$   $\beta_2\text{M}$ . The T2 cells would then be incubated with 20-40  $\mu\text{M}$  or less of RMFPNAPYL, LLDFVRFMGV or any number of irrelevant peptides at 37°C for 3-5 hours. Studies with BLCLs were done in the same manner as with T2 cells with the occlusion of  $\beta_2\text{M}$  in the media. The Pulse-Chase experiment with DIMT BLCLs was done by first incubating the BLCLs in serum-free IMDM with 20  $\mu\text{M}$  LLDFVRFMGV for 5 hours at 37°C. The cells were then washed with fresh RPMI 1640 + 10% FBS, transferred back into this culture medium and cultured further at 37°C for 5 and 24 hours, followed by flow cytometric analysis at each time point using EBNA Clone 315 scFv.

*Binding kinetics using surface plasmon resonance*

Kinetic measurements were performed by surface plasmon resonance using the BIAcore T100 (GE Biosciences). Briefly, the first two flow cells of a CM5 chip (GE Biosciences) were activated using the standard amine coupling reagents in HBS-EP running buffer (0.01 M HEPES, 0.15 M NaCl, 3 mM EDTA, 0.005% Tween 20) with flow cell 2 immobilized with the purified EBNA Clone 315 scFv-Fc fusion protein using 10 mM Acetate (pH 5). Subsequently, the target HLA-A2-peptide monomer (222 nM-13.875 nM) was injected over both the 1st (reference) and 2nd flow cells at 20  $\mu$ l/min. for 120 sec., followed by the addition of running buffer for an extra 180 sec. Kinetics values were determined using the BIAcore T100 Evaluation Software 2.0 and 1:1 binding model (local Rmax).

### *Flow cytometry*

Peptide-pulsed and unpulsed cells were transferred to plastic polystyrene round-bottom tubes (Becton Dickinson Labware) and washed with PBS. The cells were subsequently incubated with 5 µg of either targeted or non-specific purified scFv or scFv-Fc on ice for 40 min. The cells were washed with PBS and then incubated with 1 µg of biotinylated mouse-anti-myc antibody (Clone 9E10; Sigma Aldrich) to target the scFv or PE-conjugated goat-anti-human IgG Fc-specific (Jackson Immunoresearch Laboratories) on ice for 30 min. The cells were washed with PBS and then the scFv-treated cells incubated with streptavidin-PE (BD Biosciences) on ice for 20 min. Lastly, the cells were washed once more with PBS and analyzed on the BD FACS Calibur.

For CD107a cytotoxicity assays, transduced-NK92MI cells and target T2 cells or BLCLs were cocultured in a 1:1 effector:target (E:T) ratio ( $2.5-5.0 \times 10^5$  cells each) in 200 µl complete Alpha Essential medium (12.5% horse serum and 12.5% FBS) (Invitrogen) + 10-15 µl anti-CD107a-PE at 37°C for 5 Hours. The cell mixture was then washed with PBS and analyzed on the BD FACS Caliber.

For FACS sorting experiments, retrovirally-transduced NK92MI cells were sorted based on GFP intensity using the BD Aria Flow Cytometer under the guidance of the MSKCC Flow Cytometry facility.

*Quantitation of HLA-A2-LLDFVRFMGV complexes on peptide-pulsed T2 cells*

For MHC-peptide complex quantitation, the EBNA Clone 315 scFv-Fc was first directly conjugated to Alexa Fluor 647 using the APEX Alexa Fluor 647 Antibody Labeling Kit (Invitrogen). The kit yields about 10-20 µg of labeled antibody.

For quantitation, the Quantum Simply Cellular anti-Human IgG kit was used (Bangs Laboratories) along with the technical assistance of Hong-fen Guo in our laboratory. Briefly, the kit is comprised of five microsphere populations; one blank and four labeled with increasing amounts of anti-human IgG. The beads and the peptide pulsed T2 cells (37°C for 5 hours) were then labeled with the same fluorescently conjugated EBNA Clone 315 scFv-Fc on ice for 30 minutes. The cells were then washed with PBS and analyzed on the BD FACS Calibur along with the labeled beads. The Excel-based QuickCal analysis template that's provided with each kit aids in correlating fluorescence intensity with antigen density on the T2 cells. Each of the 4 data points are the average of duplicates.

### *Construction of the WT1 Clone 45 chimeric antigen receptor*

In order to generate a CAR specific for the HLA-A2-RMFPNAPYL complex, the WT1 Clone 45 scFv would typically be fused to intracellular signaling domains of immune-modulatory proteins found in immune effector cells. Through collaboration with Dr. Dario Campana at St. Jude Children's Hospital, we were able to obtain a CAR expression vector in which a CD19-specific scFv was fused to the CD8 $\alpha$  hinge/transmembrane region, 4-1BB (a tumor necrosis factor-receptor family member which has been shown to prevent activation-induced cell death, induction of T cell expansion, and enhanced T cell response (201, 202) and the CD3 $\zeta$  chain (one of five CD3 invariant polypeptide chains which play an important role in coupling antigen recognition to several intracellular signaling pathways) on the inside of the cell (154). In addition, due to an internal ribosome entry site (IRES; derived from the encephalomyocarditis virus (ECMV) (203) downstream of the CAR and directly upstream of the green fluorescence protein (GFP), both genes can be translated from a single bicistronic mRNA, allowing for direct correlation between fluorescence and CAR expression.

For our purpose, we wanted to replace the anti-CD19 scFv with our WT1 Clone 45 scFv. However, due to restriction enzyme incompatibility issues between the St. Jude CAR vector and our Tomlinson vector, we decided to have the entire CAR gene, containing the WT1 Clone 45 scFv, synthesized by Genescript. The resulting WT1 pUC57 vector contained the desired WT1 Clone 45 CAR sequence flanked by a CD8 $\alpha$  signal peptide at the N-terminus and a hinge region on the C-terminal side (pUC57 vector from Genescript; Piscataway, NJ) (Fig. 16A). Next, we digested the WT1 pUC57 vector and St. Jude CAR vector (Fig. 16B) using EcoRI (37°C for 2 hours) and XhoI (37°C for 2

hours). Afterwards, the digested and undigested plasmids were run on a 1% agarose gel along with the lambda HindIII and 100 bp markers (Fig. 17). The highlighted bands corresponded to the anticipated sizes of the St. Jude plasmid lacking the CAR sequence (~6500 bp) and the WT1 Clone 45 CAR sequence lacking the pUC57 plasmid (~1500 bp). These bands were excised from the gel, and after DNA purification, the two were ligated together and the ligation products transformed into NEB 5-alpha competent *E. coli* (New England Biolabs). The bacteria were then plated on TYE + Ampicilin (100 µg/ml), 8 colonies were picked and cultured in LB + Ampicilin (100 µg/ml) and their plasmids sequenced using the reverse primer 788A (5'-CCCTTGAACCTCCTCGTTCGACC-3') by the MSKCC Sequencing Core Facility. In addition, the plasmids were also digested with EcoRI and XhoI and ran on a 1% agarose gel along with lambda HindIII and 100 bp markers to validate their sizes (Fig. 18A). After demonstrating that both bands from each plasmid yielded their expected sizes, it was determined that the cloning was successful (Fig. 18B).



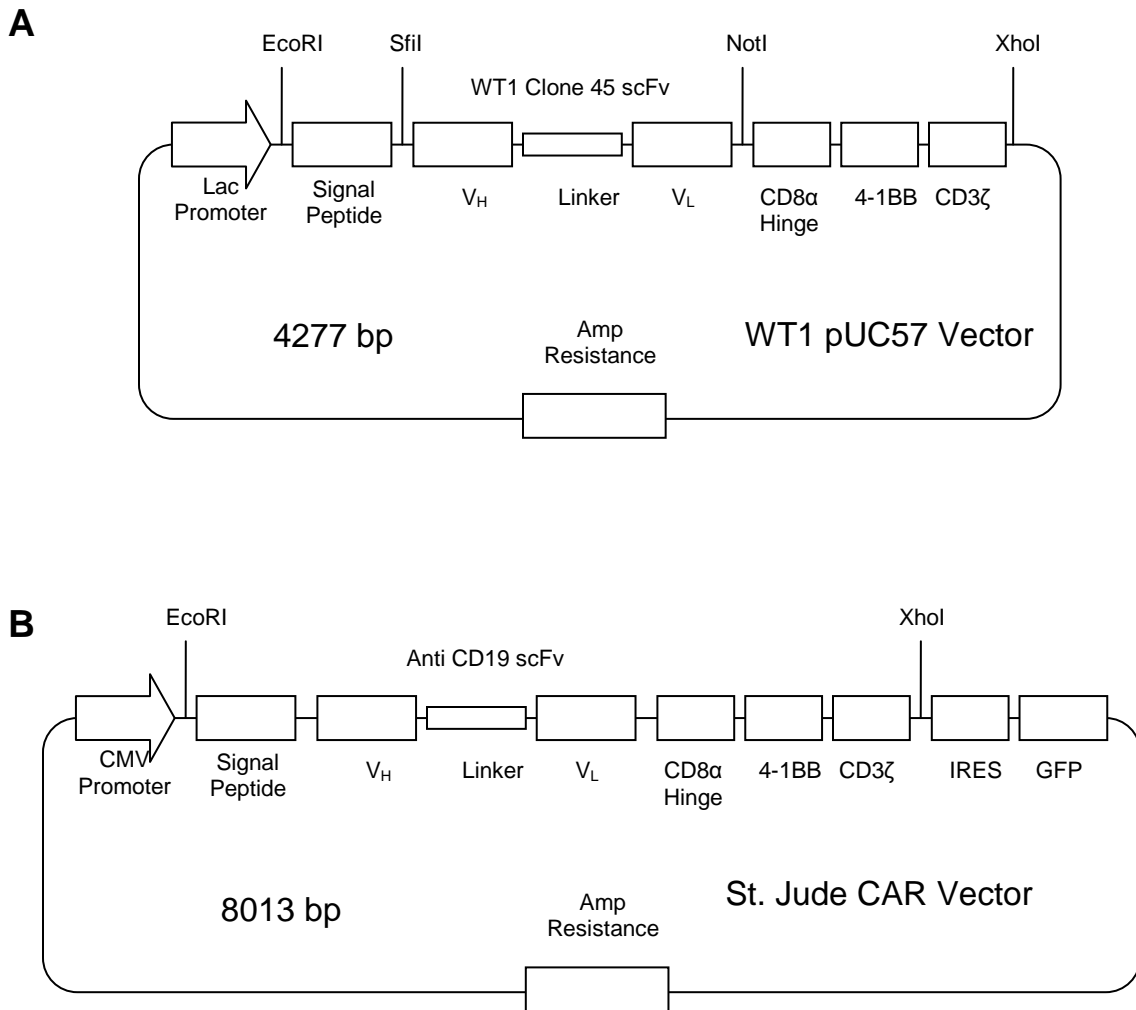


**Figure 16.** WT1 pUC57 and St. Jude CAR vectors.

*A.* The structure of the WT1 pUC57 vector (4277 bp). A gene containing a transmembrane signal peptide, WT1 Clone 45 scFv sequence, CD8 $\alpha$  hinge region, 4-1BB and CD3 $\zeta$  chain was ordered from Genescript and provided to us inside of this pUC57 vector. *B.* The St. Jude CAR vector (8013 bp) provided to us by the Campana laboratory has a similar structure to the pUC57 vector with the addition of an IRES-GFP sequence directly downstream of the CAR gene. This allows for direct correlation between CAR expression and GFP fluorescence without the need for the two to be attached to each other. Both vectors also contained an ampicillin resistance gene.

Lambda HindIII Marker	100bp Marker	St. Jude CAR Vector Uncut	St. Jude CAR Vector Cut	WT1 pUC57 Vector Uncut	WT1 pUC57 Vector Cut
-----------------------------	-----------------	---------------------------------	-------------------------------	------------------------------	----------------------------

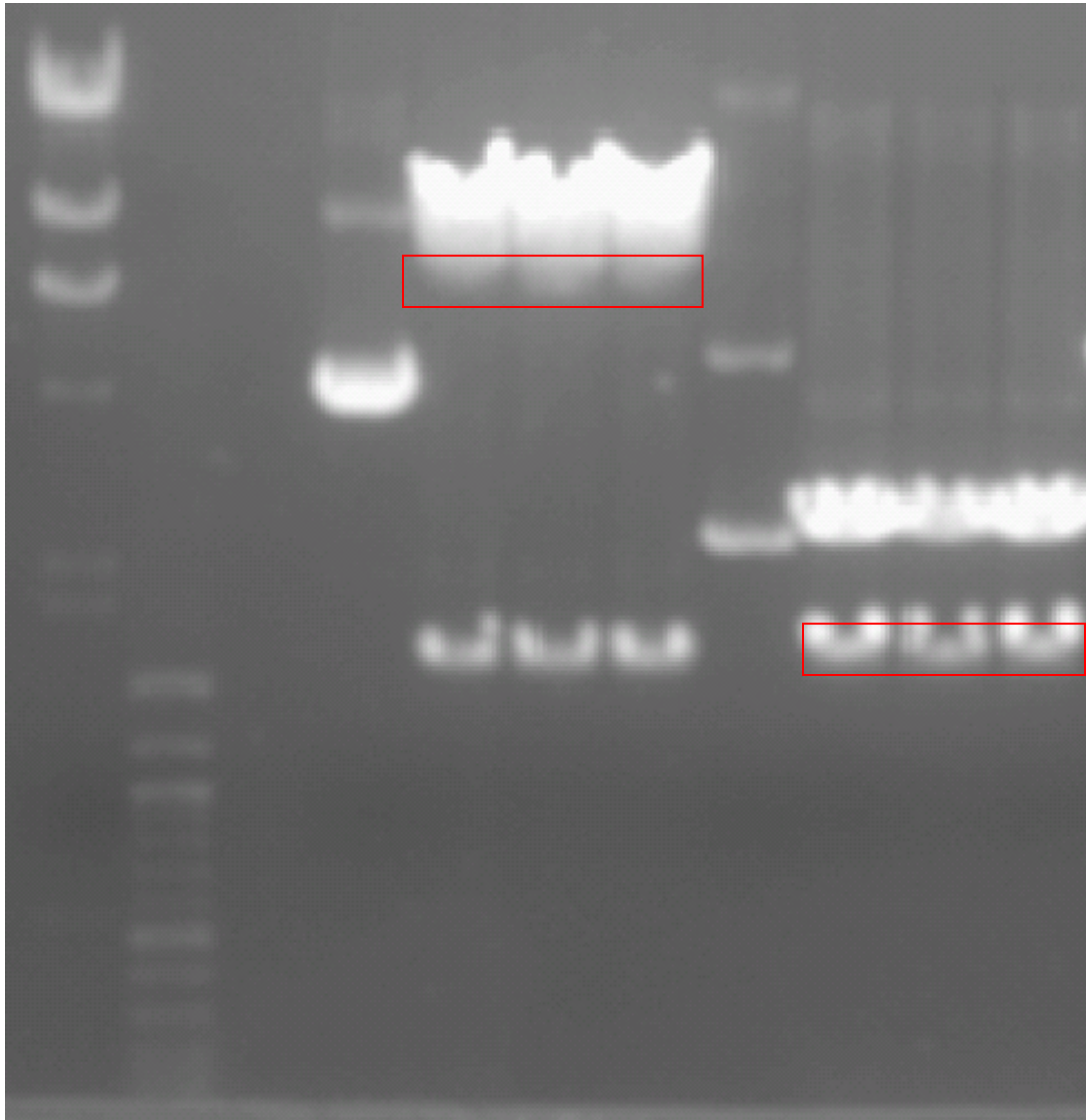


**Figure 17.** EcoRI and XhoI digestion of the WT1 pUC57 and St. Jude CAR vectors. Both the WT1 pUC57 and St. Jude CAR vectors were digested with EcoRI and XhoI and ran on a 1% agarose gel, along with undigested plasmid, a lambda HindIII marker and a 100 bp marker. As highlighted, the larger of the two bands (~6000 bp) was removed from the St. Jude CAR vector digestion while the smaller band (~1500 bp) was removed from the WT1 pUC57 digestion; these two bands were the sizes which were anticipated for the St. Jude vector and WT1 CAR insert. After purification, the vector and insert were ligated together.

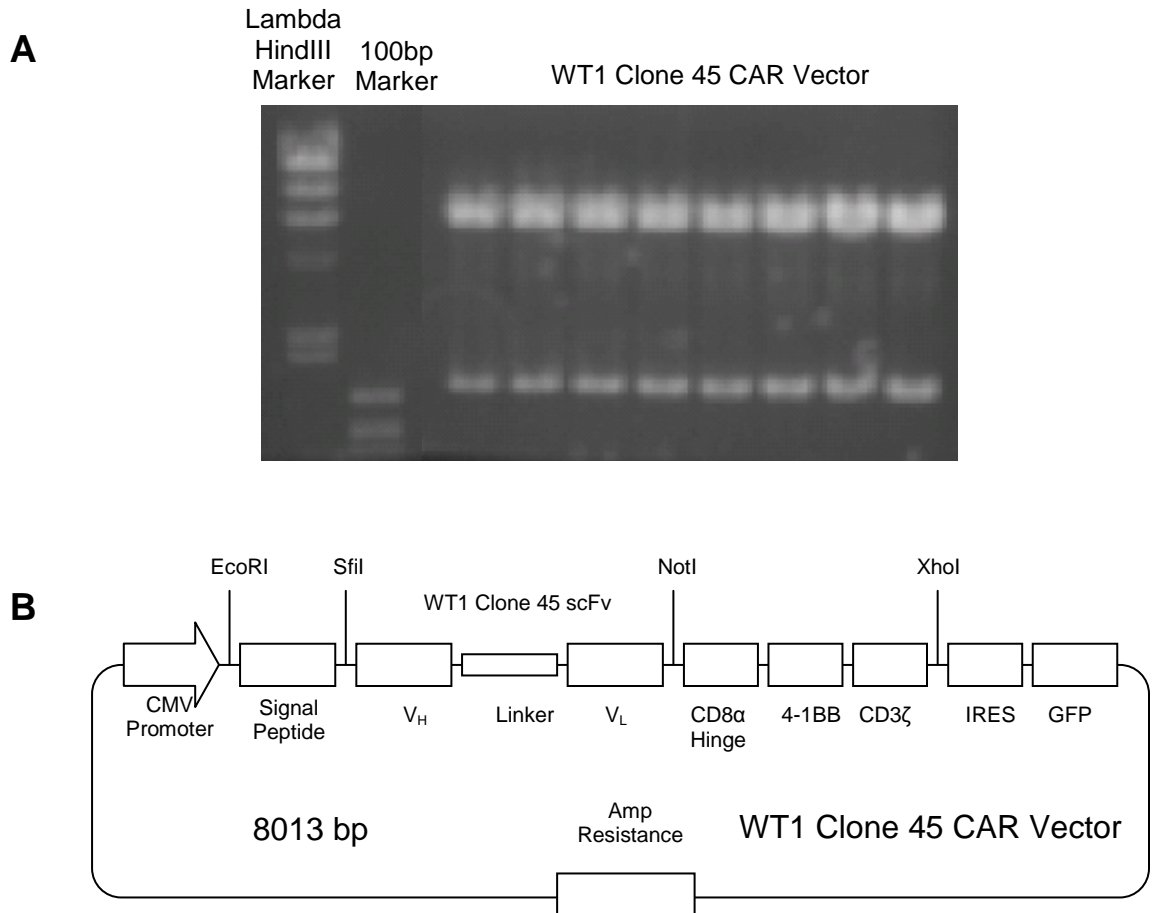


**Figure 18.** EcoRI and XhoI digestion validation of the WT1 Clone 45 CAR vector.

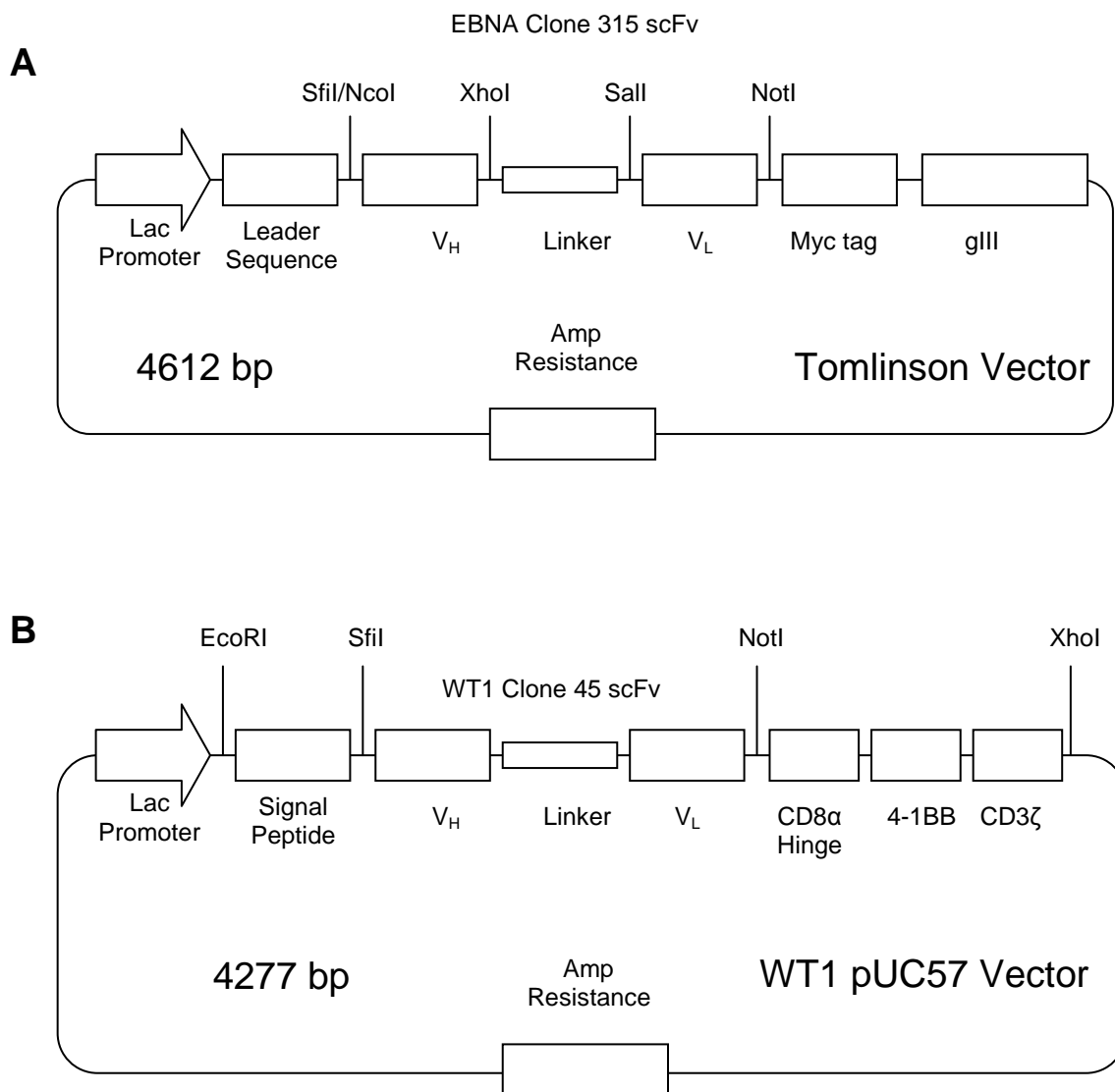
*A.* Along with sequence validation, plasmids isolated from 8 different bacterial colonies, after ligation, transformation and EcoRI and XhoI digestion, were run on a 1% agarose gel. Based on the lambda HindIII and 100 bp markers, it was determined that the bands were the correct size (~1500 bp and ~6000 bp). *B.* The structure of the resulting WT1 Clone 45 CAR vector has the same components as the original St. Jude CAR vector with the only difference being the scFv sequence.

### *Construction of the EBNA Clone 315 chimeric antigen receptor*

Since the WT1 Clone 45 CAR required us to purchase the WT1 pUC57 vector, additional restriction sites were added to this construct for greater ease when swapping different scFvs (Fig. 19B). As a result, the EBNA Clone 315 scFv sequence could directly be cloned out of the Tomlinson vector in which it was derived from (Fig. 19A).

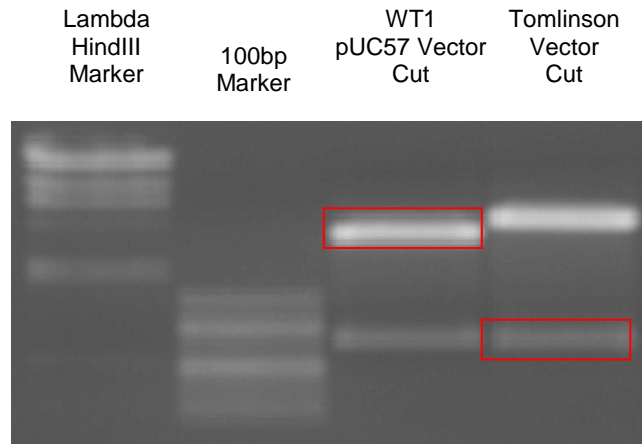
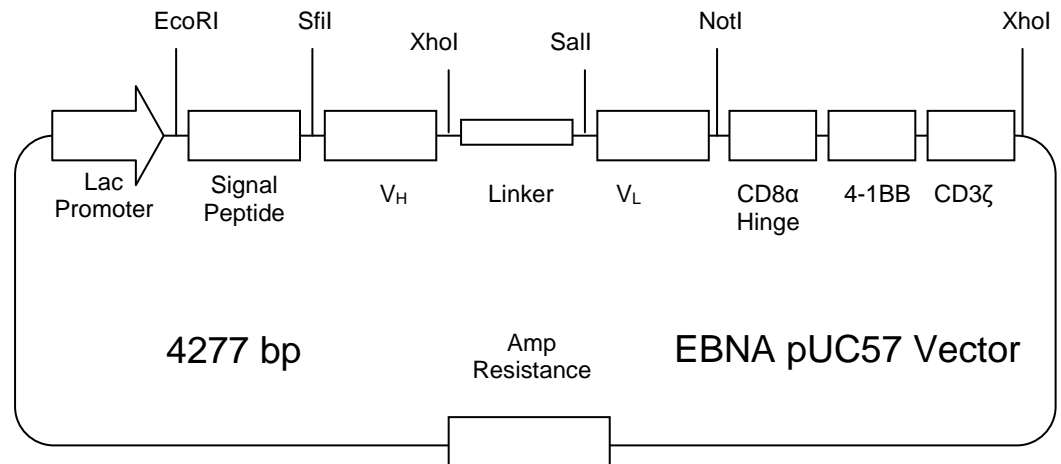
The first cloning step involved the removal of the WT1 Clone 45 scFv from the WT1 pUC57 vector using SfiI (50°C for 2 hours) and NotI (37°C for 2 hours). The same digestion was done to the Tomlinson vector containing the EBNA Clone 315 scFv sequence. Once digested, both plasmids were run on a 1% agarose gel along with lambda HindIII and 100 bp markers (Fig. 20A). The highlighted bands corresponded to the WT1 pUC57 vector without a scFv, and the EBNA Clone 315 scFv from the Tomlinson vector. These bands were excised from the gel and ligated together, resulting in a predicted structure illustrated in Figure 20B. After ligation, the product was transformed into *E. coli*, plated on TYE + Ampicilin (100 µg/ml), 10 colonies were picked, cultured overnight, their plasmids were purified, and each DNA digested with EcoRI alone or EcoRI and XhoI. As anticipated, due to an inherent XhoI site within every scFv sequence derived from the Tomlinson vector (with the exception of WT1 Clone 45 scFv in the context of pUC57 since the site was removed when purchased as a CAR from Genescript), the double digestion yielded three separate bands (Fig. 21). To overcome this issue, a partial digestion of the EBNA pUC57 vector using XhoI was necessary. The EBNA pUC57 plasmids isolated from the 10 colonies above were combined and digested with XhoI at room temperature for 1 minute. The reaction was quickly stopped by adding it to 4 separate wells of a 1% agarose gel and running the DNA along with uncut

plasmid, lambda HindIII and 100 bp markers (Fig. 22A). The highlighted bands were determined to be the expected size of the linearized EBNA pUC57 plasmid (~4300 bp); this linearized plasmid is a result of a random cut at either of the two XhoI sites. Subsequently, to obtain the complete CAR sequence (~1500 bp), the linearized plasmid was isolated from the gel and digested completely with EcoRI. The resulting double and single digests were run on a 1% agarose gel along with the lambda HindIII and 100 bp markers (Fig. 22B). The highlighted band corresponded to the anticipated size of the EBNA Clone 315 CAR gene, and as a result was excised from the gel, DNA purified, and ligated to the predigested (EcoRI and XhoI) St. Jude CAR vector. After insertion into the vector provided to us by the Campana laboratory, the ligation products were then transformed into *E.coli* as above, plated on TYE + Amplicilin (100 µg/ml), 10 colonies were picked and their plasmids sequenced using the reverse primer 788A (5'-CCCTTGAACCTCCTCGTTCGACC-3') at the MSKCC Sequencing Core Facility. Once the isolated plasmids were validated to contain the EBNA Clone 315 scFv sequence in the context of the CAR, the plasmids were digested with EcoRI and ran on a 1% agarose gel along with the lambda HindIII marker to validate their sizes (Fig. 23A). After demonstrating that the bands yielded the expected sizes, it was determined that the cloning was successful (Fig. 23B).



**Figure 19.** Tomlinson and WT1 pUC57 vectors.

*A.* The structure of the Tomlinson library vector (4612 bp). A beta-galactosidase promoter drives the expression of the EBNA Clone 315 scFv ( $V_H$  – 15 amino acid Glycine/Serine Linker –  $V_L$ ) fused to a myc-tag and gIII by ways of an amber codon. An ampicillin resistance gene is also present. *B.* The structure of the WT1 pUC57 vector (4277 bp). A gene containing a transmembrane signal peptide, WT1 Clone 45 scFv sequence, CD8 $\alpha$  hinge/transmembrane region, 4-1BB and CD3 $\zeta$  chain was ordered from Genescript and provided to us inside of this pUC57 vector. The vector also contained an ampicillin resistance gene.

**A****B**

**Figure 20.** SfiI and NotI digestion of the WT1 pUC57 and Tomlinson vectors.

Both the WT1 pUC57 and Tomlinson (containing the EBNA Clone 315 scFv) vectors were digested with SfiI and NotI and ran on a 1% agarose gel, along with a lambda HindIII marker and a 100 bp marker. As highlighted, the larger of the two bands (~3500 bp) was removed from the WT1 pUC57 digestion while the smaller band (~800 bp) was removed from the Tomlinson digestion; these two bands were the sizes which were anticipated for the WT1 pUC57 vector and EBNA Clone 315 scFv insert. After purification, the vector and insert were ligated together. *B.* The predicted structure of the resulting plasmid after the EBNA Clone 315 scFv was cloned into the pUC57 vector (EBNA pUC57).

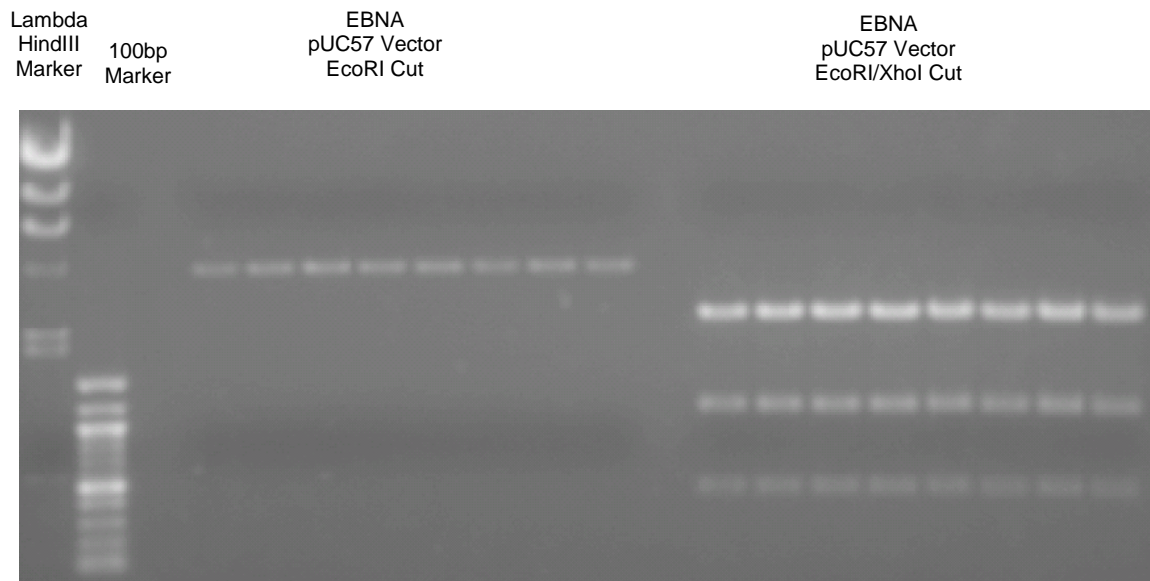


**Figure 21.** EcoRI and XhoI digestion validation of the EBNA pUC57 vector. After ligation and transformation, EBNA pUC57 plasmids isolated from 8 different bacterial colonies were digested with EcoRI alone (left) or EcoRI and XhoI together (right). The sizes of the bands were as anticipated based on the predicted structure of the EBNA pUC57 vector.



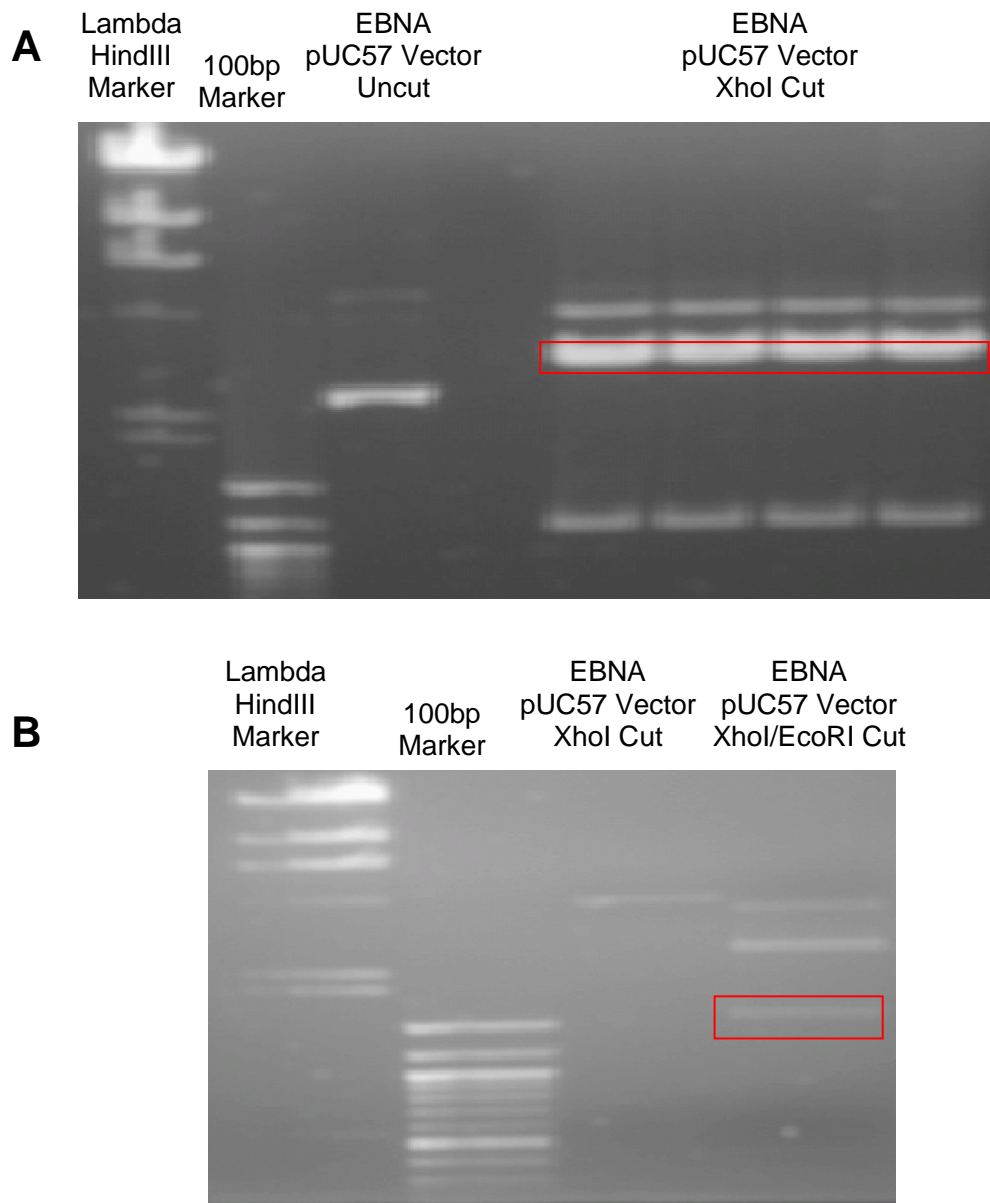


**Figure 22.** XhoI partial and EcoRI complete digestion of the EBNA pUC57 vector.

*A.* The EBNA pUC57 vector was digested at room temperature for 1 minute with XhoI and subsequently loaded onto 4 separate wells of a 1% agarose gel, along with the uncut vector, a lambda HindIII marker and 100 bp marker. The highlighted bands were excised from the gel since they were predicted to represent the linearized vector (~4200 bp). *B.* After the partially digested XhoI bands were isolated and DNA purified, it was then completely digested with EcoRI and loaded onto a 1% agarose gel along with some of the partially digested vector, a lambda HindIII marker and 100 bp marker. Since the partial digestion randomly cut at either of the two XhoI sites, the EcoRI digestion allowed us to resolve the correct XhoI digest by selecting for a DNA fragment which is around 1200 bp long (highlighted). This fragment was then excised from the gel, purified, and ligated to the pre-digested St. Jude CAR vector.

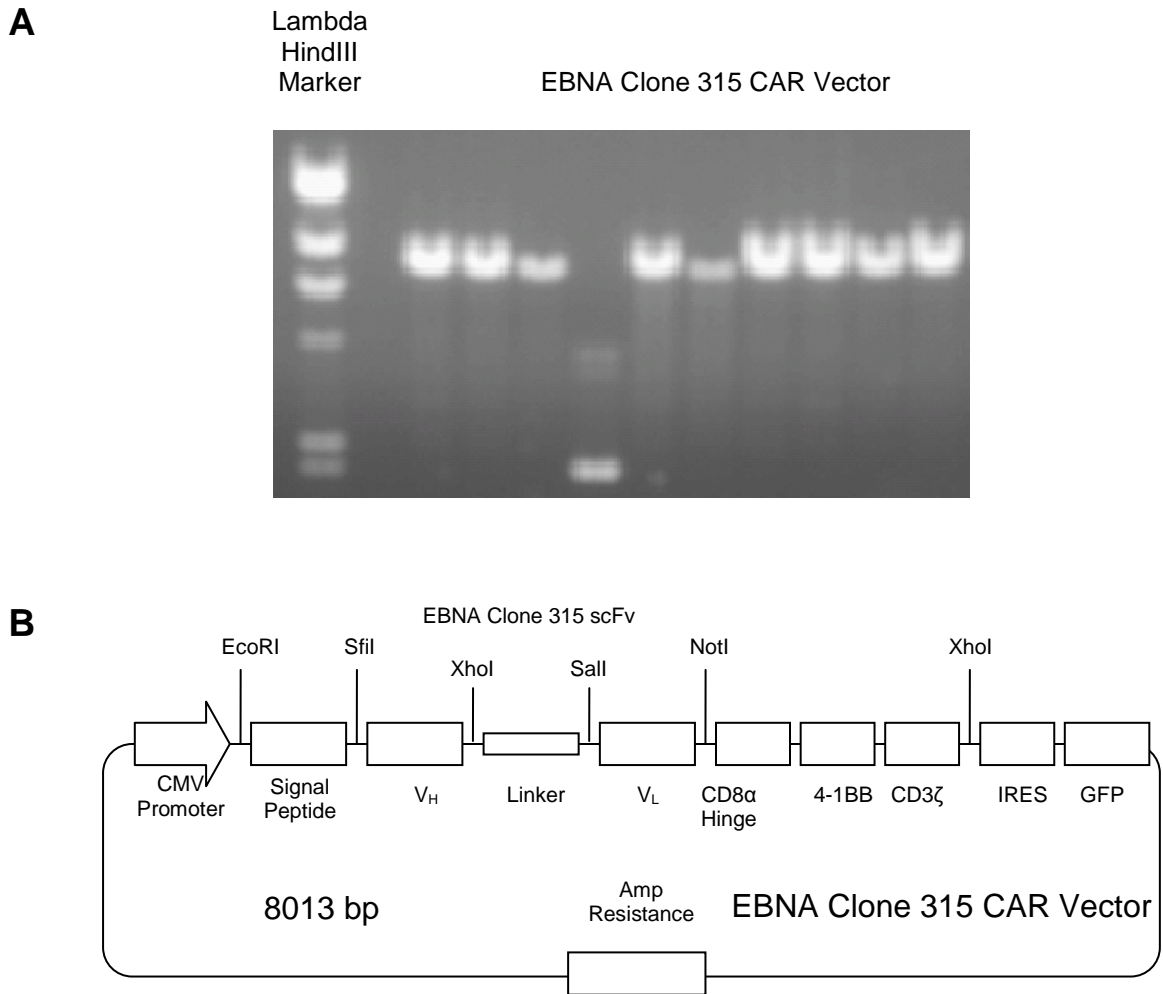


**Figure 23.** EcoRI digestion validation of the EBNA Clone 315 CAR vector.

*A.* Along with sequence validation, plasmids isolated from 10 different bacterial colonies, after ligation, transformation and EcoRI digestion, were run on a 1% agarose gel. Based on the lambda HindIII marker, it was determined that all but one of the bands were the correct size (~8000 bp). *B.* The structure of the resulting EBNA Clone 315 CAR vector has the same components of the original St. Jude CAR vector with the only difference being the scFv sequence.

*Retroviral production, DNA packaging, and infection of NK92MI cells*

To produce CAR-containing retrovirus, the following procedure was employed which used a 293T-based retroviral production cell line (GP2). Briefly, 7 µg of CAR DNA was combined with 3.5 µg of PCLAmpho helper construct and 3.5 µg pVSVg in 1 ml of serum-free DMEM. This mixture was then combined with 1 ml serum-free DMEM containing 36 µl of Lipofectamine 2000 (Invitrogen) and incubated at RT for 20 min. Afterwards, the DNA-Lipofectamine complex (2 ml) was mixed with GP2 cells ( $3-5 \times 10^6$ ) in 10 ml of DMEM + 10% FBS and cultured at 37°C for 72 hours. Subsequently, the supernatant (12 ml) was depleted of GP2 cells during recovery and incubated with 3 ml Lenti-X Concentrator solution (Clontech) at 4°C for 12-16 hours. Afterwards, the solution was centrifuged at 3000 rpm for 15 min., the supernatant discarded, and the pellet dissolved in 1 ml complete Alpha Essential medium containing  $5 \times 10^5$  NK92MI cells. The cells were then incubated for 72 hours and checked by flow cytometry for CAR expression via GFP (the CAR gene is expressed under a CMV promoter which is followed by IRES-GFP).

### *<sup>51</sup>Cr release cytotoxicity assay*

The capacity of CAR-equipped NK92MI cells to lyse target cells was evaluated using a <sup>51</sup>Chromium release assay. Peptide pulsed or unpulsed <sup>51</sup>Cr-labeled cells (100 µCi/sample in 50 µl at 37°C for 1 hour) were plated in round-bottom 96-well plates (5 x 10<sup>3</sup> cells/well) in RPMI 1640 with 10% FBS. Subsequently, CAR-equipped NK92MI cells were added to the labeled target cells at different effector (E)/target (T) ratios and incubated for 2-4 hours at 37°C, with or without blocking antibodies (scFv-Fc fusion proteins; 10-30 µg/ml. Anti-HLA-A2 and irrelevant IgG<sub>2b</sub> antibodies; 5-10 µg/ml), after which the cultures were depleted of cells and <sup>51</sup>Cr-release was measured in the supernatants.

The capacity of EBNA Clone 315 scFv-Fc to lyse peptide-pulsed target cells was also evaluated using a <sup>51</sup>Chromium release assay. LLDFVRFMGV-pulsed DIMT or LUY BLCL (20 µM at 37°C for 2-3 hours) were labeled with <sup>51</sup>Cr (100 µCi/sample in 50 µl at 37°C for 1 hour) and plated in round-bottom 96-well plates (5 X 10<sup>3</sup> cells/well) in RPMI 1640 with 10% FBS. Subsequently, CD16(V)-equipped NK92MI cells were added to the labeled target cells at different E:T ratios and incubated for 3-4 hours at 37°C with or without EBNA Clone 315 scFv or an irrelevant scFv at varying concentrations. Afterwards, the cultures were depleted of cells and <sup>51</sup>Cr-release was measured in the supernatants.

All E:T ratios were done in triplicate, with the average plotted on the graphs. Percent (%) <sup>51</sup>Cr Release was determined using the following formula: ((Sample Release – Spontaneous Release) / (Total Release – Spontaneous Release) x 100).

## CHAPTER 1

### *SELECTING HLA-A2-RESTRICTED, PEPTIDE-SPECIFIC MONOCLONAL ANTIBODIES USING PHAGE DISPLAY TECHNOLOGY*

#### *1.1 Introduction*

Recombinant antibodies against a variety of MHC-peptide complexes have been isolated over the past several decades. While hybridoma technology is still used by some groups since the turn of the century, the majority of these antibodies have been isolated using human phage display libraries. To date, the size of the human phage display libraries used for selection have been in the order of  $10^{10}$  in diversity, with the most common being an Fab library of  $3.7 \times 10^{10}$  (204). The majority of these libraries have been derived from the immune repertoires of non-immunized healthy donors, however there has been a report of a phage library derived from an HLA-A2 transgenic mouse which was immunized with a gp100-derived peptide on HLA-A2 (205); the resulting library was determined to have  $1 \times 10^8$  independent clones. Selections have typically been done on recombinant, biotinylated single-chain MHC-peptide complexes using a solution-phase biopanning approach without negative selection (25). Initial screening for TCR-like specificity is first done using an ELISA assay on recombinant MHC-peptide complexes. Subsequently, antigen presenting cells expressing the restricted HLA haplotype are incubated with the target peptide and the antibodies are then tested for their ability to stain the cells using flow cytometry or fluorescence microscopy.

In our study, we decided to use a commercially available naïve scFv human phage display library of relatively small diversity ( $\sim 3 \times 10^8$ ) (199) to select for antibodies with

TCR-like specificity against both viral and non-viral HLA-A2-peptide complexes using a solution-phase biopanning approach with an irrelevant HLA-A2-peptide complex for negative selection. We believe that antibody sequences which can recognize MHC-peptide complexes are relatively common in the human immune repertoire, and hypothesize that such antibodies can be recovered from non-immunized phage display libraries with 100 fold less diversity than what has been previously published.

## *1.2 Affinity selection of phage on virally-derived recombinant HLA-A2-peptide complexes*

Biotinylated and non-biotinylated recombinant HLA-A2-peptide complexes presenting various different peptides previously shown to bind to HLA-A2 were obtained from the MSKCC Tetramer Core Facility. For selection purposes, the Tomlinson I and J phage display libraries were combined and first preincubated with non-biotinylated, irrelevant HLA-A2-YVDPVITSI complex along with streptavidin paramagnetic beads so that any phage which expresses an antibody that may bind to the general framework of HLA-A2, or the streptavidin beads themselves, are eventually discarded during the washing steps. Subsequently, the contents (phage and irrelevant complex) were incubated with biotinylated HLA-A2-LLDFVRFMGV (EBNA3C) and biotinylated HLA-A2-NLVPMVATV (pp65) simultaneously in equimolar ratios and captured using streptavidin paramagnetic beads. Once the beads were bound to the biotinylated complexes, the beads were washed with PBS containing Tween 20 and the bound phage were eluted from the beads using trypsin. After two additional rounds of selection, the recovered phage were used to infect HB2151 *E. coli* and plated on ampicillin-containing agar. The next morning, individual colonies were picked, cultured overnight in 48-well culture plates, and their supernatants tested for the presence of scFv on 96-well ELISA plates pre-coated with recombinant HLA-A2-peptide complexes.

The first three rounds of selection resulted in a 55-fold increase in phage recovery, based on output/input ratio, and scFvs which only bound to the HLA-A2-EBNA3C complex (Table 4). These results were somewhat surprising since both of the peptides on HLA-A2 were derived from viral-related proteins, which are not seen in the

human protein repertoire. To confirm these findings, an additional round of selection was undertaken on just the HLA-A2-EBNA3C complex alone which resulted in a further amplification of recovered phage (109-fold) and a similar percentage of clones which bound to the HLA-A2-EBNA3C complex (83% positive after Round 3 and 77% after Round 4). During the screening processes, several different scFv were found to bind to the targeted HLA-A2-EBNA3C complex, however only a few scFv sequences resulted in absolute specificity and did not bind to HLA-A2-peptide complexes of different origins (Fig. 24A). Of those clones which were tested, EBNA Clones 315 and 327 had the same peptide sequence and were further characterized. After scFv purification, a subsequent validation ELISA demonstrates that EBNA Clone 315 maintained its specificity towards the targeted HLA-A2-EBNA complex, in addition to failing to bind to the LLDFVRFMGV peptide by itself (Fig. 24B). These initial binding assays demonstrate the TCR-like binding ability of this antibody.



**Table 4.** Phage display selection results on recombinant HLA-A2-LLDFVRFMGV and HLA-A2-NLVPMVATV complexes.

	<b>Round 1*</b>	<b>Round 2*</b>	<b>Round 3*</b>	<b>Round 4**</b>
Input	$7.5 \times 10^{12}$	$4.9 \times 10^{12}$	$2.4 \times 10^{12}$	$1.8 \times 10^{12}$
Output	$4.7 \times 10^6$	$6 \times 10^6$	$8.4 \times 10^7$	$1.25 \times 10^8$
Output/Input	$6.3 \times 10^{-7}$	$1.22 \times 10^{-6}$	$3.5 \times 10^{-5}$	$6.9 \times 10^{-5}$
Fold Enrichment (From Rd 1)	—	2	55.5	109.5
HLA-A2-EBNA3C Peptide-Specific Clones***	—	—	40/48 (83%)	37/48 (77%)
HLA-A2-pp65 Peptide-Specific Clones***	—	—	0/48 (0%)	0/48 (0%)

\* Rd 1-3: Panning against Biotinylated-HLA-A2-pp65 Peptide + Biotinylated-HLA-A2-EBNA Peptide

\*\* Rd 4: Panning against Biotinylated HLA-A2-EBNA3C Peptide Only

\*\*\* Relative signal at least 2-fold greater than background.

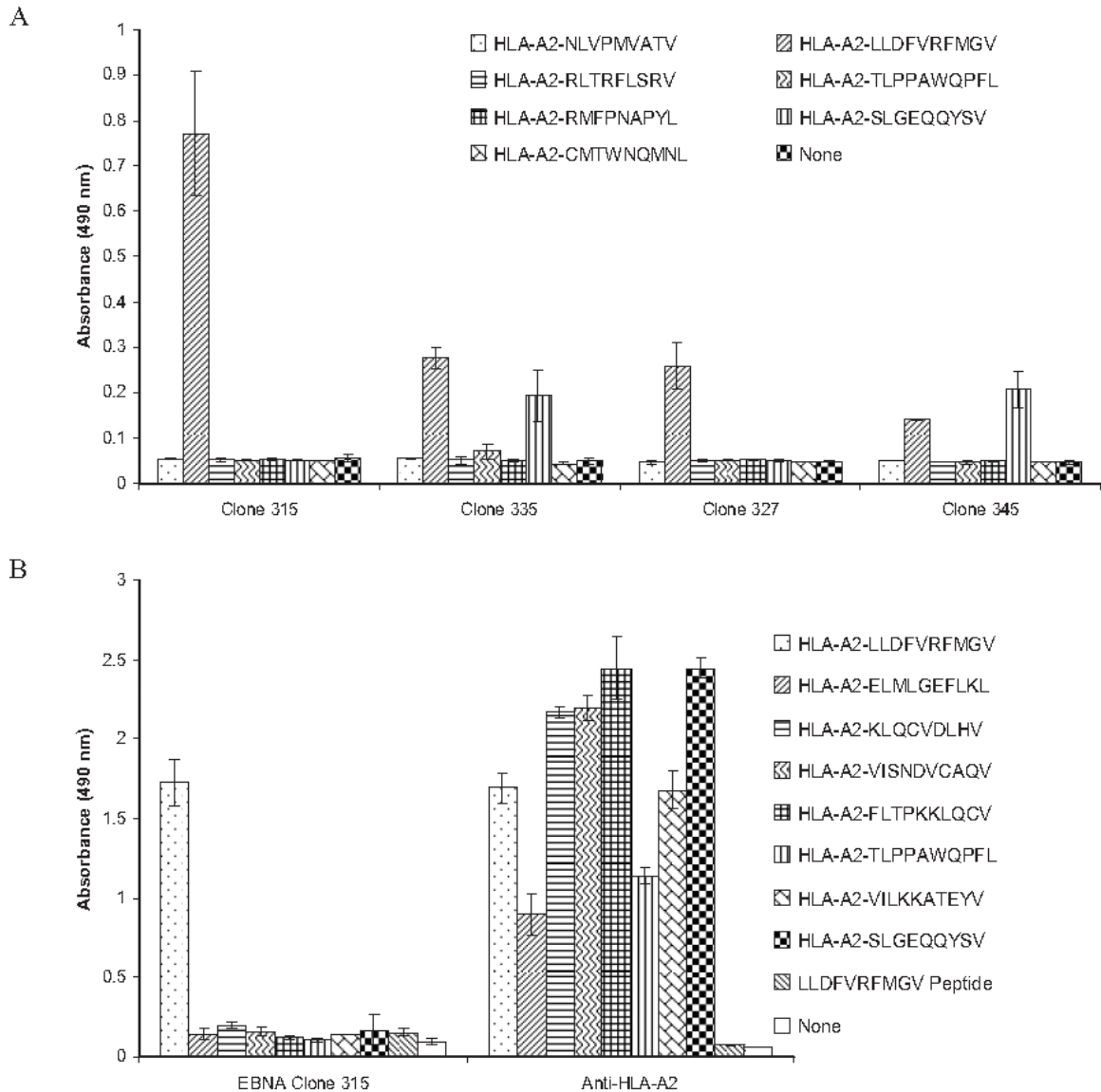


**Figure 24.** EBNA Clone 315 scFv is highly specific for the recombinant HLA-A2-LLDFVRFMGV complex.

**A.** Bacterial supernatant from individual clones after 3 rounds of phage selection were tested for binding to recombinant, biotinylated-HLA-A2-peptide complexes on vinyl microtiter plates. While several clones resulted in cross-reactivity to more than just the targeted HLA-A2-LLDFVRFMGV complex (Clones 335 and 345), Clones 315 and 327 were found to have the desired specificity. **B.** Purified EBNA Clone 315 scFv was retested against a similar panel of recombinant, biotinylated HLA-A2-peptide complexes. Purified EBNA Clone 315 scFv maintained its specificity over a panel of HLA-A2-peptide complex in addition to its inability to bind to the native peptide by itself. The anti-HLA-A2 antibody BB7.2 was included to demonstrate that all HLA-A2-peptide complexes are adherent and presented properly on the plate.

### *1.3 Affinity selection of phage on WT1-derived recombinant HLA-A2-peptide complex*

Antibody selection using phage against biotinylated HLA-A2-RMFPNAPYL (WT1-derived) was done in a similar manner to that which was described above. Briefly, the Tomlinson I and J phage display libraries were first combined and preincubated with non-biotinylated, irrelevant HLA-A2-NLVPMVATV complex and streptavidin paramagnetic beads. Subsequently, the contents (phage and irrelevant complex) were incubated with biotinylated HLA-A2-RMFPNAPYL and captured using fresh streptavidin paramagnetic beads. Once bound to the biotinylated complex, the beads were washed with PBS containing Tween 20 and the bound phage were eluted from the beads using trypsin. After two additional rounds of selection, the recovered phage were used to infect HB2151 *E. coli* and plated on ampicillin-containing agar. The next morning, individual colonies were picked, cultured overnight in 48-well culture plates, and their supernatants tested for the presence of scFv on 96-well ELISA plates pre-coated with recombinant HLA-A2-peptide complexes.

The first three rounds of selection resulted in a 90-fold enrichment in phage when comparing the output/input ratios (Table 5). After screening 48 clones for binding to the specific HLA-A2-RMFPNAPYL complex, three clones were found to bind specifically to their targeted complex but failed to bind to complexes which displayed an irrelevant peptide (Fig. 25A). Of the clones which were tested, all of them were found to have the same peptide sequence and WT1 Clone 45 was chosen for further characterization. After scFv purification, a subsequent validation ELISA demonstrates that WT1 Clone 45 maintained its specificity towards the targeted HLA-A2-WT1 complex, in addition to

failing to bind to the RMFPNAPYL peptide by itself (Fig. 25B). These initial binding assays demonstrate the TCR-like binding ability of this antibody.

**Table 5.** Phage display selection results on recombinant HLA-A2-RMFPNAPYL complex.

	<b>Round 1*</b>	<b>Round 2**</b>	<b>Round 3**</b>
Input	$3.7 \times 10^{12}$	$5.6 \times 10^{11}$	$1.55 \times 10^{11}$
Output	$4.0 \times 10^6$	$3.2 \times 10^6$	$1.52 \times 10^7$
Output/Input	$1.08 \times 10^{-6}$	$5.7 \times 10^{-6}$	$9.8 \times 10^{-5}$
Fold Enrichment (From Rd 1)	—	5.3	90.7
HLA-A2-RMFPNAPYL-Specific Clones***	—	—	3/48

\* Rd 1: Panning against 5  $\mu$ g Complex.

\*\* Rd 2-3: Panning against 2.5  $\mu$ g Complex.

\*\*\* Relative signal at least 3-fold greater than background (Irrelevant HLA-A2-Complex).

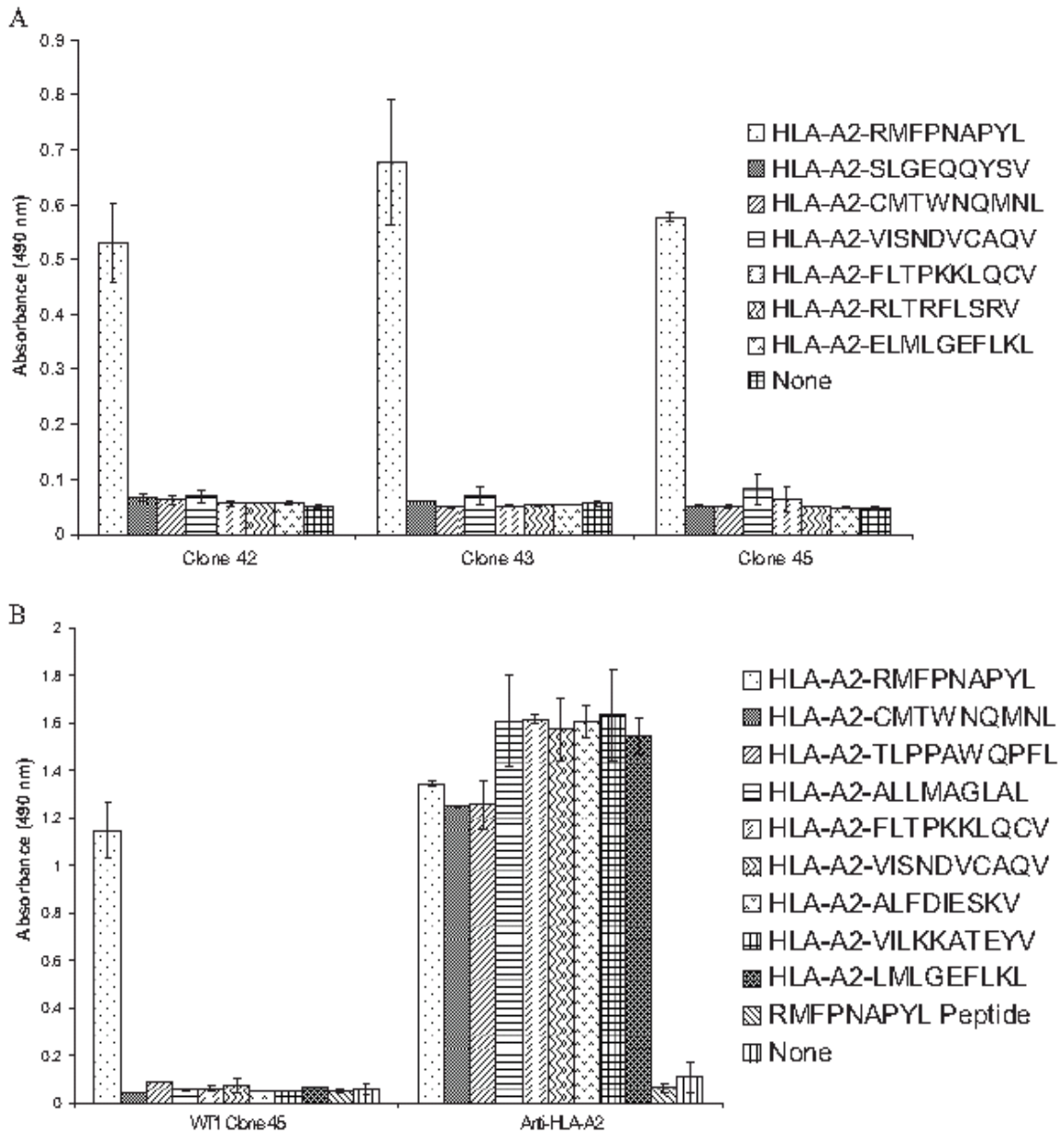


**Figure 25.** WT1 Clone 45 scFv is highly specific for the recombinant HLA-A2-RMFPNAPYL complex.

A. Bacterial supernatant from three individual clones after three rounds of phage selection were tested for binding to recombinant, biotinylated-HLA-A2-peptide complexes on vinyl microtiter plates. All three clones which were tested had the necessary specificity to only recognize the HLA-A2-RMFPNAPYL complex. It was discovered that all three clones had the same DNA sequence. B. Purified WT1 Clone 45 scFv was retested against a similar panel of recombinant, biotinylated HLA-A2-peptide complexes. Purified WT1 Clone 45 scFv maintained its specificity over a panel of HLA-A2-peptide complex in addition to its inability to bind to the native peptide outside of the context of MHC. The anti-HLA-A2 antibody BB7.2 was included to demonstrate that all HLA-A2-peptide complexes are adherent and presented properly on the plate.

#### *1.4 Binding kinetics and specificity of purified scFv (EBNA Clone 315 and WT1 Clone 45) on peptide-pulsed T2 cells*

To demonstrate that the isolated EBNA Clone 315 and WT1 Clone 45 scFvs are able to recognize and bind to their native complexes on the surface of peptide-pulsed antigen presenting cells (APCs), the TAP-deficient T2 cell line was used. T2 cells were first incubated for 5 hours at 37°C with either LLDFVRFMGV (EBNA3C-derived), RMFPNAPYL (WT1-derived) or irrelevant peptide KLQCVDLHV in serum-free medium containing  $\beta_2$ M. The cells were subsequently washed and stained with the purified WT1 Clone 45, EBNA Clone 315 or an irrelevant scFv. In addition, peptide pulsed and unpulsed T2 cells were also incubated with an anti-HLA-A2-FITC (BB7.2) antibody. This BB7.2 staining control was included due to previous studies which demonstrate that if a peptide is able to bind HLA-A2 on the T2 cell surface, the HLA-A2 molecule is stabilized, and the stabilization can be visualized by an increase in fluorescence intensity (206). As shown in Figure 26A, T2 cells which have been pulsed with either the LLDFVRFMGV or KLQCVDLHV peptides resulted in a fluorescence shift, consistent with their binding to the HLA-A2 pocket. However, EBNA Clone 315 was only able to stain T2 cells pulsed with its specific target peptide LLDFVRFMGV and not an irrelevant peptide (Fig. 26B). Similar results were obtained when T2 cells were pulsed with either the RMFPNAPYL or LLDFVRFMGV peptides and stained with WT1 Clone 45 scFv. While both peptides were able to stabilize the HLA-A2 molecule (Fig. 27A), WT1 Clone 45 scFv was only able to detect the T2 cells pulsed with the RMFPNAPYL peptide (Fig. 27B). This further validates their utility in detecting the native complex on the surface of cells.

Next, we became interested in the detection sensitivity of the EBNA Clone 315 scFv using flow cytometry. This data will become useful in the subsequent chapter of this thesis when we correlate sensitivity with antigen density using flow cytometric quantitative beads. By titrating down the amount of peptide used for incubation with the T2 cells, it was determined that concentrations as low as 78 nM were still able to produce a fluorescence signal above background when stained with EBNA Clone 315 scFv (Fig. 26C). With decreasing concentrations of peptide used for loading, there was a corresponding reduction in overall HLA-A2 intensity (data not shown) as one would expect.



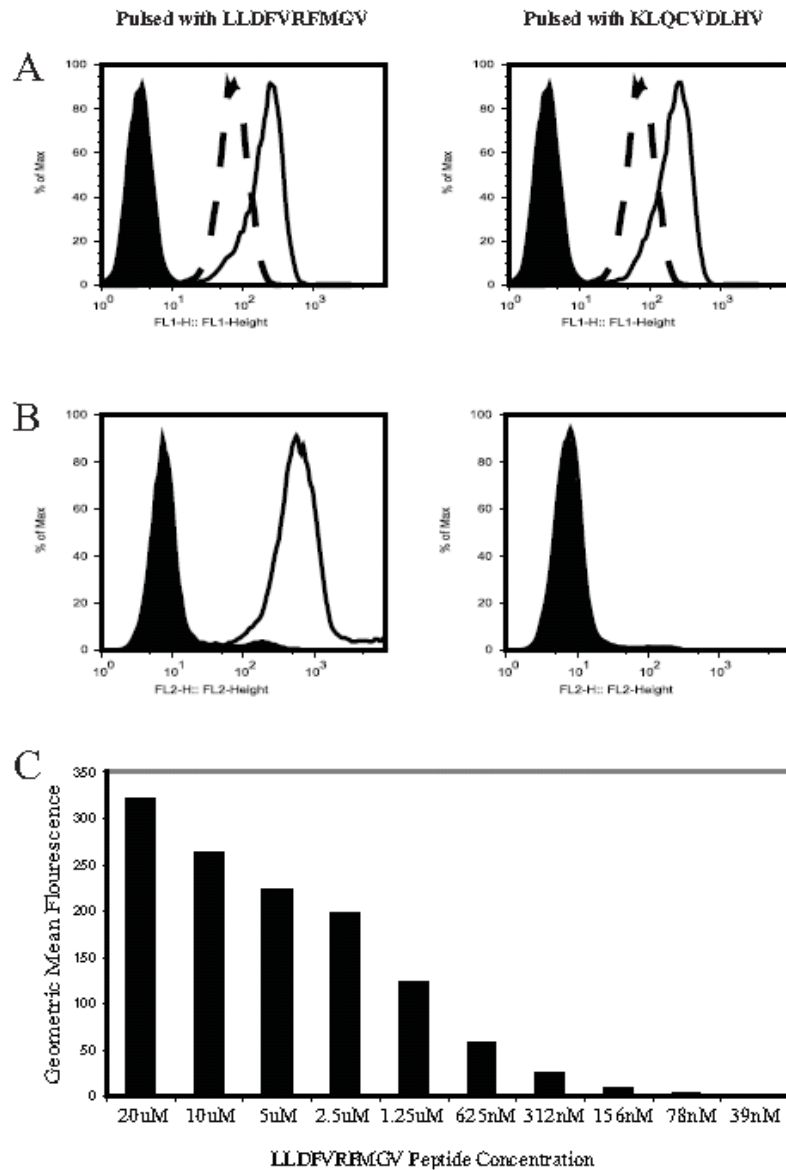


**Figure 26.** EBNA Clone 315 can recognize HLA-A2-LLDFVRFMGV on peptide-pulsed T2 cells.

A. TAP-deficient T2 cells were pulsed with (solid, unfilled lines) or without (dashed, unfilled lines) LLDFVRFMGV (left panel) or KLQCVDLHV peptides (right panel) at 20  $\mu$ M in serum-free IMDM media at 37°C for 5 hours. The cells were then stained with a mouse-anti-human HLA-A2-FITC conjugated antibody (unfilled lines) or a control mouse IgG<sub>1</sub>-FITC conjugated antibody (filled lines) and analyzed on the FACS machine. B. Peptide-pulsed T2 cells from A were stained with EBNA Clone 315 scFv (unfilled lines) or a control scFv (filled lines). Only T2 cells which had been pulsed with the LLDFVRFMGV peptide (left panel), but not ones which had been pulsed with KLQCVDLHV (right panel), could be stained by the EBNA Clone 315 scFv. C. T2 cells were incubated with decreasing concentrations of the LLDFVRFMGV peptide and subsequently stained with EBNA Clone 315 scFv as above.

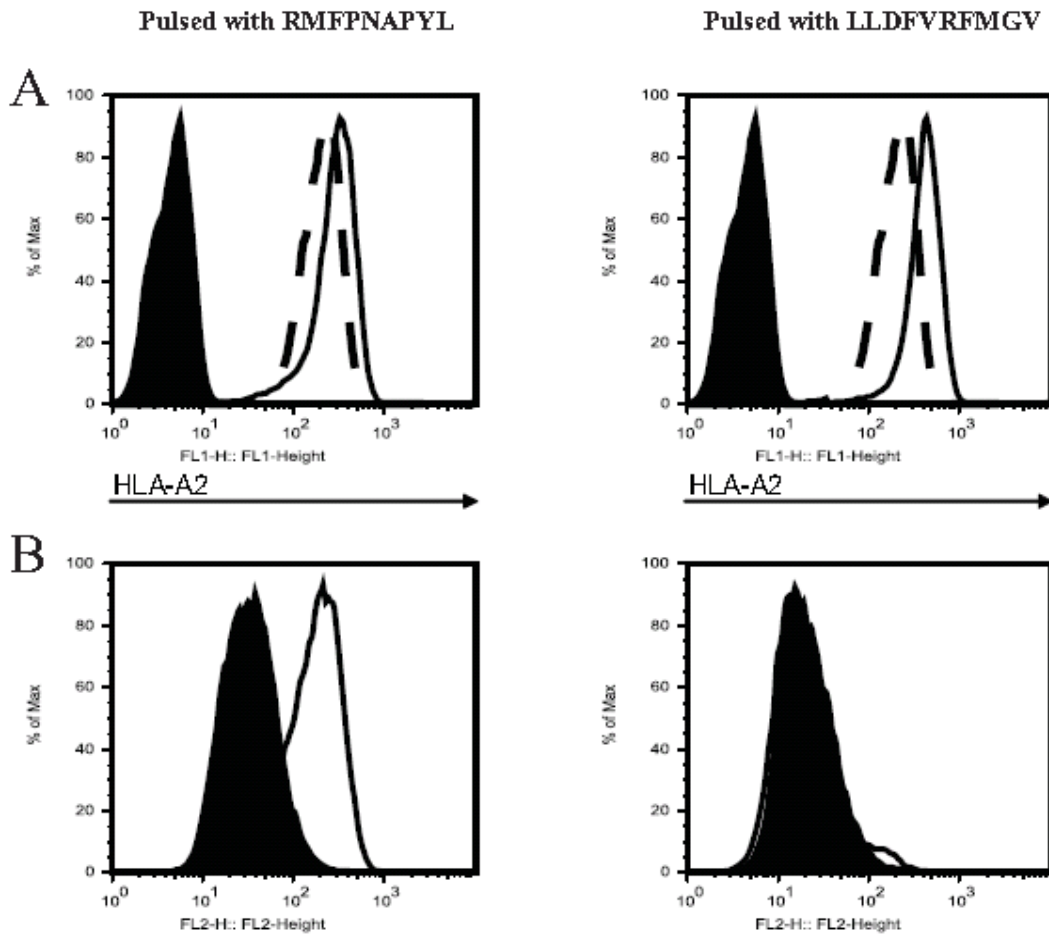


**Figure 27.** WT1 Clone 45 can recognize HLA-A2-RMFPNAPYL on peptide-pulsed T2 cells.

A. TAP-deficient T2 cells were pulsed with (solid, unfilled lines) or without (dashed, unfilled lines) RMFPNAPYL (left panel) or LLDFVRFMGV peptides (right panel) at 40  $\mu$ M in serum-free IMDM media at 37°C for 5 hours. The cells were then stained with a mouse-anti-human HLA-A2-FITC conjugated antibody (unfilled lines) or a control mouse IgG1-FITC conjugated antibody (filled lines) and analyzed on the FACS machine.

B. Peptide-pulsed T2 cells from A were stained with WT1 Clone 45 (unfilled lines) or a control scFv (filled lines). Only T2 cells which had been pulsed with the RMFPNAPYL peptide (left panel), but not ones which had been pulsed with LLDFVRFMGV (right panel), could be stained by the WT1 Clone 45.

*1.5 Demonstrating HLA restriction of the LLDFVRFMGV peptide and EBNA Clone 315 using peptide-pulsed BLCLs*

We next examined the expression of these peptides on BLCLs, especially since BLCLs are used routinely as APCs (207). Two BLCL lines were used, one HLA-A2<sup>+</sup> (DIMT) (Fig. 28A) and one HLA-A2<sup>-</sup> (6268A) (Fig. 28B). The BLCLs were incubated in serum-free IMDM media for 5 hours at 37°C with either the specific LLDFVRFMGV or irrelevant KLQCVDLHV peptides. When incubated with the specific peptide, only the HLA-A2<sup>+</sup> DIMT BLCL could be stained by EBNA Clone 315. Similarly to results seen with T2 cells, DIMT cells loaded with the irrelevant peptide, or 6268A loaded with the specific/irrelevant peptide, could not be stained with EBNA Clone 315. It is interesting to note that without peptide pulsing we were unsuccessful at staining DIMT. While our staining approach has been optimized to detect low levels of antigen through signal amplification involving secondary and tertiary reagents to detect the scFv, the amount of peptide that the cell naturally presents seems to be below our level of detection.

Subsequently, in an attempt to study the duration of peptide presentation on HLA-A2, a pulse-chase experiment was set up to monitor the levels of the HLA-A2-EBNA3C complex on DIMT cells over time. Initially, DIMT cells were incubated in serum-free IMDM media for 5 hours at 37°C with the LLDFVRFMGV peptide. Afterwards, the cells were washed twice with RPMI + 10% FBS and further cultured in this media for an additional 5 hours and 24 hours. At each of these three time points, cells were harvested and stained with either the purified EBNA Clone 315 scFv or an irrelevant scFv. The results show that after pulsing, the HLA-A2-EBNA3C complex could easily be detected

on the cell surface (Fig. 29). Furthermore, even after the cells were transferred to fresh media and cultured for an additional 5 and 24 hours, the MHC-peptide complex could still be detected, signifying that peptide-pulsed BLCLs are able to hold onto and present antigen for at least a day after the peptide had been removed from the media. This data further supports the use of autologous BLCLs in the generation of antigen specific T cells and the utility of TCE-specific antibodies like EBNA Clone 315 in precise visualization of TCE expression on APCs or target cells.

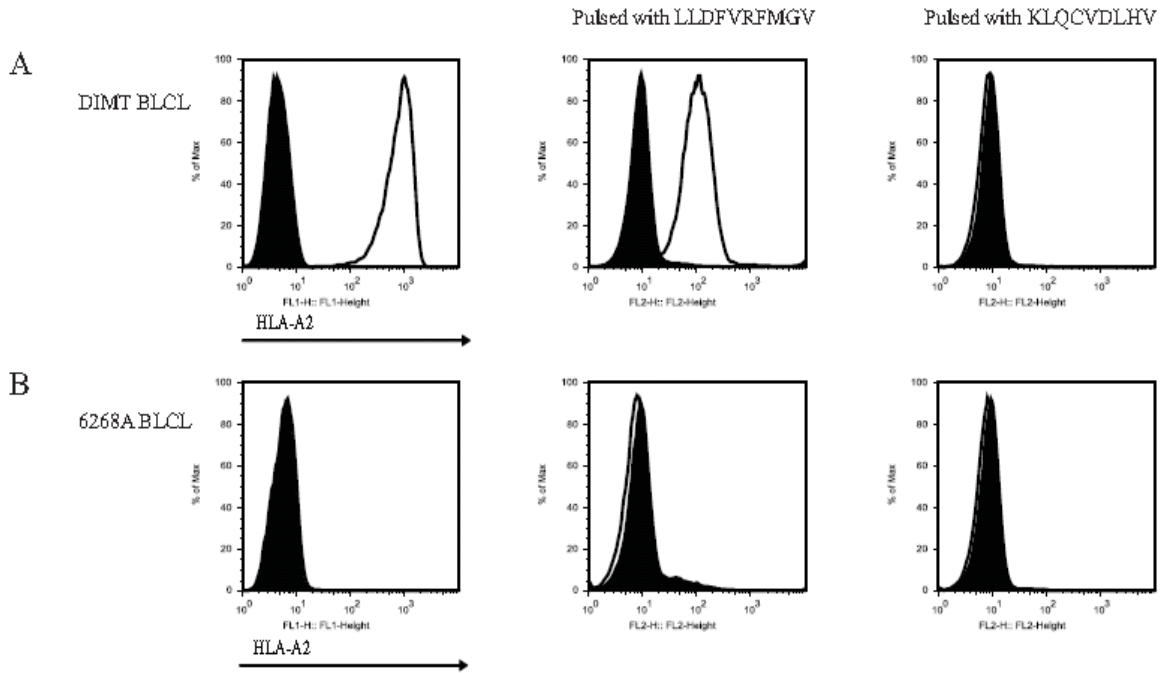


**Figure 28.** EBNA Clone 315 is LLDFVRFMGV peptide specific and HLA-A2-restricted.

*A and B.* In the left panels, DIMT (*A*) and 6268A (*B*) BLCLs were stained with an HLA-A2-FITC conjugated antibody (unfilled lines) or an isotype control (filled lines). The BLCLs were then incubated with LLDFVRFMGV (middle panel) or KLQCVDLHV peptides (right panel) with 20  $\mu$ M in serum-free IMDM media at 37°C or 5 hours. Subsequently, the peptide-pulsed BLCLs were stained with EBNA Clone 315 scFv (unfilled lines) or a control scFv (filled lines). Only the HLA-A2-positive DIMT BLCLs which had been pulsed with the LLDFVRFMGV peptide could be stained.

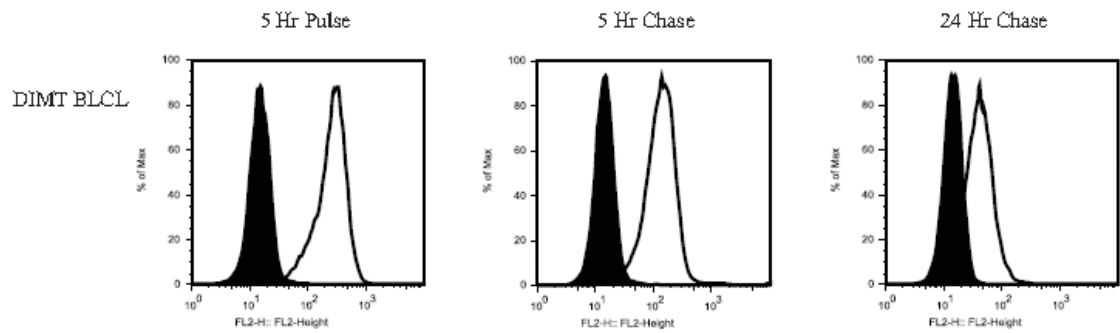


**Figure 29.** The HLA-A2-LLDFVRFMGV complex is stable on the cell surface. DIMIT BLCLs were incubated with LLDFVRFMGV at 20  $\mu$ M in serum-free IMDM media at 37°C for 5 hours (left panel), washed twice with RPMI + 10% FBS, and then further incubated for 5 hours (middle panel) or 24 hours (right panel) in fresh RPMI + 10% FBS. At each of these time points, the BLCLs were stained with EBNA Clone 315 scFv (unfilled lines) or an irrelevant scFv (filled lines). Incredibly, even 24 hours after removal from the medium, the BLCLs are still able to present a detectable amount of peptide.

## *1.6 Conclusions*

Traditionally, the MHC-peptide complex could only be recognized by a TCR, limiting our ability to detect an epitope of interest to a T cell-based readout assay. In this work, we demonstrate that monoclonal antibodies, in the form of scFvs, can be selected for using recombinant HLA-A2-peptide complexes after 3-4 rounds of selection by way of a human scFv phage display library. It is interesting to note that our library was relatively small (100-fold) compared to previously published reports which used far more diverse human naïve scFv and Fab libraries. Our scFvs demonstrated exquisite specificity, with EBNA Clone 315 and WT1 Clone 45 recognizing only the HLA-A2-LLDFVRFMGV and HLA-A2-RMFNPAPYL complexes, respectively. In addition, along with their inability to bind to HLA-A2 complexes which carried other peptides, the scFvs were also unable to bind to the free peptides themselves, further demonstrating their TCR-like specificity.

Next, the scFvs were tested for their ability to bind to peptide presented on the surface of HLA-A2-positive cells. After T2 cells and BLCLs were incubated in the presence of peptide, the cells could selectively recognize them using flow cytometry. In addition, in the case of LLDFVRFMGV, the complex which it formed with HLA-A2 could be detected on the surface of a BLCL even 24 hours after pulsing, further demonstrating the utility of these antibodies for the study of antigen presentation. As a result, we believe that these antibodies have potential implications in the field of vaccine development, as others have demonstrated before us.

## CHAPTER 2

### *GENERATING SCFV-FC FUSION PROTEINS FOR ANTIGEN QUANTITATION, AFFINITY DETERMINATION AND ANTIBODY-DEPENDENT CELL CYTOTOXICITY*

#### *2.1 Introduction*

Most antibodies in clinical development are full length IgGs (~150 kD). The main advantages of these immunoglobulins are their long serum half-lives (persisting in the patient for weeks depending on their specific IgG subclass) and their ability to induce ADCC and CDC. In the setting of TCR-like antibodies, the majority have been isolated using scFv and Fab phage display libraries; these fragments were subsequently engineered to act as toxin fusion proteins and/or chimeric antigen receptors. While the Fabs have proven useful in several settings, other groups have begun to isolate full length immunoglobulins and gone onto show that they are capable of inducing ADCC and/or CDC in cell lines which express the targeted MHC-peptide complex (38-40). In addition, these antibodies were also useful in quantifying antigen density on the surface of antigen presenting cells (29, 31, 33, 37, 38) and cancer cell lines (31, 36), with similar detection sensitivities when fluorescence was correlated with number of cell surface MHC-peptide complexes (100-400 complexes (29, 31, 33)).

In our study, we decided to go one step further and determine whether we can test ADCC using engineered scFvs. In addition, we hypothesized that scFv-Fc fusion proteins would allow us determine antibody affinity, study antigen presentation and gain a better understanding of antigen density. These fusion proteins allow for the conversion of monovalent scFvs into dimers, increasing the overall avidity and stability of our scFvs.



We believe the Fc portion will also allow us to directly conjugate the antibody to fluorescent dyes for antigen quantitation studies, immobilize the antibody for affinity measurements using surface plasmon resonance (SPR), and test for Fc-mediated cytotoxicity using CD16-expressing NK cells. To date, there has not been any documentation in which MHC-restricted, peptide-specific scFv-Fc fusion proteins have been engineered and tested for their ability to carry out the studies that we undertake in this work.

## *2.2 Binding kinetics and sensitivity of EBNA Clone 315 scFv-Fc on recombinant HLA-A2-peptide complex and peptide-pulsed T2 cells*

To further understand the affinity of the interaction between EBNA Clone 315 and the HLA-A2-EBNA3C complex, surface plasmon resonance was used to determine the binding kinetics between these two proteins. First, the EBNA Clone 315 scFv-Fc was constructed, expressed in DG44 CHO cells, purified, and its binding ability was tested using ELISA (Fig. 30A) along with flow cytometry via peptide-pulsed T2 cells at varying concentrations (Fig. 30B and C). These initial studies demonstrate that the antibody maintains its binding characteristics when expressed as a fusion protein. In addition, it is important to note that the flow cytometric sensitivity of the scFv and scFv-Fc were very comparable (20–200 nM), further highlighting the utility of the scFv as a monomeric binding fragment.

Next, using the Biacore T100 (GE Healthcare), a CM5 chip (flow cells 1 and 2) was initially activated for amine coupling based on manufacturer recommendation. The purified EBNA Clone 315 scFv-Fc was subsequently immobilized onto the second flow cell and the purified HLA-A2-EBNA3C complex passed over both flow cells as part of the soluble phase. After background subtraction (signal from flow cell 2 minus that of flow cell 1), the association rate ( $k_{on}$ ) and dissociation rate ( $k_{off}$ ) were determined ( $2.361 \times 10^5 \text{ M}^{-1}\text{s}^{-1}$  and  $6.891 \times 10^{-2} \text{ s}^{-1}$ , respectively), resulting in an overall  $K_D$  ( $k_{off}/k_{on}$ ) of 291 nM using a 1:1 binding model (Fig. 31); these kinetic rates were very similar to previously isolated Fabs against different MHC-peptide complexes (26, 35). Relative to published TCR:MHC Class I-peptide  $K_D$  measurements, which typically range in the neighborhood of 2-50  $\mu\text{M}$  (208), our scFv:MHC Class I-peptide interaction seems to be

at best 150-fold stronger, with the most significant improvement attributed to a slower  $k_{\text{off}}$ . Previous studies which support an affinity-based T cell activation model argue that a greater overall affinity or slower dissociation rate leads to higher interferon-gamma release and target cell lysis (209, 210).

Lastly, in an attempt to quantify the amount of HLA-A2-LLDFVRFMGV complex on the surface of peptide-pulsed T2 cells, we decided to use flow cytometric quantitation beads. This data will also be useful in determining the detection threshold of EBNA Clone 315 scFv and scFv-Fc. First, purified EBNA Clone 315 scFv-Fc was conjugated to a fluorescent label, Alexa Fluor 647, using a commercially available kit. Subsequently, T2 cells were pulsed with 20, 10, 5, or 0  $\mu\text{M}$  of LLDFVRFMGV peptide at 37°C for 5 hours. After pulsing, the peptide-pulsed T2 cells, along with beads containing known quantities of anti-human IgG<sub>1</sub> antibodies, were incubated with the fluorescently-labeled EBNA Clone 315 scFv-Fc. Once the cells and beads were analyzed on the FACS machine, the fluorescence intensities were correlated to each other, resulting in an estimation of the number of complexes on the surface of the T2 cells relative to the quantity of peptide used for pulsing. These four values (337,091 sites with 20  $\mu\text{M}$ , 149,688 sites with 10  $\mu\text{M}$ , 76,040 sites with 5  $\mu\text{M}$ , and no sites with 0  $\mu\text{M}$ ) were plotted on a graph and a trendline was used to create a standard curve ( $R^2 = 0.9948$ ) (Fig. 32A). Furthermore, when looking at the lower end of the spectrum, we have determined that an amount less than 40 nM of peptide will correspond to less than 100 complexes on the surface of the cell (Fig. 32B), placing the detection level of the EBNA Clone 315 scFv-Fc fusion within that range.

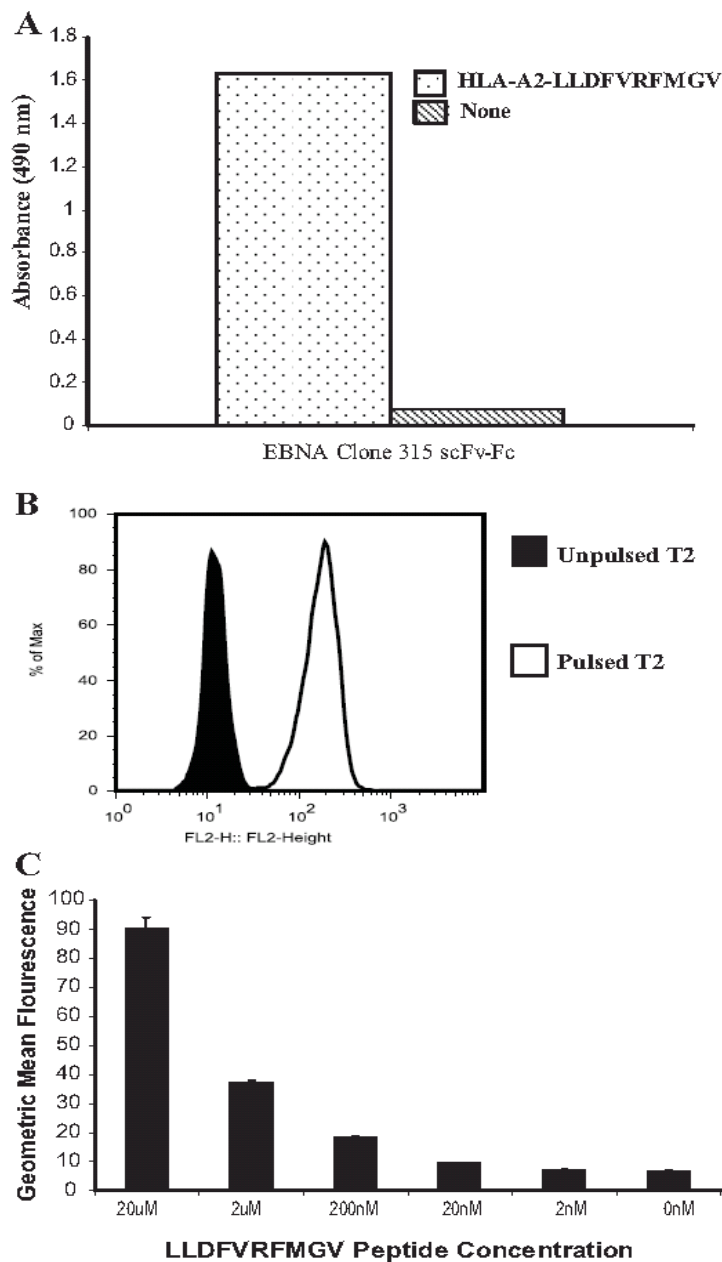
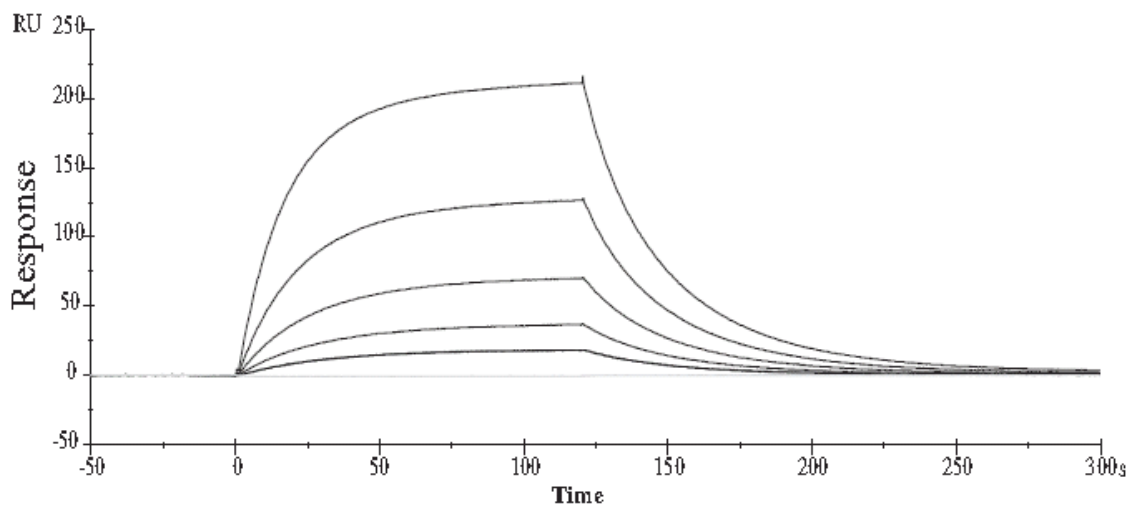


**Figure 30.** Binding studies using EBNA Clone 315 scFv-Fc.

A. Purified EBNA Clone 315 scFv-Fc was tested for binding on an ELISA plate coated with or without HLA-A2-LLDFVRFMGV. The scFv-Fc maintained its binding ability towards the recombinant complex. B. Purified EBNA Clone 315 scFv-Fc was tested for binding on T2 cells pulsed with or without the LLDFVRFMGV peptide (20  $\mu$ M) in serum-free IMDM media at 37°C for 5 hours. The scFv-Fc was only able to recognize peptide-pulsed T2 cells (unfilled lines). C. T2 cells were incubated with decreasing concentrations of the LLDFVRFMGV peptide in serum-free IMDM media at 37°C for 3 hours and subsequently stained with EBNA Clone 315 scFv-Fc as above. Based on geometric mean fluorescence, the lower limit of detection seems to be in the same range as the scFv (200 nM- 20 nM).



$$k_{\text{on}} (\text{M}^{-1} \text{s}^{-1}) = 2.361 \times 10^5 \quad k_{\text{off}} (\text{s}^{-1}) = 6.891 \times 10^{-2} \quad K_D (\text{nM}) = 291$$

**Figure 31.** Kinetics determination of EBNA Clone 315 to HLA-A2-LLDFVRFMGV. Affinity measurements were done using surface plasmon resonance by way of the Biacore T100 and a CM5 sensor chip. EBNA Clone 315 scFv-Fc was amine coupled to flow cell 2 using 10 mM Acetate (pH 5) while an empty flow cell 1 was used as a reference. Subsequently, different concentrations (222 nM – 13.875 nM) of the recombinant HLA-A2-LLDFVRFMGV complex were injected at 20  $\mu\text{l}/\text{min}$  over both the target and reference flow cells and the affinity determined using the Biacore T100 Evaluation Software Version 2.0. Affinity measurements were calculated using all 5 separate concentrations curves.

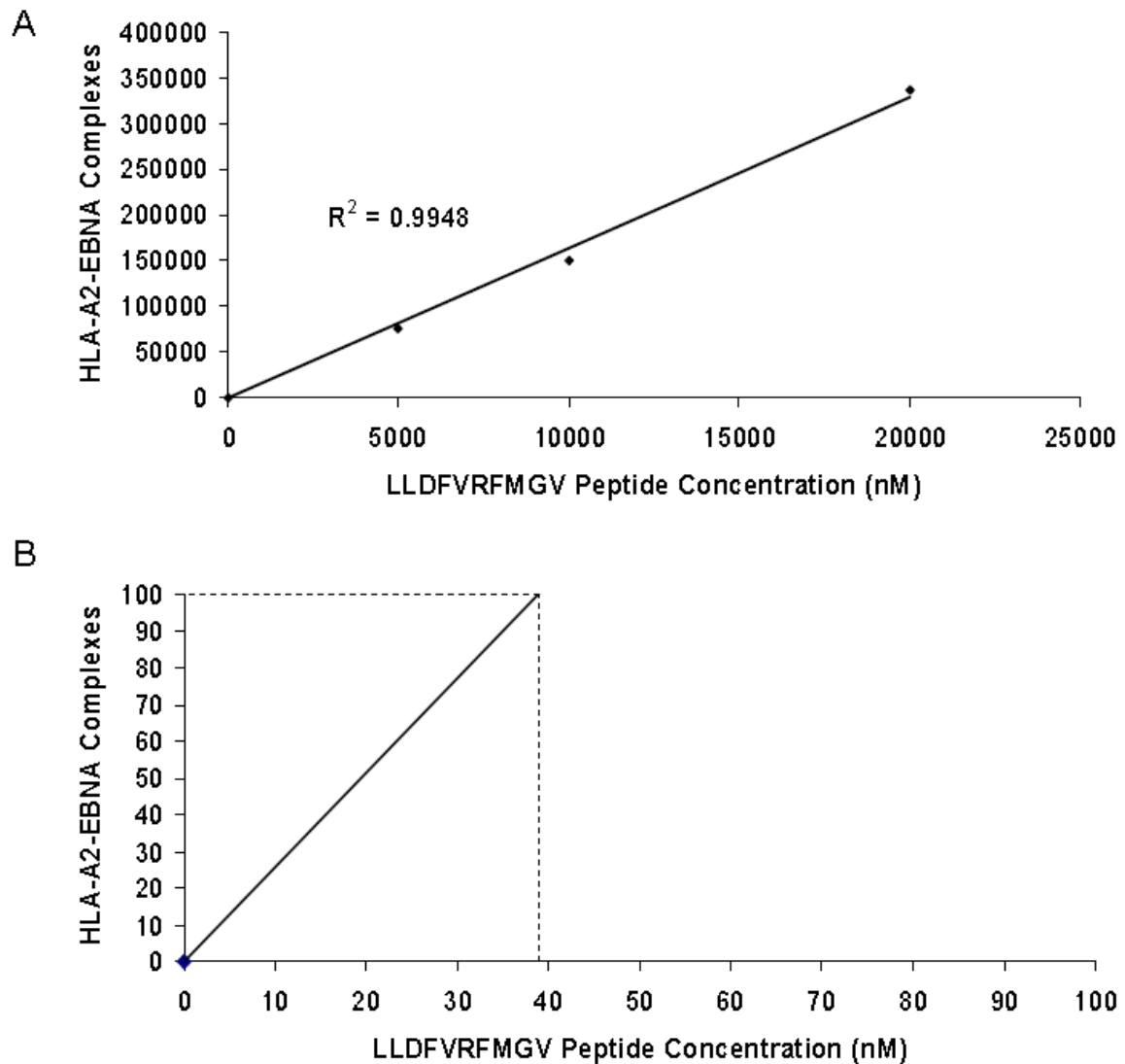


**Figure 32.** Quantitation of HLA-A2-LLDFVRFMGV complex on T2 cells.

*A.* Fluorescently-conjugated EBNA Clone 315 scFv-Fc was tested for binding on T2 cells pulsed with (20, 10, or 5  $\mu$ M) or without (0  $\mu$ M) the LLDFVRFMGV peptide in serum-free IMDM media at 37°C for 5 hours. The cells, in addition to beads containing known amounts of anti-human IgG<sub>1</sub> antibodies, were stained with the scFv-Fc and the cell's fluorescence intensity was correlated to that of the beads and their number of binding sites. Using these four peptide concentrations and corresponding number of complexes, a standard curve was created with an  $R^2$  value of 0.9948. *B.* A close-up view of the lower end of the peptide and complex spectrum allows for the determination of antigen detection threshold, with 40 nM of peptide resulting in the formation of approximately 100 complexes.

### *2.3 Binding and specificity studies of WT1 Clone 45 scFv-Fc on recombinant HLA-A2-peptide complex and peptide-pulsed cells*

In order to do further studies regarding the presentation of the RMFPNAPYL peptide on the surface of APCs, the WT1 Clone 45 scFv-Fc fusion protein was also constructed, expressed in DG44 CHO cells, purified, and validated for binding to its targeted recombinant HLA-A2-peptide complex (Fig. 33A). As was shown with the scFv, the fusion protein maintained its binding ability on the ELISA plate. Next, we decided to check and see if the scFv-Fc maintained its binding ability and specificity on peptide-pulsed T2 cells. T2 cells were pulsed with the RMFPNAPYL peptide or an irrelevant peptide in serum-free media with  $\beta_2M$  at 37°C for 5 hours. Using flow cytometry, the scFv-Fc was able to detect T2 cells which had been pulsed with the RMFPNAPYL peptide, but failed to recognize the cells pulsed with an irrelevant peptide (Fig. 33B). These two assays further validated that the fusion protein acts in the same way as the original scFv.

Subsequently, we decided to test whether the binding of the RMFPNAPYL peptide and scFv-Fc fusion protein were restricted to HLA-A2. HLA-A2<sup>+</sup> and HLA-A2<sup>-</sup> BLCLs (DIMIT and 6268A, respectively) were pulsed with the RMFPNAPYL peptide in serum-free media at 37°C for 5 hours. Similarly to EBNA Clone 315, the WT1 Clone 45 scFv-Fc fusion protein was only able to recognize the peptide pulsed DIMIT and not the HLA-A2<sup>-</sup> 6268A BLCL (Fig. 34). These results demonstrate that the RMFPNAPYL peptide is restricted to HLA-A2 and WT1 Clone 45 is only able to recognize it in the context of this complex.

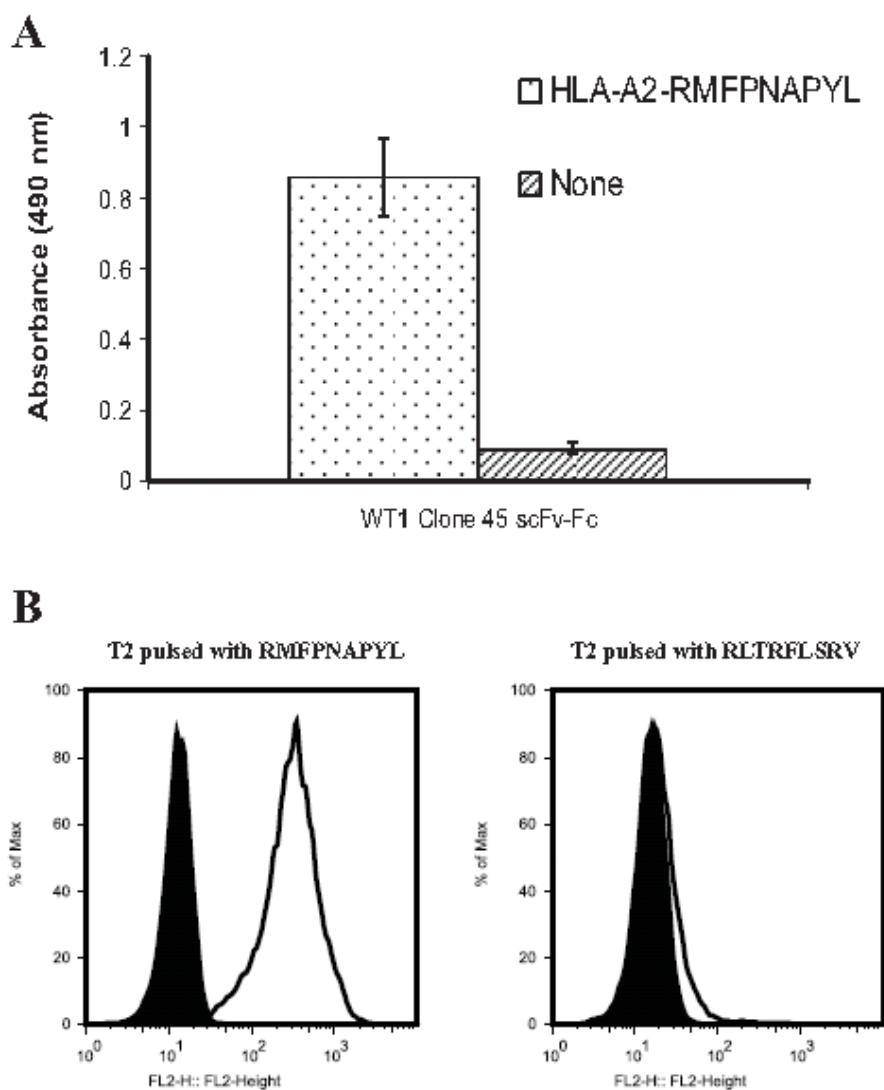


**Figure 33.** Binding and specificity studies of WT1 Clone 45 scFv-Fc.

*A.* Purified WT1 Clone 45 scFv-Fc was tested for binding on an ELISA plate coated with or without HLA-A2-RMFPNAPYL. The bound scFv-Fc was detected using a goat-anti-human-HRP-conjugated antibody. The scFv-Fc maintained its binding ability towards the recombinant complex. *B.* Purified WT1 Clone 45 scFv-Fc was tested for binding on T2 cells pulsed with the RMFPNAPYL or RLTRFLSRV peptide (40  $\mu$ M) in serum-free IMDM media at 37°C for 5 hours. The scFv-Fc (unfilled lines) was only able to recognize RMFPNAPYL-pulsed T2 cells.



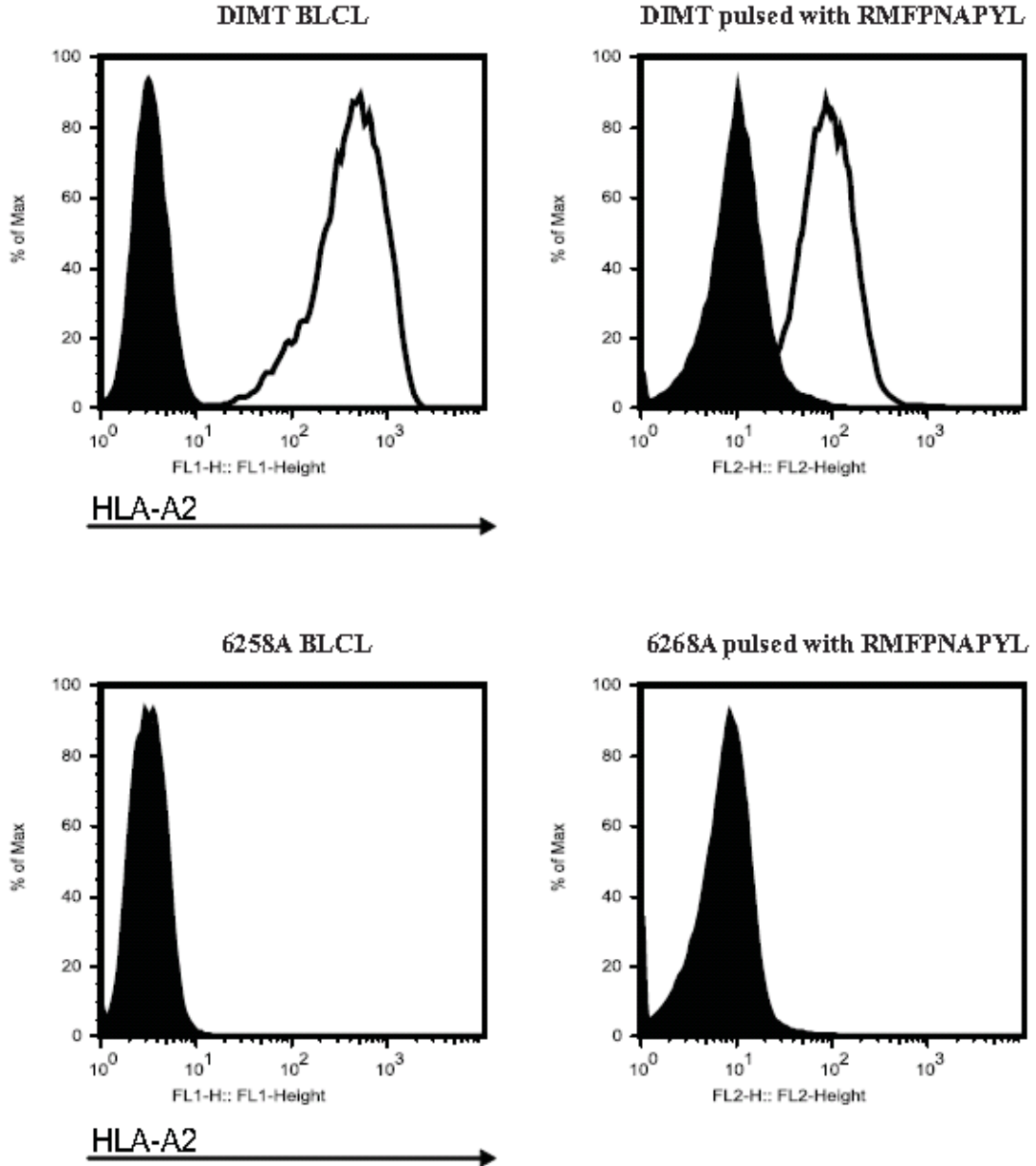


**Figure 34.** WT1 Clone 45 is RMFPNAPYL peptide specific and HLA-A2 restricted. Purified WT1 Clone 45 scFv-Fc was tested for peptide recognition on BLCLs. In the left panels, DIMT (top) and 6268A (bottom) BLCLs were stained with an HLA-A2-FITC conjugated antibody (unfilled lines) or an isotype control (filled lines). The BLCLs were incubated with RMFPNAPYL (right panel) at 40  $\mu$ M in serum-free IMDM media at 37°C for 5 hours. Subsequently, the peptide-pulsed BLCLs were stained with WT1 Clone 315 scFv-Fc (unfilled lines) or a control scFv (filled lines). Only the HLA-A2-positive DIMT BLCLs which had been pulsed with the RMFPNAPYL peptide could be stained.

#### *2.4 Antibody-dependent cellular cytotoxicity (ADCC) of EBNA Clone 315 scFv-Fc on peptide-pulsed cells*

In addition to using the scFv-Fc for antigen presentation studies, we tested whether the truncated human IgG<sub>1</sub> Fc region is capable of inducing antibody-dependent cellular cytotoxicity (ADCC). In order to avoid variability amongst human donor lymphocytes, and in an effort to increase the chances of observing cytotoxicity, Hong-fen Guo in our laboratory generated a CD16(V)-transduced NK92MI cell line. This NK92 cell variant is transduced with both IL-2 and the human CD16 activating Fc receptor (FcγRIIIA) containing a high affinity polymorphism (valine instead of phenylalanine at position 158 on CD16) responsible for an enhancement in ADCC and clinical response to antibody-based immunotherapy (211, 212).

We used this cell line in combination with the EBNA Clone 315 scFv-Fc or an irrelevant, isotype-matched scFv-Fc to test whether the fusion protein can induce NK92MI-mediated ADCC against LLDFVRFMGV-pulsed LUY (HLA-A2<sup>+</sup>) BLCL. At an E:T ratio of 42:1, EBNA Clone 315 scFv-Fc led to greater killing over background (with or without an irrelevant scFv-Fc) at the two highest concentrations tested (27-32% versus 13-15%) (Fig. 35). A similar magnitude of killing (over background) was also observed with other peptide-pulsed, HLA-A2<sup>+</sup> target BLCLs (DIMIT and JG19; data not shown). This data demonstrates that these truncated scFv-Fc fusion proteins maintain their Fc-mediated effector functions, despite being about 33% smaller than a full immunoglobulin.

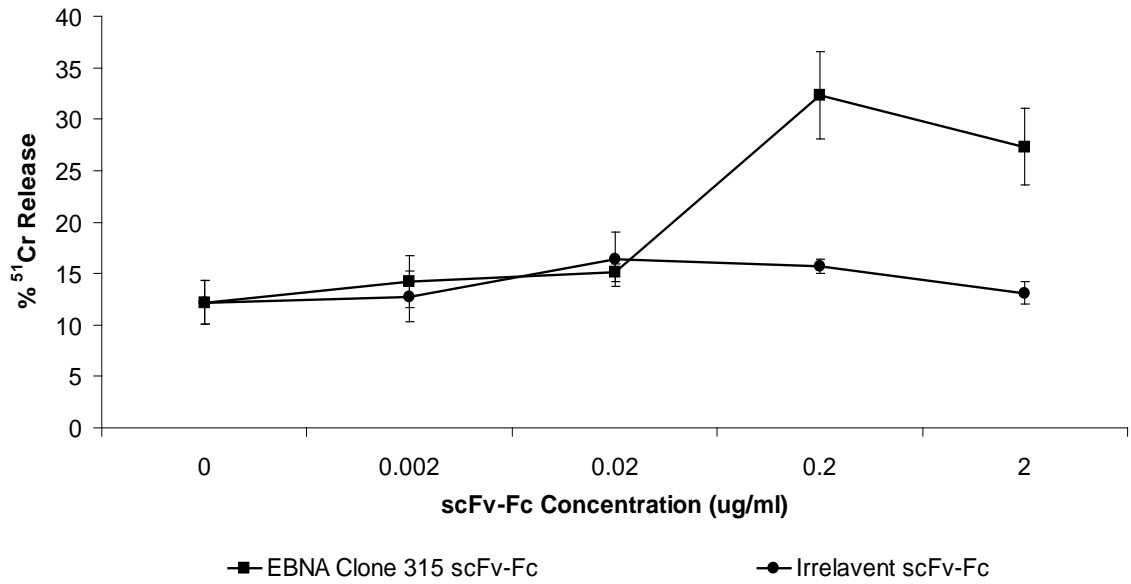


**Figure 35.** EBNA Clone 315 scFv-Fc mediates ADCC of peptide-pulsed cells. LUY BLCL was incubated with 20  $\mu$ M LLDFVRFMGV peptide in serum-free IMDM media at 37°C for 3 hours. The peptide pulsed cells were then labeled with <sup>51</sup>Cr and cocultured with CD16(V)-expressing NK92MI cells (E:T ratio of 42:1), in addition to varying concentrations of EBNA Clone 315 or an irrelevant scFv-Fc, at 37°C for 4 hours. EBNA Clone 315 scFv-Fc is able to lyse the peptide pulsed target cells better than effector cells alone or in combination with an irrelevant scFv-Fc.

## *2.5 Conclusions*

While antibodies in the form of scFvs were sufficient for most binding and specificity studies (as demonstrated in Chapter 1), generating scFv-Fc fusion proteins became necessary for several reasons: 1) The scFv-Fc fusion proteins are bivalent, which increases the overall avidity of the antibodies by a factor of two. This enhancement also correlated with a slightly better detection sensitivity of peptide-pulsed T2 cells, where the EBNA Clone 315 scFv-Fc fusion protein could detect fewer MHC-peptide complexes than the scFv using flow cytometry. The increase in binding strength will also become useful in CAR blocking assays discussed in the subsequent chapter due to the necessity to out compete a monovalent scFv-based receptor. 2) The scFv-Fc fusion proteins are larger, allowing for direct conjugation to fluorescent dyes without destroying the binding ability of the antibody. This became useful in helping us quantify the number of complexes on the surface of peptide-pulsed cells based on the amount of peptide used for pulsing. 3) The Fc region of the fusion proteins is functionally useful. First, we were able to demonstrate that these Fc fusion proteins can induce ADCC using CD16(V)-transduced NK92MI cells. Second, the Fc domain allowed us to determine the monovalent interaction affinity of EBNA Clone 315 through immobilization of the scFv-Fc to the gold dextrane surface of a CM5 Biacore chip. Compared to previously previous studies, our EBNA Clone 315 seemed to have a better affinity than a typical TCR (1-50  $\mu$ M (208)) yet comparable affinity to other TCR-like scFv or Fab fragments (2-300 nM).

## CHAPTER 3

### *ENGINEERING AND USE OF HLA-A2-RESTRICTED, PEPTIDE-SPECIFIC CHIMERIC ANTIGEN RECEPTORS*

#### *3.1 Introduction*

While the majority of the CAR field focuses on targeting conventional transmembrane proteins, several groups have been successful in generating constructs which target the MHC-peptide complex. The first study which used such a CAR came in 2001, where a Fab fragment (specific for an MAGE-A1-restricted peptide presented on HLA-A1) was fused to the Fc $\epsilon$ RI- $\gamma$  signaling molecule (43). This first generation construct was expressed in primary human T lymphocytes and was able to confer tumor specificity by inducing cytokine production (TNF- $\alpha$  and IFN- $\gamma$ ) and target specific cytotoxicity. Furthermore, when the Fab was affinity matured, researchers were able to demonstrate an improvement in CAR-mediated target cell lysis (44). In a subsequent study by the same group, researchers compared the first generation construct to one which contained both the Fc $\epsilon$ RI- $\gamma$  and CD28 signaling domains (45). The researchers were able to show that the addition of the CD28 signaling domain to the CAR resulted in substantially greater IL-2, TNF- $\alpha$  and IFN- $\gamma$  production, in addition to an increase in cytolytic activity, compared to the Fc $\epsilon$ RI- $\gamma$  alone.

The CARs which were used in this thesis are based off of a 2<sup>nd</sup> generation construct in which signaling is provided by CD3 $\zeta$  and 4-1BB (154). 4-1BB is a member of the tumor necrosis factor receptor (TNFR) family of proteins which signal through specific TNFR-associated factors (TRAFs). TRAF1 and TRAF2 are recruited to TRAF-

binding motifs on the cytoplasmic region of 4-1BB upon aggregation, which results in activation of NF- $\kappa$ B and downstream signaling involving extracellular signal regulated kinase (ERK), c-Jun N-terminal kinase (JNK) and p38 mitogen-associated protein (MAP) kinase (213-219). In T cells, this has been shown to induce survival through the upregulation of prosurvival members of the Bcl-2 family (214) and downregulation of the proapoptotic molecule Bim (215). While most studies which incorporate 4-1BB as a signaling molecule in the context of a CAR use it in the T cell setting, one study examined the function of a 2<sup>nd</sup> generation CAR (containing both CD3 $\zeta$  and 4-1BB) in CD56<sup>+</sup>CD3<sup>-</sup> NK cells (220). In that study, researchers showed that the addition of 4-1BB to CD3 $\zeta$  not only increased NK cell activation (as measured by IFN- $\gamma$  and GM-CSF production), but also led to greater cytotoxicity when compared to CD3 $\zeta$  alone; coincidentally, this same construct was used for the generation of the CARs used in this thesis.

In this work, we decided to test whether our scFvs, in the form of chimeric antigen receptors (CARs) have the ability to activate NK92MI cells. We hypothesized that converting scFvs to chimeric antigen receptors (CARs) would be a very sensitive method of detecting low level of antigen due to previous work showing the sensitivity of T cell activation requires interaction with as few as 10 MHC-peptide complexes on the target cell surface (221). In addition, we believe that NK92MI cells are ideal effector cells for CAR-based immunotherapy due to their strong cytolytic activity combined with their ease of maintenance in cell culture.

### *3.2 EBNA Clone 315 CAR-equipped NK92MI cells can detect cells bearing the specific HLA-A2-LLDFVRFMGV complex via CD107a expression*

After the EBNA Clone 315 CAR was generated, the DNA was packaged into retrovirus using the 293T-based GP2 cell line. Once the retrovirus was generated in the culture media, it was recovered and concentrated using a polyethylene glycol solution. The concentrated virus was then used to infect 500,000 to 1,000,000 NK92MI cells in NK92MI growth media. After 3-4 days of culture, the NK92MI cells infected with the CAR-containing retrovirus were compared to mock-infected cells (infected with empty retrovirus) by detecting GFP expression using flow cytometry. While the infection efficiency was approximately 27.5%, flow assisted cytometric cell sorting (FACS) allowed us to enrich the GFP-positive population to more than 98% positive (Fig. 36).

Once the NK92MI cells were enriched for EBNA Clone 315 CAR expression, they were tested for their ability to recognize the targeted HLA-A2-EBNA3C complex. As an initial readout of NK92MI activation by target cells, we assayed for cell surface expression of CD107a, a marker of NK cell and T cell degranulation (222, 223). T2 cells were loaded with 20  $\mu$ M of the targeted peptide (LLDFVRFMGV), an irrelevant peptide (YMFNPAPYL) or no peptide. Using a 1:1 E:T ratio, the T2 cells were cocultured with EBNA Clone 315 CAR-expressing NK92MI cells in the presence of an anti-CD107a-PE conjugated antibody at 37°C for 5 hours. As shown in Figure 37A, NK92MI cells equipped with the EBNA Clone 315 CAR did not react to unpulsed T2 cells or T2 cells pulsed with the irrelevant peptide, showing CD107a levels comparable to those of NK92MI cells cultured in the absence of targets. On the other hand, when the CAR-equipped NK92MI cells were cocultured with T2 cells that had been pulsed with the

LLDFVRFMGV peptide, 27% of GFP<sup>+</sup> cells expressed CD107a above background levels. These results show that after scFv engineering, the CAR is able to maintain its specificity towards the targeted HLA-A2-peptide complex.

Next, in order to get a quantitative measurement of how sensitive this CAR is at activating NK92MI cells, we titrated down the LLDFVRFMGV peptide concentration used to pulse T2 cells and measured their ability to activate the CAR-equipped NK92MI cells. As can be seen in Figure 37B, the lower limit of response by the CAR-equipped NK92MI was at a peptide concentration of 10 nM, with a clear dose response curve beginning at the 600 nM concentration. Based on our earlier quantitation studies, this peptide concentration corresponds to approximately 25 complexes on the cell surface. Compared to the levels necessary for epitope detection using the EBNA Clone 315 scFv or scFv-Fc (20-200 nM), the CAR seems to be a more sensitive approach at detecting low levels of MHC-peptide complex on the surface of APCs using flow cytometric analysis.

While T2 cells can present any peptide of interest, BLCLs naturally present their own peptides on their MHC Class I molecules. Similarly to T2, these endogenous peptides can be replaced by simple incubation with a substitute peptide of high enough affinity. Using a 1:1 E:T ratio, HLA-A2<sup>+</sup> (DIMIT) and HLA-A2<sup>-</sup> (6268A) BLCLs were pulsed with serum-free IMDM medium or medium containing the LLDFVRFMGV, cocultured with EBNA Clone 315 CAR-expressing NK92MI cells as discussed above, and assayed for CD107a expression using flow cytometry. Peptide pulsed DIMIT (HLA-A2<sup>+</sup>) induced 25% of GFP<sup>+</sup> NK92MI cells to express CD107a (Fig. 38), in contrast to 0.54% for peptide pulsed 6268A (HLA-A2<sup>-</sup>) and 1.09% for unpulsed DIMIT. This data



further demonstrates both peptide specificity and HLA-A2 exclusivity of the EBNA  
Clone 315 CAR.

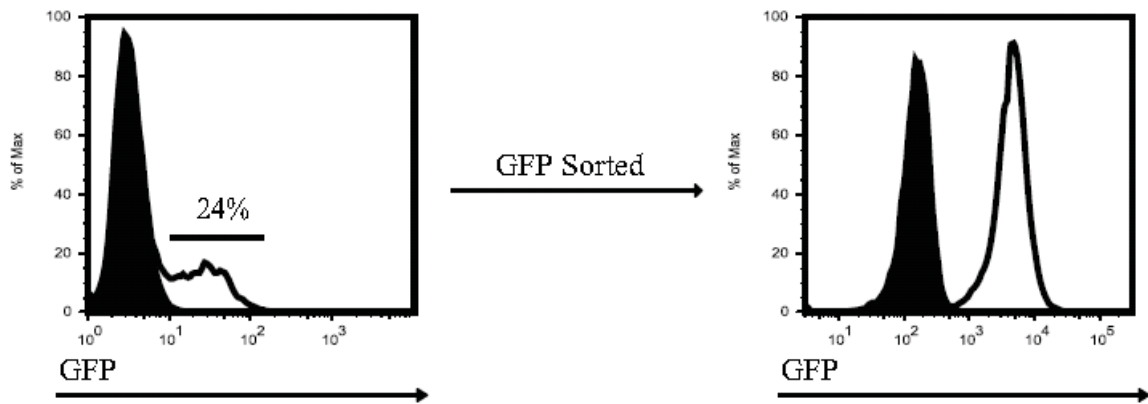


**Figure 36.** Retroviral transduction of EBNA Clone 315 CAR into NK92MI cells. After retroviral packaging using 293T GP2 cells and transduction into NK92MI cells, approximately 24% of the NK92MI cells contained the construct based on GFP expression (left panel; unfilled lines) when compared to mock transduced (empty retrovirus) NK92MI cells (left panel; filled lines). Of the GFP-positive cells, the top 20% were flow cytometrically sorted and expanded to yield a population of stably transduced cells which were greater than 90% GFP positive (right panel). Retroviral transduction was done on three separate occasions, with 24% being the highest efficiency.

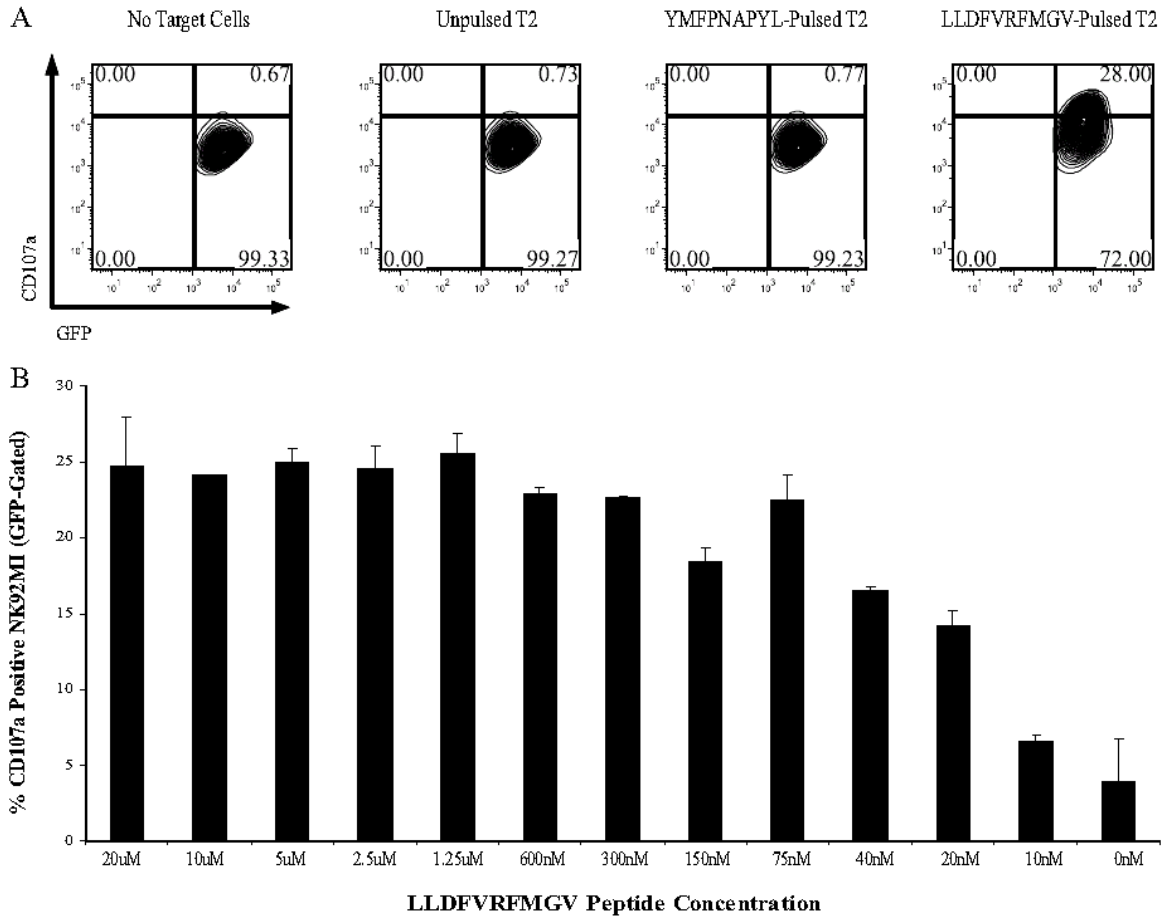


**Figure 37.** EBNA Clone 315 CAR-expressing NK92MI cells can specifically detect the HLA-A2-EBNA3C complex on peptide-pulsed T2 cells via CD107a expression. T2 cells were pulsed with or without LLDFVRFMGV or YMFPNAPYL peptides at 20  $\mu$ M in serum-free IMDM media at 37°C for 5 hours. CAR-equipped NK92MI cells were then cultured in media containing an anti-CD107a-PE conjugated antibody at 37°C for 5 hours with or without peptide pulsed or unpulsed cells. **A.** CAR-equipped NK92MI cells were gated based on GFP fluorescence and analyzed for CD107a expression. NK92MI cells which were cultured without any T2 cells or those which were cocultured with unpulsed and YMFPNAPYL-pulsed T2 cells were unreactive while NK92MI cells which were cocultured with LLDFVRFMGV-pulsed T2 cells led to a 27% increase in CD107a expression above background levels. **B.** T2 cells were pulsed with decreasing concentrations of LLDFVRFMGV and subsequently cocultured with CAR-equipped NK92MI cells. NK92MI cells presented noticeable amounts of CD107a on their cell surface even when T2 cells were pulsed with only 10 nM of peptide.

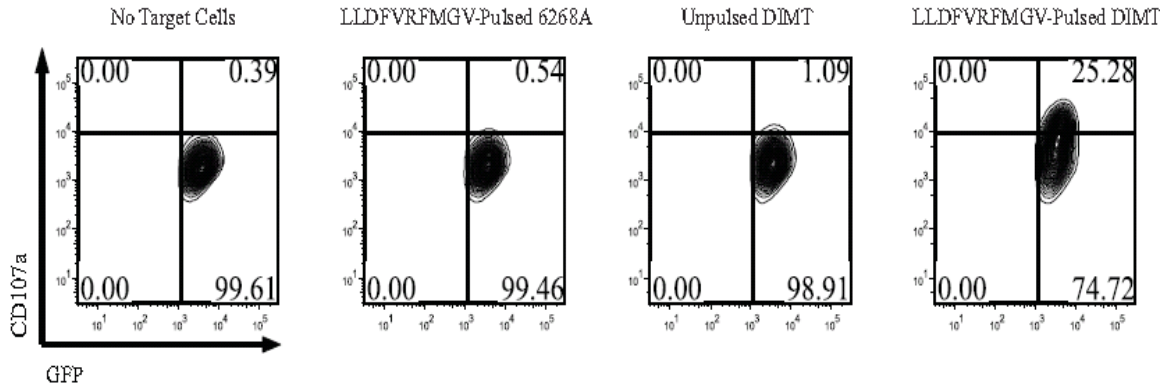


**Figure 38.** EBNA Clone 315 CAR-expressing NK92MI cells can specifically detect the HLA-A2-EBNA3C complex on peptide-pulsed BLCLs via CD107a expression. HLA-A2<sup>+</sup> (DIMT) and HLA-A2<sup>-</sup> (6268A) BLCLs were pulsed with LLDFVRFMGV at 20  $\mu$ M in serum-free IMDM media at 37°C for 5 hours. CAR-equipped NK92MI cells were then cultured in media containing an anti-CD107a-PE conjugated antibody at 37°C for 5 hours with or without peptide pulsed or unpulsed cells. CAR-equipped NK92MI cells were gated based on GFP fluorescence and analyzed for CD107a expression. NK92MI cells which were cultured without any BLCL or those which were cocultured with LLDFVRFMGV-pulsed 6268A BLCL were unreactive while NK92MI cells which were cocultured with unpulsed DIMT BLCL or LLDFVRFMGV-pulsed DIMT BLCL led to a 0.5% and 25% increase in CD107a expression above background levels (pulsed 6268A).

### *3.3 EBNA Clone 315 CAR-equipped NK92MI cells can destroy cells bearing the specific HLA-A2-LLDFVRFMGV complex via <sup>51</sup>Cr release*

While CD107a expression on NK cells and T cells reflect their activation, target cell lysis can also be measured using a conventional <sup>51</sup>Cr cytotoxicity assay. First, to get an idea of how sensitive the <sup>51</sup>Cr cytotoxicity assay is with regards to killing HLA-A2-EBNA3C expressing targets, T2 cells were pulsed with decreasing concentrations of the LLDFVRFMGV peptide at 37°C for 3 hours and subsequently labeled with <sup>51</sup>Cr as described in the Materials and Methods. The labeled T2 cells were then cocultured with EBNA Clone 315 CAR-expressing NK92MI cells at 37°C for 2 hours at a 3:1 E:T ratio. Similar to the results seen in the CD107a assay (Fig. 37B), EBNA Clone 315 CAR expressing NK92MI cells were able kill T2 cells in a peptide-dependent manner, with 13.2% of 2 nM peptide-pulsed T2 cells being killed compared to 10.1% with unpulsed T2 cells (Fig. 39). This relationship between antigen density and cytolytic sensitivity is similar to what has been seen previously using antigen-specific T cells directed at a HER2-derived peptide on HLA-A2 (224). Relative to that which can be detected using flow cytometric antibody staining, the level of sensitivity is in the order of 10-100 fold greater in favor of the CAR using two separate assays (CD107a and <sup>51</sup>Cr).

Next, DIMT and 6268A BLCLs pulsed with the LLDFVRFMGV peptide (20 µM) in serum-free IMDM (Fig. 40A and B) were used as targets in the <sup>51</sup>Cr release assay; this experiment was carried out by Ming Cheng in our laboratory. Similar to the results from the CD107a assay (Fig. 38), only the HLA-A2<sup>+</sup> DIMT BLCL was lysed by the CAR-equipped NK92MI cells (Fig. 40A), which could be blocked using the purified EBNA Clone 315 scFv-Fc (Fig. 40B). In addition, the ability to block cytotoxicity was

not restricted to the scFv-Fc protein since a commercial anti-HLA-A2 (BB7.2) antibody also possessed blocking ability (Fig. 41). This blocking data recapitulates results seen with other MHC-restricted, peptide-specific antibodies on antigen-specific cytolytic T cells (28, 34).

Although the lytic potential of the CAR-equipped NK92MI cells was clearly evident when targets were artificially pulsed with the relevant peptide, cytotoxicity against naturally processed HLA-A2-peptide complexes is of clinical relevance. Here, CAR-equipped NK92MI cells were tested against a panel of HLA-A2<sup>+</sup> (DIMIT and JG19) and HLA-A2<sup>-</sup> (6268A and GKO) unpulsed BLCLs. While the level of cytotoxicity was low, 23.0% for DIMIT and 8.9% for JG19 (30:1 E:T ratio), this was highly significant when compared to 3.6% for GKO and 1.8% for 6268A (Fig. 42A). In addition, when the cytotoxicity assay was performed in the presence of EBNA Clone 315 scFv-Fc, the killing capacity could be reduced by approximately 46% when compared to that with an irrelevant scFv-Fc or in the absence of antibody (Fig 42B). These findings demonstrate the utility and specificity of TCR-like CARs in reprogramming effector immune cells to engage antigen whose expression is below the detection limit using conventional flow cytometry.

Lastly, since both the EBNA Clone 315 CAR and scFv-Fc fusion protein have the same variable sequences used for detecting the HLA-A2-LLDFVRFMGV complex, we decided to directly compare CAR-mediated cytotoxicity with ADCC since both approaches are currently being used independently for the treatment of cancer patients. First, the DIMIT BLCL was pulsed with the LLDFVRFMGV peptide at 20  $\mu$ M in serum-free IMDM media at 37°C for 2 hours. The pulsed BLCL was then labeled with <sup>51</sup>Cr and

cocultured with either EBNA Clone 315 CAR or CD16(V)-expressing NK92MI cells along with EBNA Clone 315 scFv-Fc or an irrelevant scFv-Fc at an E:T ratio of 15:1 for 3 hours at 37°C. At a EBNA Clone 315 scFv-Fc concentration of 0.5 µg/ml, CD16(V) NK92MI cells were able to kill about 30-35% of cells, compared to 10-15% with an irrelevant scFv-Fc or no antibody at all (Fig. 43A). When the ADCC experiment was carried out using higher scFv-Fc concentrations, the cytotoxicity percentage did not change (data not shown). On the other hand, at the same E:T ratio, EBNA Clone 315 CAR-equipped NK92MI cells were able to kill 80-90% of the same peptide-pulsed target cells; the EBNA Clone 315 scFv-Fc was included as a blocking control (Fig. 43B). These results demonstrate that the CAR-mediated killing involving NK92MI cells is a far more potent means of target cell lysis compared to ADCC in our setting.

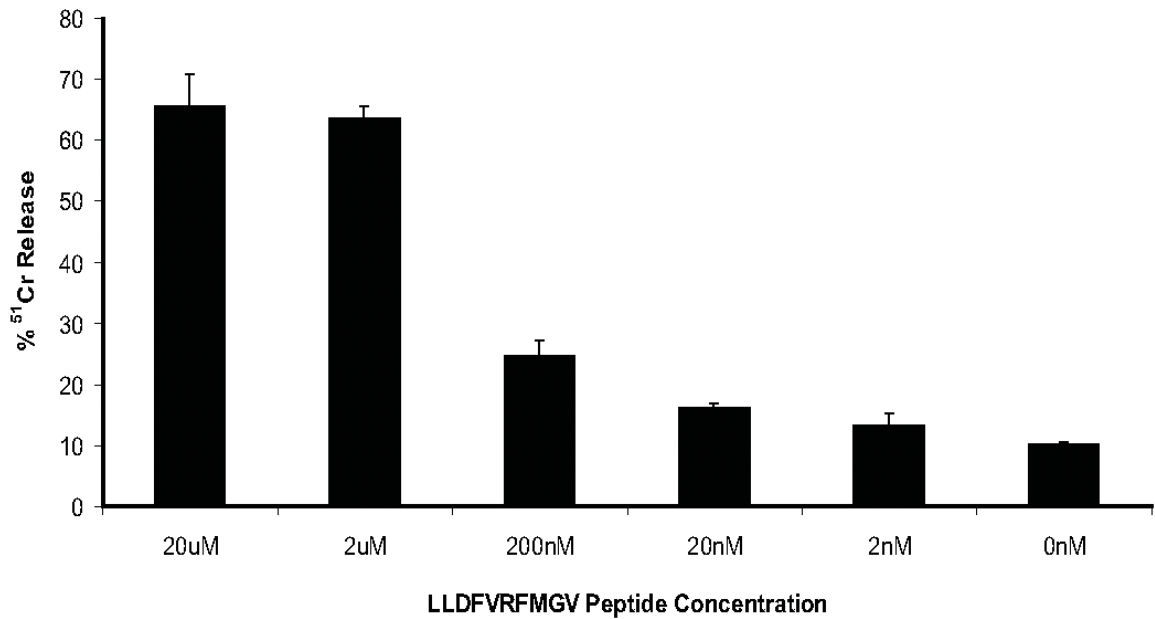


**Figure 39.** EBNA Clone 315 CAR-expressing NK92MI cells can specifically detect the HLA-A2-EBNA3C complex on peptide-pulsed T2 cells via <sup>51</sup>Cr release. T2 cells were pulsed with or without decreasing concentrations of LLDFVRFMGV in serum-free IMDM media at 37°C for 5 hours. CAR-equipped NK92MI cells were cocultured for 2 hours with <sup>51</sup>Cr-labeled T2 cells at a 3:1 E:T ratio. Even with 2 nM of peptide, peptide-specific cytotoxicity could be observed when compared to unpulsed T2 cells.



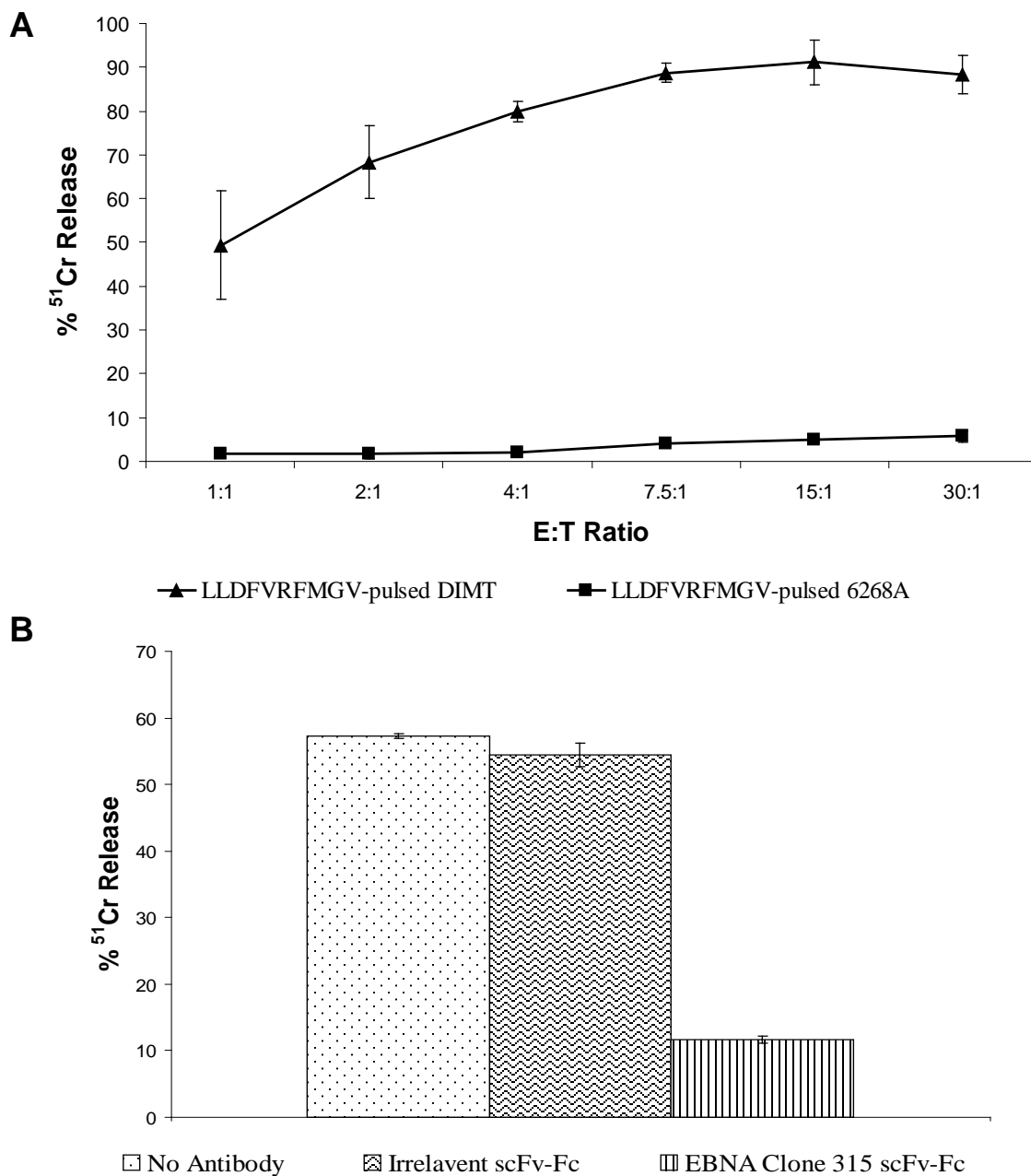


**Figure 40.** EBNA Clone 315 CAR-expressing NK92MI cells can specifically detect the HLA-A2-EBNA3C complex on peptide-pulsed BLCLs via <sup>51</sup>Cr release.

*A-B.* BLCLs were pulsed with LLDFVRFMGV in serum-free IMDM media at 37°C for 3-5 hours. CAR-equipped NK92MI cells were then cultured in RPMI + 10% FBS with <sup>51</sup>Cr labeled target cells at 37°C for 4 hours. *A.* CAR equipped NK92MI cells were able to specifically differentiate between peptide pulsed DIMT and 6268A BLCL, with a clear difference in cytotoxicity between the two different targets. *B.* CAR-mediated killing of peptide-pulsed DIMT BLCL could be blocked using the EBNA Clone 315 scFv-Fc fusion protein (1.25 µg/ml), but not by an irrelevant, isotype-matched scFv-Fc (1.25 µg/ml), at a 20:1 E:T ratio.

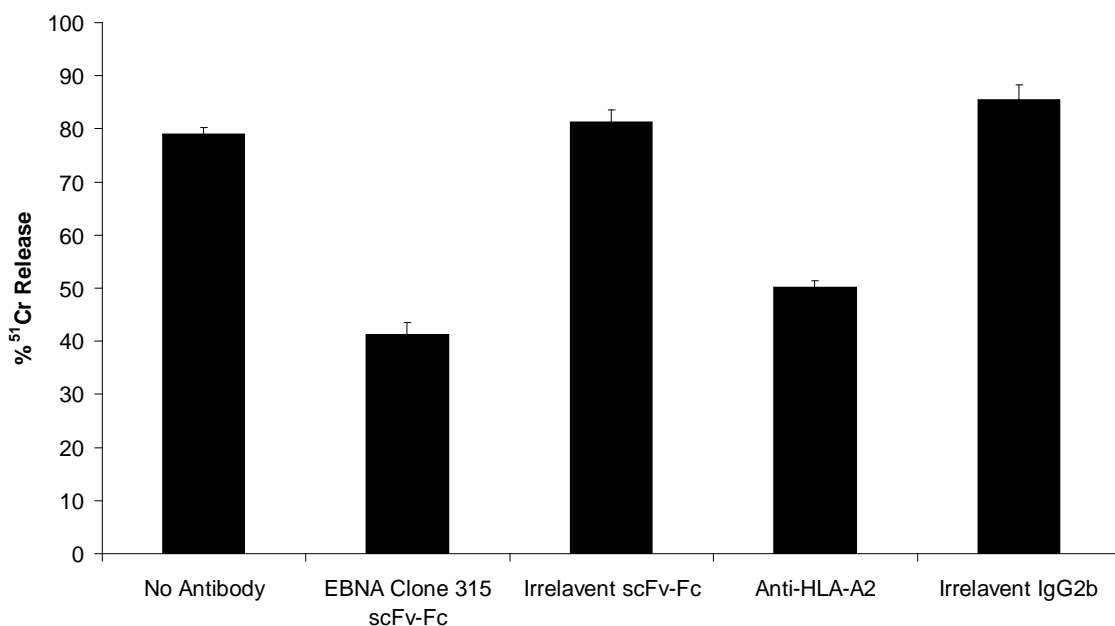


**Figure 41.** EBNA Clone 315 CAR-mediated cytotoxicity can be blocked using scFv-Fc fusion protein and anti-HLA-A2 full immunoglobulin.

DIMT BLCL was pulsed with LLDFVRFMGV in serum-free IMDM media at 37°C for 3-5 hours. CAR-equipped NK92MI cells were then cultured in RPMI + 10% FBS with <sup>51</sup>Cr labeled target cells at 37°C for 4 hours. CAR-mediated killing of peptide-pulsed DIMT BLCL could be blocked using the EBNA Clone 315 scFv-Fc fusion protein or a commercial anti-HLA-A2 antibody (66.6 nM), but not by irrelevant, isotype-matched antibodies (66.6 nM), at a 6:1 E:T ratio.

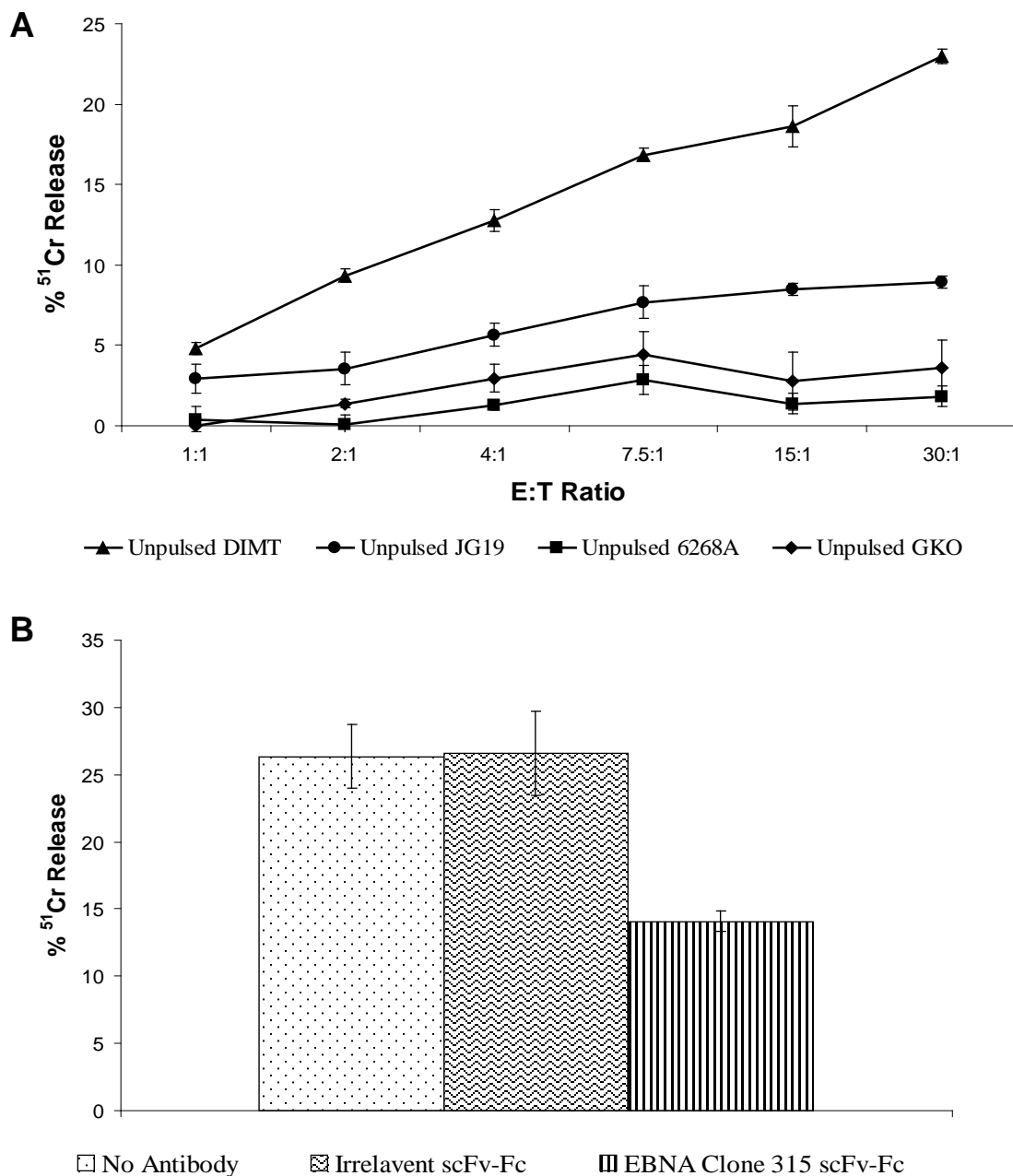


**Figure 42.** EBNA Clone 315 CAR-expressing NK92MI cells can specifically detect the HLA-A2-EBNA3C complex on HLA-A2<sup>+</sup> BLCLs via <sup>51</sup>Cr release.

*A-B.* CAR-equipped NK92MI cells were cultured in RPMI + 10% FBS with <sup>51</sup>Cr labeled, unpulsed BLCLs at 37°C for 4 hours. *A.* CAR-equipped NK92MI cells were more reactive towards the HLA-A2<sup>+</sup> DIMT and JG19 BLCL versus the HLA-A2<sup>-</sup> 6268A and GKO BLCL when cocultured in the absence of any exogenous peptide. *B.* CAR-mediated killing of unpulsed DIMT BLCL could be blocked using the EBNA Clone 315 scFv-Fc fusion protein (20 µg/ml), but not by an irrelevant, isotype-matched scFv-Fc, at a 10:1 E:T ratio.

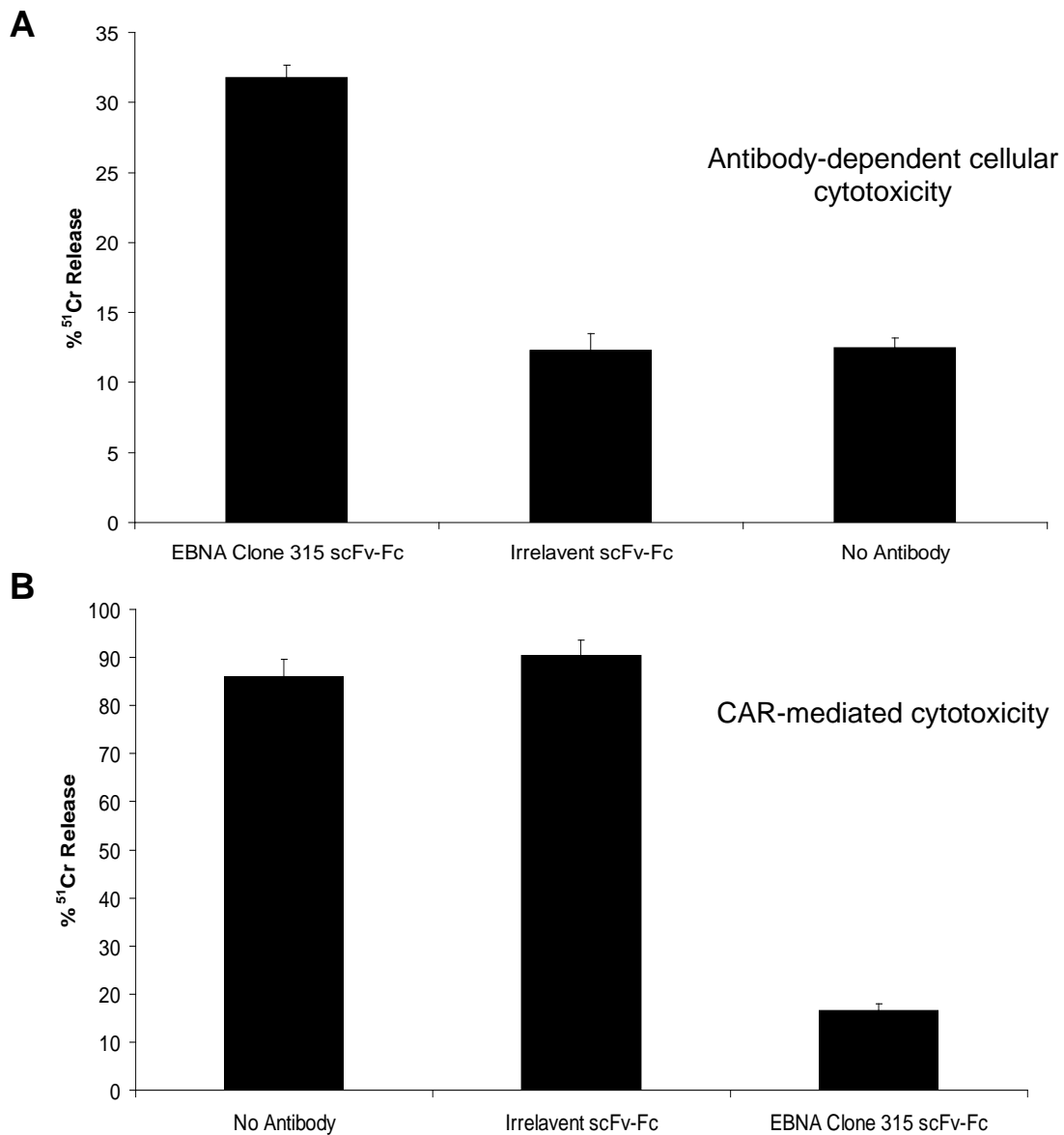


**Figure 43.** CAR-mediated killing is more potent than scFv-Fc-mediated ADCC on peptide-pulsed DIMT BLCL.

A. CD16(V)-expressing NK92MI cells were cultured in RPMI + 10% FBS with <sup>51</sup>Cr labeled, LLDFVRFMGV-pulsed DIMT BLCL and either EBNA Clone 315 or an irrelevant scFv-Fc (0.5 µg/ml) at 37°C for 3 hours. At an E:T ratio of 15:1, EBNA Clone 315 scFv-Fc was able to kill 30-35% of target cells. B. EBNA Clone 315 CAR-expressing NK92MI cells were cultured with LLDFVRFMGV-pulsed DIMT BLCL as above and either EBNA Clone 315 or an irrelevant scFv-Fc (30 µg/ml) at 37°C for 3 hours. At the same E:T ratio as in A, the CAR-equipped cells were able to kill 80-90% of target cells, with specific inhibition using EBNA Clone scFv-Fc.

### *3.4 WT1 Clone 45 CAR-equipped NK92MI cells can destroy cells bearing the specific HLA-A2-RMFPNAPYL complex via <sup>51</sup>Cr release*

Once the WT1 Clone 45 CAR was generated, the DNA was packaged into retrovirus and used to infect NK92MI cells in the same way as with the EBNA Clone 315 CAR. After 3-4 days of culture, the GFP expression level of the infected NK92MI cells were compared to mock-infected cells. The initial infection efficiency was approximately 24%, and after flow assisted cytometric cell sorting (FACS), the GFP-positive population was enriched to more than 90% positive (Fig. 44).

Along with the EBNA Clone 315 CAR, we decided to test the cytolytic ability of the WT1 Clone 45 CAR in the context of NK92MI cells. First, DIMT and 6268A BLCLs were pulsed with the RMFPNAPYL peptide (40 µg/ml) in serum-free IMDM at 37°C for 3-5 hours. Subsequently, the target cells were labeled with <sup>51</sup>Cr and cocultured with the CAR-equipped NK92MI cells at 37°C for 4 hours. Of the two peptide-pulsed BLCLs, only the HLA-A2<sup>+</sup> DIMT could be lysed (~70% versus ~5% with 6268A) at a 10:1 E:T ratio (Fig. 45A). In addition, CAR-mediated cytotoxicity could be blocked using a commercial anti-HLA-A2 antibody by approximately 45% (Fig. 45B), further demonstrating specificity.

Next, we decided to test the cytolytic capacity of WT1 Clone 45 CAR-equipped NK92MI cells against cell lines which might natively express the HLA-A2-RMFPNAPYL complex. Due to previously published data (225), and conversations with Dr. Richard O'Reilly's laboratory here at MSKCC, researchers have demonstrated that WT1 can be constitutively activated in all BLCLs derived from EBV immortalization. More specifically, O'Reilly's group was able to show WT1 transcript in the DIMT BLCL

(data not shown). As a result, we first decided to test WT1 Clone 45 CAR-mediated killing against unpulsed HLA-A2<sup>+</sup> DIMT and HLA-A2<sup>-</sup> 6268A BLCL. Similarly to what was seen with the EBNA Clone 315 CAR, WT1 Clone 45 CAR-equipped NK92MI cells were able to kill unpulsed DIMT at a lower capacity than peptide-pulsed DIMT. While the level of cytotoxicity was lower, ~35% for DIMT at a 20:1 E:T ratio, it was far greater when compared to 6268A (~5%) (Fig. 46A). In addition, when the cytotoxicity assay was performed in the presence of the WT1 Clone 45 scFv-Fc, the killing capacity could be reduced by approximately 43% relative to an irrelevant scFv-Fc or in the absence of antibody (Fig. 46B). These findings correspond well with what was seen using the EBNA Clone 315 CAR and further demonstrate the utility and specificity of TCR-like CARs in reprogramming effector immune cells to engage antigen.

Lastly, we decided to test CAR-mediated cytotoxicity against two cell lines which are HLA-A2-positive and previously shown to express WT1. OVCAR-3 is a cell line established from malignant ascites of a patient with progressive adenocarcinoma of the ovary (226) and later shown to contain WT1 mRNA (227). In addition, 697 is a human pre-B cell leukemia established from bone marrow cells obtained from a child with relapsed acute lymphocytic leukemia (ALL) (228). Since then, several groups have shown that this cell line also expresses high levels of both WT1 transcript and protein (229, 230). WT1 Clone 45 CAR-expressing NK92MI cells were cocultured with <sup>51</sup>Cr labeled OVCAR-3 and 697 cells at 37°C for 4 hours. CAR-equipped NK92MI cells were able to lyse approximately 20-30% of 697 and OVCAR-3 cells at a 20:1 E:T ratio, which decreased with the number of effector cells used in the assay (Fig. 47). This data demonstrates that these two cell types are sensitive to WT1 Clone 45 CAR-equipped

NK92MI cells and provides further evidence for their utility in the treatment of HLA-A2<sup>+</sup>/WT1<sup>+</sup> malignancies.

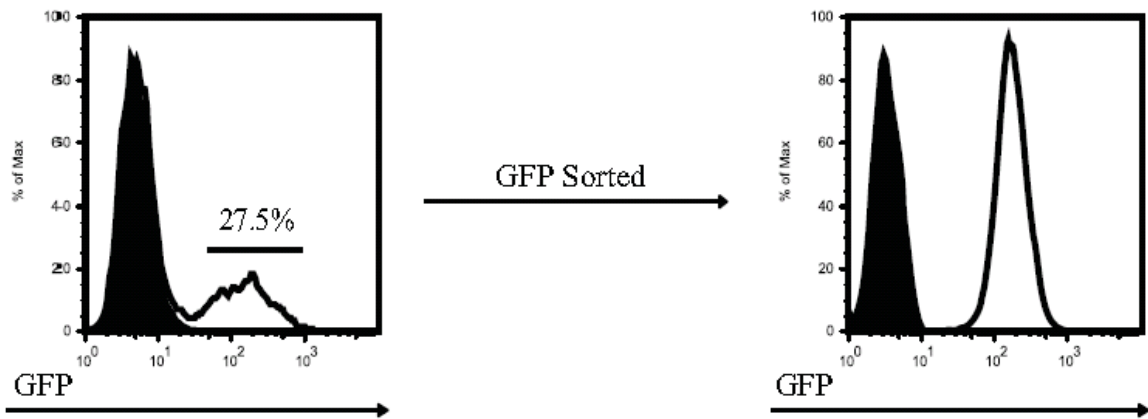


**Figure 44.** Retroviral transduction of WT1 Clone 45 CAR in NK92MI cells. After retroviral packaging using 293T GP2 cells and transduction into NK92MI cells, approximately 27.5% of the NK92MI cells contained the construct based on GFP expression (unfilled lines) when compared to mock transduced (empty retrovirus) NK92MI cells (filled lines). Of the GFP-positive cells, the top 20% were flow cytometrically sorted and expanded to yield a population of stably transduced cells which were greater than 98% GFP positive (right panel).



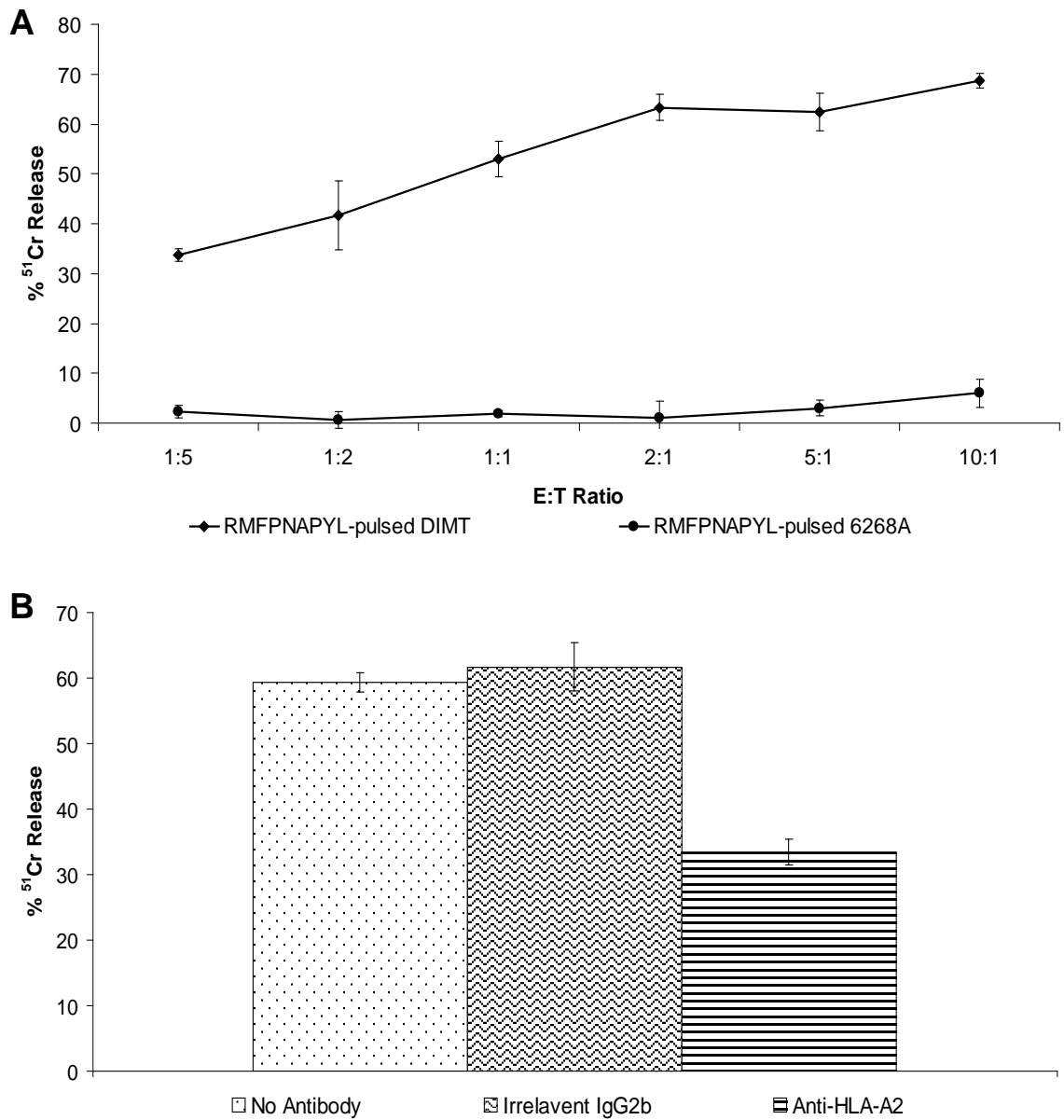


**Figure 45.** WT1 Clone 45 CAR expressing NK92MI cells can specifically detect the HLA-A2-RMFPNAPYL complex on peptide-pulsed BLCLs via <sup>51</sup>Cr release.

*A-B.* BLCLs were pulsed with RMFPNAPYL in serum-free IMDM media at 37°C for 3-5 hours. CAR-equipped NK92MI cells were then cultured in RPMI + 10% FBS with <sup>51</sup>Cr labeled target cells at 37°C for 4 hours. *A.* CAR equipped NK92MI cells were able to specifically differentiate between peptide pulsed DIMT and 6268A BLCL, with a clear difference in cytotoxicity between the two different targets. *B.* CAR-mediated killing of peptide-pulsed DIMT BLCL could be blocked using a commercial anti-HLA-A2 antibody (5 µg/ml), but not by an irrelevant, isotype-matched antibody (5 µg/ml), at a 9:1 E:T ratio.

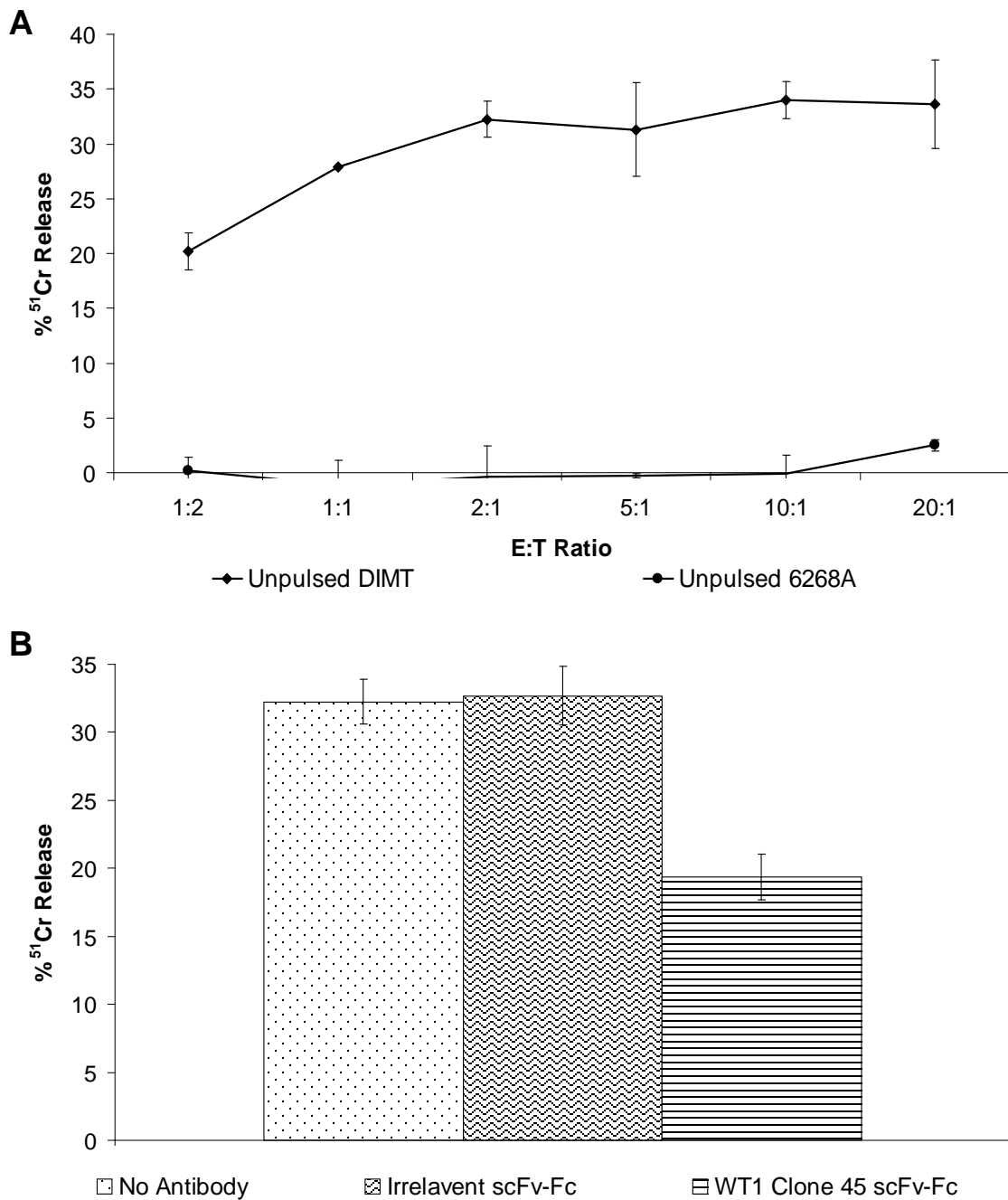


**Figure 46.** WT1 Clone 45 CAR expressing NK92MI cells can specifically detect the HLA-A2-RMFPNAPYL complex on unpulsed DIMT BLCL via <sup>51</sup>Cr release.

*A-B.* CAR-equipped NK92MI cells were cultured in RPMI + 10% FBS with <sup>51</sup>Cr labeled target cells at 37°C for 4 hours. *A.* CAR equipped NK92MI cells were able to specifically differentiate between DIMT and 6268A BLCL, with a clear difference in cytotoxicity between the two different targets. *B.* CAR-mediated killing of DIMT BLCL could be blocked using the WT1 Clone 45 scFv-Fc fusion protein (20 µg/ml), but not by an irrelevant, isotype-matched scFv-Fc, at a 2:1 E:T ratio.

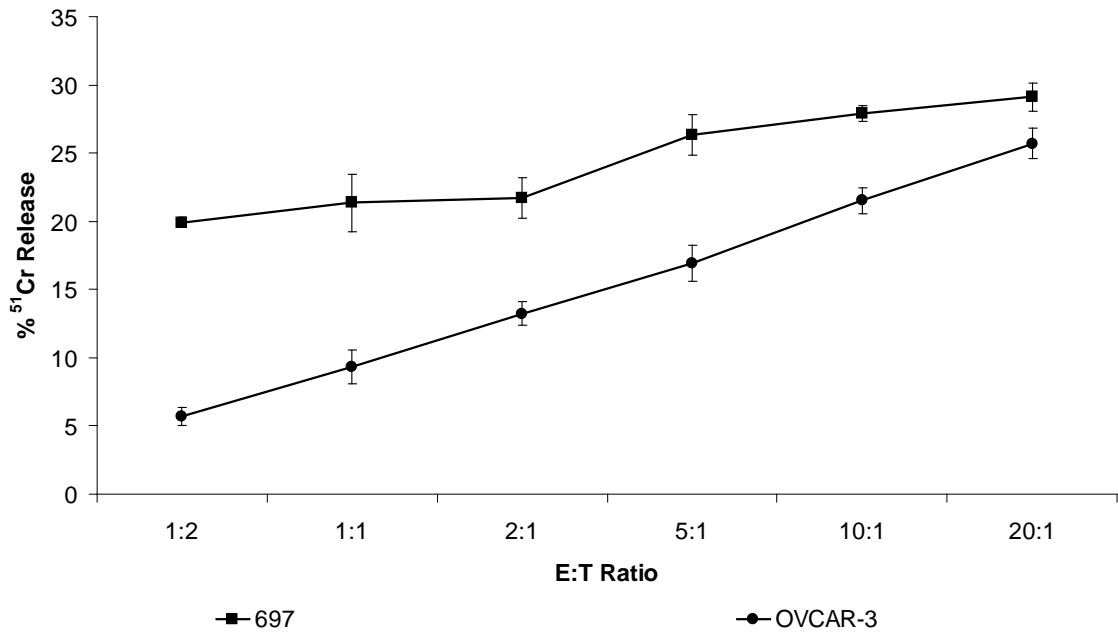


**Figure 47.** WT1 Clone 45 CAR expressing NK92MI cells can specifically detect the HLA-A2-RMFPNAPYL complex on 697 and OVCAR-3 cells via <sup>51</sup>Cr release. CAR-equipped NK92MI cells were cultured in RPMI + 10% FBS with <sup>51</sup>Cr labeled target cells at 37°C for 4 hours. CAR equipped NK92MI cells were able to kill 20-30% of cells at the highest E:T ratio tested (20:1).

### *3.5 Conclusions*

CARs have previously been shown to have great promise by several groups, in both the preclinical and clinical settings (231-235). In this work, we were able to generate two different CARs from two different scFvs derived from the same human phage display libraries (Tomlinson I and J). Unlike conventional CARs which typically target the extracellular domain of transmembrane proteins such as CD19 and HER2, the CARs discussed here targeted different peptides in the context of HLA-A2 in a similar manner to a TCR. In addition, while other MHC-restricted, peptide-specific CARs have only been used in the context of T cells, we were able to reprogram NK92MI cells using a 2<sup>nd</sup> generation CAR containing the CD3 $\zeta$  and 4-1BB signaling domains.

Due to an IRES-GFP sequence downstream of the CAR, the relative protein level could be monitored without directly conjugating both proteins. This allowed us to determine that our initial retroviral transduction efficiency was between 20 and 30%, which was further enriched using FACS. Next, we were able to demonstrate that the CARs maintained their original specificity towards their targeted HLA-A2-peptide complexes via peptide pulsing assays using antigen presenting cells. This was further validated by blocking target cell lysis to similar extents using both a commercial anti-HLA-A2 antibody (BB7.2) as well as the targeting scFv-Fc fusion protein. Furthermore, we were also able to demonstrate that the CAR in the context of NK92MI cells was a very sensitive way of detecting low levels of antigen; resulting in a 10-100 fold more sensitive readout using CD107a expression and <sup>51</sup>Cr release relative to flow cytometric staining using the scFv and scFv-Fc fusion proteins. Based on antigen quantitation studies done in Chapter 2, the level of NK92MI CAR-mediated detection was in the order

of 25 HLA-A2-peptide complexes. Even more so, we could show that CAR-mediated cytotoxicity was far better at killing target-expressing cells than scFv-Fc-mediated ADCC.

Lastly, we were able to demonstrate peptide-specific, CAR-mediated killing of both peptide-pulsed and unpulsed DIMT BLCL through antigen blockage on the target cells using the purified scFv-Fc fusion proteins. This specificity experiment could be seen using both EBNA Clone 315 CAR and WT1 Clone 45 CAR-expressing NK92MI cells and their respective antibody fragments. While the magnitude of killing was far greater in the peptide-pulsed setting (due to high levels of antigen on the cell surface), it is important to note that unpulsed cells were also sensitive. These results further justify the use of these CARs to retarget NK92MI cells towards a desired TCE.

## DISCUSSION

T-cell based cancer immunotherapy gained momentum from studies which showed a correlation of increased numbers of tumor infiltrating lymphocytes (TILs) in surgical specimens and patient outcome (236, 237). It is generally believed that tumor specificity underlined this infiltration of TILs and that this was mediated through the expression of tumor associated peptides in the context of MHC. These findings eventually led researchers to try and take advantage of antigen-specific T cells for the treatment of cancer. Antigen-specific T cells have been generated in several ways, either by *ex vivo* stimulation with APCs, *in vivo* sensitization using dendritic cell-based stimulation, or TCR gene transfer using retroviral or lentiviral vectors. When generated *ex vivo*, these cells are expanded by culturing with IL-2 or other cytokines before adoptively transferring them back into the patient. While these procedures are feasible, they can be laborious and time consuming. On the other hand, TCR gene transfer is a more efficient means of generating antigen-specific T cells; however, the antigen specific population of cells still need to be selected for and expanded, in addition to issues regarding the mispairing of the exogenous TCR proteins with those of the endogenous. An alternative adoptive cell therapy approach would be to engineer the targeting TCR into NK cells. NK cells have well known cytolytic properties but limited growth and longevity when adoptively transferred into a host (238). To further improve the longevity of killer cells, cytokine genes (e.g. IL-2) can be transduced, as was the case for using NK92MI in our studies. NK92MI is a human NK cell line derived from a non-Hodgkin's lymphoma and transduced with human IL-2 cDNA; previous studies have demonstrated its strong cytotoxic abilities in mouse models (239, 240). In addition, NK92 cells have

also been used in the clinical setting and proven safe after a number of Phase I studies in patients with renal cell carcinoma and melanoma (241). Because of their ease of maintenance *in vitro* and relatively short doubling-times, these cells are ideal effectors for various cytotoxicity assays to test a variety of targeting approaches.

MHC-restricted, peptide-specific antibodies have been studied for over a decade. In addition to their value in studying antigen presentation, researchers have used these antibodies as targeting agents in the form of full length immunoglobulin, antibody-toxin fusions and chimeric antigen receptors. In this thesis, we detail the generation of two MHC-restricted, peptide-specific antibodies and their ability to function as CARs. As a proof of principle, we first focused our efforts on a scFv which bound to a peptide derived from EBNA3C. While most EBV-related tumors do not express EBNA3C (176), and as a result may not be candidates for therapy, targeting the LLDFVRFMGV TCE was chosen for the following reasons: 1) The peptide binds very tightly to HLA-A2 and does not bind to other HLA molecules; this has been established based on the peptide's ability to displace naturally presented peptides on HLA-A2<sup>+</sup> but not HLA-A2<sup>-</sup> BLCLs. 2) The recovered scFv was highly specific for its targeted complex and had the necessary affinity to allow us to carry out flow cytometric cell staining assays. 3) EBNA3C has previously been shown to be essential for B cell transformation after EBV infection (242), allowing us to look at natural peptide presentation and specific cell lysis using EBV-transformed BLCLs.

In addition to viral TCEs, we focused our efforts on a scFv which was able to specifically recognize a known WT1-derived peptide in the context of HLA-A2. The significance of such an antibody, especially in the context of adoptive cell therapy, is

highlighted by the large number of T cell-based clinical trials currently being carried out which target this antigen. WT1 overexpression has been demonstrated in leukemias, lymphomas and a wide variety of solid tumors including astrocytic tumors, sarcomas, breast, lung and colorectal cancer, and neuroblastoma (181, 182). The EBNA Clone 315 and WT1 Clone 45 CARs were introduced into NK92MI cells. These CAR-equipped effector cells were shown to have the capacity to specifically lyse peptide-pulsed HLA-A2<sup>+</sup> APCs in a peptide specific, HLA-restricted manner using CD107a effector cell expression and <sup>51</sup>Cr target cell release as markers of activation and cytotoxicity, respectively. More importantly, CAR-equipped NK92MI cells were shown to be able to recognize and kill BLCLs even when the targeted MHC-peptide complex is below the detection limit of the specific scFv or scFv-Fc fusion protein using flow cytometry. In support of killing being specific towards their targeted HLA-A2-peptide complexes, the scFv-Fc fusion proteins and anti-HLA-A2 antibodies could substantially inhibit CAR-mediated cytotoxicity. While the inhibition of killing of the unpulsed BLCL was not as complete as the peptide-pulsed BLCL, we interpreted that as residual nonspecific cytolytic activity of NK92 cells particularly at high E:T ratios. When expressed in T cells, we expect that they will have lower background killing, especially when the therapy is applied to the autologous setting.

In this thesis, we have explored CARs directed at the class I MHC-peptide complex. We believe that there are several advantages of using this targeting approach over a typical TCR or CAR directed at cell surface antigens: First, unlike CARs, mispairing between transduced and endogenous TCR  $\alpha$  and  $\beta$  chains can lead to impaired T cell functionality. This TCR chain mispairing has also been linked to changes in



receptor specificity which has previously been shown to lead to autoimmunity (243). Second, to build CARs, scFvs can be selected from naïve and immunized phage display libraries with diversities of more than  $10^{10}$ , which is not routinely feasible since TCR libraries are not available. Third, while TCR signaling requires a variety of other adapter and costimulatory molecules, 2<sup>nd</sup> and 3<sup>rd</sup> generation CARs come equipped with these signaling domains, allowing for costimulation of the effector cell without depending on the corresponding ligand on the target cell, which in the cancer setting is typically unavailable. Fourth, most CARs are built from scFvs directed at surface antigens; however, this repertoire is quite limited. Through the MHC class I window, peptide antigens derived from proteins inside the cytoplasm and the nucleus become exposed, as is the case with EBNA3C and WT1. MHC-peptide complexes offer a huge opportunity to identify the next generation of tumor-specific TCEs, which include mutations (e.g. HER2/neu) (244), fusion transcripts from chromosomal translocations (e.g. the bcr-abl translocation-derived TCE) (245), overexpressed oncoproteins (e.g. WT1), or viral antigens from virus-associated malignancies (e.g. EBV, HPV). Depending on the stringency used in selecting the scFv, the affinity for the targeted complex can be modified from 20 to 1000-fold, which can have profound influence on effector functions based on previously published work comparing CAR affinity and cytotoxicity at different antigen densities (44, 246).

A finding of potential importance is the ability of MHC-restricted, peptide-specific antibodies to efficiently block CAR-mediated killing. While the presence of such natural antibodies in normal or diseased individuals has yet to be proven, the B lymphocyte immune repertoire does appear to have the capacity to generate them, as

demonstrated by the human scFv phage display library used in our studies. In addition, due to a recent study which looked at maternal immunoglobulins towards the fetus' HLA, peptide-specificity seems to be present against specific TCEs, at least in the allogeneic settings (256). If these antibodies do exist naturally, they may function in inhibiting T cell mediated cytotoxicity against particular TCEs, which could be a humoral approach by which our immune system prevents unwanted autoimmune disease or help viruses evade a T cell response. On the other hand, these antibodies may be responsible in inducing antibody-dependent cell cytotoxicity (ADCC) or complement mediated cytotoxicity (CMC) in settings where T cells are otherwise ineffective, providing the immune system with yet another method of regulation and efficacy. As a result, MHC-restricted, peptide-specific antibodies should be studied in more detail in the context of immune regulation and therapeutic potential in human diseases.

While this thesis does encompass a large body of work, there are many questions which still need to be addressed. We believe these issues would be ideal future directions for the field of adoptive cell therapy using MHC-restricted, peptide-specific monoclonal antibodies and chimeric antigen receptors: 1) What properties constitute an ideal target? While it is plausible to target highly expressed antigens, in most cases those antigens are self proteins and could lead to unwanted toxicity. On the other hand, antigens which are highly tumor specific are relatively rare and in most cases expressed at very low levels. In this thesis, we try to address this antigen density threshold issue and what is required for CAR activation and target cell lysis by correlating MHC-peptide density with cytotoxicity. We were able to demonstrate that very low levels of antigen (25-100 complexes) were sufficient in activating NK92MI cells through CAR recognition. 2)

What is the optimal range of a CARs affinity towards its target antigen? While previous studies have shown that too high of an affinity can be detrimental to TCR-mediated cytotoxicity (247), other studies reveal a more complex relationship between CAR density, CAR affinity, CAR expression levels and antigen expression levels (248). We believe that our CARs have high affinity relative to a typical TCR, while being in the normal range of a typical TCR-like antibody. Since our scFv off-rate is only 10-fold greater than a typical TCR, our construct probably binds long enough to induce a signaling cascade inside NK92 cells while eventually releasing the target antigen and serially engaging other MHC-peptide complexes.

3) What is the optimal target epitope? Recent studies suggest that the distance of the epitope to the target cell surface, along with length and flexibility of the CAR hinge region, matter in regards to cytolytic efficiency (156, 249). These studies argue that longer and more flexible linkers seem to be essential for epitopes which are closer to the cell membrane. While this makes sense for large cell surface proteins, the epitopes we target in this work are at the top of the target antigen (the MHC-peptide interface), resulting in easy presentation of the epitope to the CAR. This epitope accessibility of the MHC-peptide complex may have to do with an evolutionary pressure put onto the MHC to efficiently present a peptide epitope to the TCR.

4) What cell types are ideal for CAR-based therapy? Currently, most researchers use bulk human peripheral T cells, however others have recently began to use EBV-specific T cells (250), lymphoid progenitor cells (251, 252), and unfractionated bone marrow cells (253, 254). We believe that our CAR has been positioned in an ideal cell type (NK92MI) since it is both highly cytolytic and easy to culture, providing a continuous supply of CAR expressing effector cells for pre-clinical and clinical testing.

5) Do TCR-like antibodies exist naturally in normal or diseased individuals? The implications behind such a finding would be enormous, as we discuss in the previous paragraph. To answer this question, it may be possible to first use an ELISA-based method to screen patient serum against a panel of recombinant MHC-peptide complexes. Subsequently, one would have to demonstrate that one or several B cell clones which generate these types of antibodies exist by potentially generating hybridoma's from patient blood after isolation using flow cytometry and fluorescently-labeled HLA-peptide tetramers. Similar work has been done in identifying and isolating HLA-A2-specific B lymphocytes using MHC Class I tetramers from pregnant women (255). Furthermore, the same group has even shown a link between the peptide sequence on the HLA pocket with the pattern of antibody recognition (256). If our hypothesis behind the role of these antibodies is true, then one ideal disease setting would be patients who fail WT1-specific adoptive T cell therapy, since these patients could potentially be making antibodies which block the T cells from recognizing the targeted TCE.

6) Can these antibodies be used to find new ways of enhancing antigen presentation? This may be possible due to a recent finding which shows that heat shock protein 90 (HSP90) regulates, among other things, the stability of WT1 in myeloid leukemias, and helps the protein fold properly while preventing it from ubiquitination (257). As a result, HSP90 inhibitors may be useful in enhancing epitope presentation by targeting proteins for degradation and potentially synergizing with adoptive cell therapies such as the ones used in our studies. More importantly, given the large repertoire of possible peptides derived from any single protein, a precise knowledge of which peptide is modulated by proteasome inhibitors or HSP90 inhibitors is critically important for the TCR or CAR-based therapy field.

7) Are

our CAR-equipped NK92MI cells able to kill and/or prevent tumor growth *in vivo*? While other groups have been successful using conventional CARs which target typical transmembrane receptors, targeting the MHC-peptide complex might be a different story. For this experiment, a model cell line would be the HLA-A2<sup>+</sup> DIMT BLCL, due to the fact that it can be killed naturally without peptide pulsing by both EBNA Clone 315 and WT1 Clone 45 CARs. Using severe combined immunodeficiency (SCID) mice, this cell line may be implanted along with the CAR-equipped NK92MI cells and tested for efficacy.

8) Can these CAR constructs be used in the context of T cells? While others have already demonstrated the functionality of their CARs in this setting, none have targeted a WT1-derived TCE using CAR-equipped T cells. Using our approach, it may be possible to establish long-lived WT1-specific T cells by specifically introducing the WT1 Clone 45 CAR into a memory T cell population which is already specific for EBV-derived TCEs. This will allow us to avoid TCR mispairing while making bispecific T cells which would get constant stimulation from EBV-infected cells naturally present in 90% of the patient population (258).

9) What is the key predictive factor in presentation of a targeted TCE? Several other groups have already demonstrated a strong link between the protein stability (or lack thereof) and antigen presentation, disproving the hypothesis that gene and protein expression alone will predict whether an epitope is presented (36, 224, 259). In addition, when we consider the fact that both EBNA3C and WT1 suppression leads to cancer cell senescence and growth inhibition (172, 260), the persistence of these proteins seems vital for cancer survival, although the equilibrium concentration is more a function of the kinetics of protein metabolism. Our studies demonstrated similar findings, with marked differences in CAR-mediated cytotoxic

sensitivity amongst HLA-A2<sup>+</sup> BLCLs and tumor cell lines. We believe that this is an important question to consider due to our predominant dependence on protein and gene expression in deciding whether patients should receive T cell-based immunotherapy. 10) Is it possible to target several TCEs of interest at the same time using a variety of MHC-restricted, peptide-specific CARs? Several groups have published promising data for the treatment of CMV and human papillomavirus (HPV) infections in which antigen-specificity was developed against a variety of TCEs using overlapping pools of peptides (261, 262). We believe that this therapeutic approach can be applied to most settings by targeting multiple epitopes using several MHC-restricted, peptide-specific CARs. By generating a multiclonal population of effector cells, we believe that the tumor will be less able to evade the immune system through single point mutations in a particular TCE.

As is the case with other studies, there are some potential drawbacks and pitfalls associated with this work: 1) Using 4-1BB as a CAR signaling molecule maybe inadequate or detrimental. There have been several contradictory studies which on the one hand show 4-1BB enhancing survival of T cells while on the other demonstrating that 4-1BB-deficient T cells are hyperproliferative (263-265). This paradox is even more evident when one looks at the studies which show agonistic anti-4-1BB antibodies in some cases enhancing antiviral and anti-tumor T cell responses (266, 267) while blocking B cell and CD4<sup>+</sup> T cell autoimmunity (268-271). Furthermore, in the context of NK cells, recent studies have even demonstrated that 4-1BB can act in an inhibitory manner (272, 273). While this may be of concern, a 2005 study which used the same construct that we applied to our work demonstrated enhanced activation and cytotoxicity when 4-1BB was used as a signaling molecule in regular NK cells (220). More importantly,

preliminary clinical data suggested highly favorable responses in patients receiving 4-1BB CAR-modified T cells. Nonetheless, 4-1BB may be limiting the potential of our CAR-mediated targeting strategy and further argues for the testing of our scFvs using different CAR constructs. 2) The use of NK92MI cells as clinically useful effectors could be limited. While studies using the original IL-2-dependent NK92 cell line have shown minimal toxicities in both mice and humans, the IL-2-transduced NK92MI cells may have a greater leukemogenic potential. One method by which researchers try and avoid leukemogenesis in SCID mice using NK92 cells is by irradiating the effectors with 3000 cGy before inoculation. While it is still uncertain, this may be sufficient in preventing NK92MI cells from proliferating uncontrollably inside of the patient. An alternative safety mechanism is that which involves the employment of suicide genes. One common example is the use of the herpesvirus thymidine kinase gene, which works by killing a cell which expresses the gene by administration of acyclovir or ganciclovir (274). Alternatively, other groups have included the human CD20 gene within their constructs, so that aberrantly proliferating cells can be destroyed using various anti-CD20-based therapies such as rituximab. 3) Antigen density levels may be too low for CAR-mediated cytotoxicity. While this work demonstrates that our CAR-transduced NK92MI cells are very sensitive at detecting and reacting to low levels of antigen (~25 complexes), in some cases the levels of a particular MHC-peptide complex may be even less. One of the best known mechanisms by which cancer cells avoid T lymphocyte recognition is by total or partial loss of class I MHC (275-277). This may be due to loss of heterozygosity or mutations in chromosomes which contain the class I heavy chain and  $\beta_2M$ , coordinate downregulation of HLA loci, and downregulation of antigen processing

machinery such as TAP. Fortunately in some cases, researchers have demonstrated that abnormal expression can be recovered using a variety of immunomodulators such as IFN- $\gamma$  (278, 279).

In closing, there are several truly unique and novel aspects about this work: First, MHC-restricted, peptide-specific monoclonal antibodies were isolated from a human scFv phage display library which is approximately 100-fold smaller than what has been previously published for this type of work, demonstrating that these types of antibodies are quite common in the human B-cell repertoire. Second, for the first time, scFv-Fc fusion protein versions of these antibodies have been created and used to study antigen presentation, determine affinity, assist in quantifying antigen density, and demonstrate the capacity to induce ADCC. Third, CAR versions of these antibodies were made and expressed in the highly cytolytic NK92MI cell line, leading to highly sensitive and specific target cell killing. Fourth, the CAR targeting approach was shown to be far superior to that of an antibody-mediated approach when comparing their abilities to recognize low levels of antigen or kill cells which express high levels of antigen. In our direct comparison assay, the targeting agents for the CAR and scFv-Fc fusion protein were exactly the same (EBNA Clone 315), in addition to the peptide-pulsed target cells, NK92MI cell type, assay incubation time and E:T ratio. However, with all of these factors taken into account the CAR-mediated approach proved far more effective at killing target cells compared to ADCC. Our results prove somewhat different than what others have demonstrated when targeting CD20 (280), in which they claim that both targeting methods are comparable. Fifth, CAR-mediated killing could be blocked using the scFv-Fc fusion protein from which it was originally derived from. This finding not



only demonstrates the specificity of our CAR in a manner not seen in other studies, but it also points out the potential role of these types of antibodies in inhibiting an immune response directed at an MHC-peptide complex. We believe that our findings have major implications in the field of cancer immunotherapy.

## BIBLIOGRAPHY

1. Stone, M. J. 2001. Monoclonal antibodies in the prehybridoma era: a brief historical perspective and personal reminiscence. *Clinical lymphoma* 2:148-154.
2. Van Epps, H. L. 2005. How Heidelberger and Avery sweetened immunology. *The Journal of experimental medicine* 202:1306.
3. Tassev, D. V., and N. K. Cheung. 2009. Monoclonal antibody therapies for solid tumors. *Expert opinion on biological therapy* 9:341-353.
4. Kerr, W. G., L. M. Hendershot, and P. D. Burrows. 1991. Regulation of IgM and IgD expression in human B-lineage cells. *J Immunol* 146:3314-3321.
5. Kohler, G., and C. Milstein. 1975. Continuous cultures of fused cells secreting antibody of predefined specificity. *Nature* 256:495-497.
6. Adekar, S. P., R. M. Jones, M. D. Elias, F. H. Al-Saleem, M. J. Root, L. L. Simpson, and S. K. Dessain. 2008. Hybridoma populations enriched for affinity-matured human IgGs yield high-affinity antibodies specific for botulinum neurotoxins. *Journal of immunological methods* 333:156-166.
7. Jakobovits, A., G. J. Vergara, J. L. Kennedy, J. F. Hales, R. P. McGuinness, D. E. Casentini-Borocz, D. G. Brenner, and G. R. Otten. 1993. Analysis of homozygous mutant chimeric mice: deletion of the immunoglobulin heavy-chain joining region blocks B-cell development and antibody production. *Proceedings of the National Academy of Sciences of the United States of America* 90:2551-2555.
8. Ishida, I., K. Tomizuka, H. Yoshida, and Y. Kuroiwa. 2002. TransChromo Mouse. *Biotechnology & genetic engineering reviews* 19:73-82.
9. Ishida, I., K. Tomizuka, H. Yoshida, T. Tahara, N. Takahashi, A. Ohguma, S. Tanaka, M. Umehashi, H. Maeda, C. Nozaki, E. Halk, and N. Lonberg. 2002. Production of human monoclonal and polyclonal antibodies in TransChromo animals. *Cloning and stem cells* 4:91-102.
10. Oldham, R. K., and R. O. Dillman. 2008. Monoclonal antibodies in cancer therapy: 25 years of progress. *J Clin Oncol* 26:1774-1777.
11. Castillo, J., E. Winer, and P. Quesenberry. 2008. Newer monoclonal antibodies for hematological malignancies. *Experimental hematology* 36:755-768.
12. Boyiadzis, M., and K. A. Foon. 2008. Approved monoclonal antibodies for cancer therapy. *Expert opinion on biological therapy* 8:1151-1158.
13. Fridman, W. H. 1991. Fc receptors and immunoglobulin binding factors. *Faseb J* 5:2684-2690.
14. Padlan, E. A. 1991. A possible procedure for reducing the immunogenicity of antibody variable domains while preserving their ligand-binding properties. *Molecular immunology* 28:489-498.
15. Peipp, M., J. J. Lammerts van Bueren, T. Schneider-Merck, W. W. Bleeker, M. Dechant, T. Beyer, R. Repp, P. H. van Berkel, T. Vink, J. G. van de Winkel, P. W. Parren, and T. Valerius. 2008. Antibody fucosylation differentially impacts cytotoxicity mediated by NK and PMN effector cells. *Blood* 112:2390-2399.
16. Yokota, T., D. E. Milenic, M. Whitlow, and J. Schlom. 1992. Rapid tumor penetration of a single-chain Fv and comparison with other immunoglobulin forms. *Cancer research* 52:3402-3408.

17. Gram, H., L. A. Marconi, C. F. Barbas, 3rd, T. A. Collet, R. A. Lerner, and A. S. Kang. 1992. In vitro selection and affinity maturation of antibodies from a naive combinatorial immunoglobulin library. *Proceedings of the National Academy of Sciences of the United States of America* 89:3576-3580.
18. Adams, G. P., R. Schier, A. M. McCall, R. S. Crawford, E. J. Wolf, L. M. Weiner, and J. D. Marks. 1998. Prolonged in vivo tumour retention of a human diabody targeting the extracellular domain of human HER2/neu. *British journal of cancer* 77:1405-1412.
19. Schuhmacher, J., G. Klivenyi, R. Matys, M. Stadler, T. Regiert, H. Hauser, J. Doll, W. Maier-Borst, and M. Zoller. 1995. Multistep tumor targeting in nude mice using bispecific antibodies and a gallium chelate suitable for immunoscintigraphy with positron emission tomography. *Cancer research* 55:115-123.
20. Cheung, N. K., S. Modak, Y. Lin, H. Guo, P. Zanzonico, J. Chung, Y. Zuo, J. Sanderson, S. Wilbert, L. J. Theodore, D. B. Axworthy, and S. M. Larson. 2004. Single-chain Fv-streptavidin substantially improved therapeutic index in multistep targeting directed at disialoganglioside GD2. *J Nucl Med* 45:867-877.
21. Andersen, P. S., A. Stryhn, B. E. Hansen, L. Fugger, J. Engberg, and S. Buus. 1996. A recombinant antibody with the antigen-specific, major histocompatibility complex-restricted specificity of T cells. *Proceedings of the National Academy of Sciences of the United States of America* 93:1820-1824.
22. Porgador, A., J. W. Yewdell, Y. Deng, J. R. Bennink, and R. N. Germain. 1997. Localization, quantitation, and in situ detection of specific peptide-MHC class I complexes using a monoclonal antibody. *Immunity* 6:715-726.
23. Zhong, G., C. Reis e Sousa, and R. N. Germain. 1997. Production, specificity, and functionality of monoclonal antibodies to specific peptide-major histocompatibility complex class II complexes formed by processing of exogenous protein. *Proceedings of the National Academy of Sciences of the United States of America* 94:13856-13861.
24. Dadaglio, G., C. A. Nelson, M. B. Deck, S. J. Petzold, and E. R. Unanue. 1997. Characterization and quantitation of peptide-MHC complexes produced from hen egg lysozyme using a monoclonal antibody. *Immunity* 6:727-738.
25. Lev, A., G. Denkberg, C. J. Cohen, M. Tzukerman, K. L. Skorecki, P. Chames, H. R. Hoogenboom, and Y. Reiter. 2002. Isolation and characterization of human recombinant antibodies endowed with the antigen-specific, major histocompatibility complex-restricted specificity of T cells directed toward the widely expressed tumor T-cell epitopes of the telomerase catalytic subunit. *Cancer research* 62:3184-3194.
26. Chames, P., S. E. Hufton, P. G. Coulie, B. Uchanska-Ziegler, and H. R. Hoogenboom. 2000. Direct selection of a human antibody fragment directed against the tumor T-cell epitope HLA-A1-MAGE-A1 from a nonimmunized phage-Fab library. *Proceedings of the National Academy of Sciences of the United States of America* 97:7969-7974.
27. Denkberg, G., C. J. Cohen, A. Lev, P. Chames, H. R. Hoogenboom, and Y. Reiter. 2002. Direct visualization of distinct T cell epitopes derived from a melanoma tumor-associated antigen by using human recombinant antibodies with

- MHC- restricted T cell receptor-like specificity. *Proceedings of the National Academy of Sciences of the United States of America* 99:9421-9426.
28. Held, G., M. Matsuo, M. Epel, S. Gnjatic, G. Ritter, S. Y. Lee, T. Y. Tai, C. J. Cohen, L. J. Old, M. Pfreundschuh, Y. Reiter, H. R. Hoogenboom, and C. Renner. 2004. Dissecting cytotoxic T cell responses towards the NY-ESO-1 protein by peptide/MHC-specific antibody fragments. *European journal of immunology* 34:2919-2929.
  29. Held, G., A. Wadle, N. Dauth, G. Stewart-Jones, C. Sturm, M. Thiel, C. Zwick, D. Dieckmann, G. Schuler, H. R. Hoogenboom, F. Levy, V. Cerundolo, M. Pfreundschuh, and C. Renner. 2007. MHC-peptide-specific antibodies reveal inefficient presentation of an HLA-A\*0201-restricted, Melan-A-derived peptide after active intracellular processing. *European journal of immunology* 37:2008-2017.
  30. Klechevsky, E., M. Gallegos, G. Denkberg, K. Palucka, J. Banchereau, C. Cohen, and Y. Reiter. 2008. Antitumor activity of immunotoxins with T-cell receptor-like specificity against human melanoma xenografts. *Cancer research* 68:6360-6367.
  31. Cohen, C. J., O. Sarig, Y. Yamano, U. Tomaru, S. Jacobson, and Y. Reiter. 2003. Direct phenotypic analysis of human MHC class I antigen presentation: visualization, quantitation, and in situ detection of human viral epitopes using peptide-specific, MHC-restricted human recombinant antibodies. *J Immunol* 170:4349-4361.
  32. Cohen, C. J., N. Hoffmann, M. Farago, H. R. Hoogenboom, L. Eisenbach, and Y. Reiter. 2002. Direct detection and quantitation of a distinct T-cell epitope derived from tumor-specific epithelial cell-associated mucin using human recombinant antibodies endowed with the antigen-specific, major histocompatibility complex-restricted specificity of T cells. *Cancer research* 62:5835-5844.
  33. Epel, M., I. Carmi, S. Soueid-Baumgarten, S. K. Oh, T. Bera, I. Pastan, J. Berzofsky, and Y. Reiter. 2008. Targeting TARP, a novel breast and prostate tumor-associated antigen, with T cell receptor-like human recombinant antibodies. *European journal of immunology* 38:1706-1720.
  34. Neumann, F., C. Sturm, M. Hulsmeyer, N. Dauth, P. Guillaume, I. F. Luescher, M. Pfreundschuh, and G. Held. 2009. Fab antibodies capable of blocking T cells by competitive binding have the identical specificity but a higher affinity to the MHC-peptide-complex than the T cell receptor. *Immunology letters* 125:86-92.
  35. Makler, O., K. Oved, N. Netzer, D. Wolf, and Y. Reiter. 2010. Direct visualization of the dynamics of antigen presentation in human cells infected with cytomegalovirus revealed by antibodies mimicking TCR specificity. *European journal of immunology* 40:1552-1565.
  36. Michaeli, Y., G. Denkberg, K. Sinik, L. Lantzy, C. Chih-Sheng, C. Beauverd, T. Ziv, P. Romero, and Y. Reiter. 2009. Expression hierarchy of T cell epitopes from melanoma differentiation antigens: unexpected high level presentation of tyrosinase-HLA-A2 Complexes revealed by peptide-specific, MHC-restricted, TCR-like antibodies. *J Immunol* 182:6328-6341.
  37. Weidanz, J. A., P. Piazza, H. Hickman-Miller, D. Woodburn, T. Nguyen, A. Wahl, F. Neethling, M. Chiriva-Internati, C. R. Rinaldo, and W. H. Hildebrand. 2007. Development and implementation of a direct detection, quantitation and

- validation system for class I MHC self-peptide epitopes. *Journal of immunological methods* 318:47-58.
38. Verma, B., O. E. Hawkins, F. A. Neethling, S. L. Caseltine, S. R. Largo, W. H. Hildebrand, and J. A. Weidanz. 2009. Direct discovery and validation of a peptide/MHC epitope expressed in primary human breast cancer cells using a TCRm monoclonal antibody with profound antitumor properties. *Cancer Immunol Immunother* 59:563-573.
  39. Verma, B., F. A. Neethling, S. Caseltine, G. Fabrizio, S. Largo, J. A. Duty, P. Tabaczewski, and J. A. Weidanz. 2010. TCR mimic monoclonal antibody targets a specific peptide/HLA class I complex and significantly impedes tumor growth in vivo using breast cancer models. *J Immunol* 184:2156-2165.
  40. Wittman, V. P., D. Woodburn, T. Nguyen, F. A. Neethling, S. Wright, and J. A. Weidanz. 2006. Antibody targeting to a class I MHC-peptide epitope promotes tumor cell death. *J Immunol* 177:4187-4195.
  41. Reiter, Y., A. Di Carlo, L. Fugger, J. Engberg, and I. Pastan. 1997. Peptide-specific killing of antigen-presenting cells by a recombinant antibody-toxin fusion protein targeted to major histocompatibility complex/peptide class I complexes with T cell receptor-like specificity. *Proceedings of the National Academy of Sciences of the United States of America* 94:4631-4636.
  42. Stewart-Jones, G., A. Wadle, A. Hombach, E. Shenderov, G. Held, E. Fischer, S. Kleber, N. Nuber, F. Stenner-Liewen, S. Bauer, A. McMichael, A. Knuth, H. Abken, A. A. Hombach, V. Cerundolo, E. Y. Jones, and C. Renner. 2009. Rational development of high-affinity T-cell receptor-like antibodies. *Proceedings of the National Academy of Sciences of the United States of America* 106:5784-5788.
  43. Willemsen, R. A., R. Debets, E. Hart, H. R. Hoogenboom, R. L. Bolhuis, and P. Chames. 2001. A phage display selected fab fragment with MHC class I-restricted specificity for MAGE-A1 allows for retargeting of primary human T lymphocytes. *Gene therapy* 8:1601-1608.
  44. Chames, P., R. A. Willemsen, G. Rojas, D. Dieckmann, L. Rem, G. Schuler, R. L. Bolhuis, and H. R. Hoogenboom. 2002. TCR-like human antibodies expressed on human CTLs mediate antibody affinity-dependent cytolytic activity. *J Immunol* 169:1110-1118.
  45. Willemsen, R. A., C. Ronteltap, P. Chames, R. Debets, and R. L. Bolhuis. 2005. T cell retargeting with MHC class I-restricted antibodies: the CD28 costimulatory domain enhances antigen-specific cytotoxicity and cytokine production. *J Immunol* 174:7853-7858.
  46. Hulsmeyer, M., P. Chames, R. C. Hillig, R. L. Stanfield, G. Held, P. G. Coulie, C. Alings, G. Wille, W. Saenger, B. Uchanska-Ziegler, H. R. Hoogenboom, and A. Ziegler. 2005. A major histocompatibility complex-peptide-restricted antibody and t cell receptor molecules recognize their target by distinct binding modes: crystal structure of human leukocyte antigen (HLA)-A1-MAGE-A1 in complex with FAB-HYB3. *The Journal of biological chemistry* 280:2972-2980.
  47. Rojas, R., and G. Apodaca. 2002. Immunoglobulin transport across polarized epithelial cells. *Nature reviews* 3:944-955.

48. Steinitz, M. 2009. Three decades of human monoclonal antibodies: past, present and future developments. *Human antibodies* 18:1-10.
49. Carmen, S., and L. Jeremius. 2002. Concepts in antibody phage display. *Briefings in functional genomics & proteomics* 1:189-203.
50. Schmidt, M. M., and K. D. Wittrup. 2009. A modeling analysis of the effects of molecular size and binding affinity on tumor targeting. *Molecular cancer therapeutics* 8:2861-2871.
51. Bjorkman, P. J., M. A. Saper, B. Samraoui, W. S. Bennett, J. L. Strominger, and D. C. Wiley. 1987. Structure of the human class I histocompatibility antigen, HLA-A2. *Nature* 329:506-512.
52. Elliott, T., V. Cerundolo, J. Elvin, and A. Townsend. 1991. Peptide-induced conformational change of the class I heavy chain. *Nature* 351:402-406.
53. Townsend, A., C. Ohlen, J. Bastin, H. G. Ljunggren, L. Foster, and K. Karre. 1989. Association of class I major histocompatibility heavy and light chains induced by viral peptides. *Nature* 340:443-448.
54. Falk, K., O. Rotzschke, and H. G. Rammensee. 1990. Cellular peptide composition governed by major histocompatibility complex class I molecules. *Nature* 348:248-251.
55. Falk, K., O. Rotzschke, S. Stevanovic, G. Jung, and H. G. Rammensee. 1991. Allele-specific motifs revealed by sequencing of self-peptides eluted from MHC molecules. *Nature* 351:290-296.
56. Schubert, U., L. C. Anton, J. Gibbs, C. C. Norbury, J. W. Yewdell, and J. R. Bennink. 2000. Rapid degradation of a large fraction of newly synthesized proteins by proteasomes. *Nature* 404:770-774.
57. Reits, E., J. Neijssen, C. Herberts, W. Benckhuijsen, L. Janssen, J. W. Drijfhout, and J. Neefjes. 2004. A major role for TPPII in trimming proteasomal degradation products for MHC class I antigen presentation. *Immunity* 20:495-506.
58. Stoltze, L., M. Schirle, G. Schwarz, C. Schroter, M. W. Thompson, L. B. Hersh, H. Kalbacher, S. Stevanovic, H. G. Rammensee, and H. Schild. 2000. Two new proteases in the MHC class I processing pathway. *Nature immunology* 1:413-418.
59. York, I. A., M. A. Brehm, S. Zenzian, C. F. Towne, and K. L. Rock. 2006. Endoplasmic reticulum aminopeptidase 1 (ERAP1) trims MHC class I-presented peptides in vivo and plays an important role in immunodominance. *Proceedings of the National Academy of Sciences of the United States of America* 103:9202-9207.
60. Seifert, U., C. Maranon, A. Shmueli, J. F. Desoutter, L. Wesoloski, K. Janek, P. Henklein, S. Diescher, M. Andrieu, H. de la Salle, T. Weinschenk, H. Schild, D. Laderach, A. Galy, G. Haas, P. M. Kloetzel, Y. Reiss, and A. Hosmalin. 2003. An essential role for tripeptidyl peptidase in the generation of an MHC class I epitope. *Nature immunology* 4:375-379.
61. Schatz, M. M., B. Peters, N. Akkad, N. Ullrich, A. N. Martinez, O. Carroll, S. Bulik, H. G. Rammensee, P. van Endert, H. G. Holzhutter, S. Tenzer, and H. Schild. 2008. Characterizing the N-terminal processing motif of MHC class I ligands. *J Immunol* 180:3210-3217.

62. Neefjes, J., E. Gottfried, J. Roelse, M. Gromme, R. Obst, G. J. Hammerling, and F. Momburg. 1995. Analysis of the fine specificity of rat, mouse and human TAP peptide transporters. *European journal of immunology* 25:1133-1136.
63. Sadasivan, B., P. J. Lehner, B. Ortman, T. Spies, and P. Cresswell. 1996. Roles for calreticulin and a novel glycoprotein, tapasin, in the interaction of MHC class I molecules with TAP. *Immunity* 5:103-114.
64. Lehner, P. J., M. J. Surman, and P. Cresswell. 1998. Soluble tapasin restores MHC class I expression and function in the tapasin-negative cell line .220. *Immunity* 8:221-231.
65. Li, S., K. M. Paulsson, S. Chen, H. O. Sjogren, and P. Wang. 2000. Tapasin is required for efficient peptide binding to transporter associated with antigen processing. *The Journal of biological chemistry* 275:1581-1586.
66. Morrice, N. A., and S. J. Powis. 1998. A role for the thiol-dependent reductase ERp57 in the assembly of MHC class I molecules. *Curr Biol* 8:713-716.
67. Lindquist, J. A., O. N. Jensen, M. Mann, and G. J. Hammerling. 1998. ER-60, a chaperone with thiol-dependent reductase activity involved in MHC class I assembly. *The EMBO journal* 17:2186-2195.
68. Hughes, E. A., and P. Cresswell. 1998. The thiol oxidoreductase ERp57 is a component of the MHC class I peptide-loading complex. *Curr Biol* 8:709-712.
69. Smith, G. P. 1985. Filamentous fusion phage: novel expression vectors that display cloned antigens on the virion surface. *Science (New York, N.Y)* 228:1315-1317.
70. Marks, J. D., H. R. Hoogenboom, T. P. Bonnert, J. McCafferty, A. D. Griffiths, and G. Winter. 1991. By-passing immunization. Human antibodies from V-gene libraries displayed on phage. *Journal of molecular biology* 222:581-597.
71. Griffiths, A. D., M. Malmqvist, J. D. Marks, J. M. Bye, M. J. Embleton, J. McCafferty, M. Baier, K. P. Holliger, B. D. Gorick, N. C. Hughes-Jones, and et al. 1993. Human anti-self antibodies with high specificity from phage display libraries. *The EMBO journal* 12:725-734.
72. Marks, J. D., W. H. Ouwehand, J. M. Bye, R. Finnern, B. D. Gorick, D. Voak, S. J. Thorpe, N. C. Hughes-Jones, and G. Winter. 1993. Human antibody fragments specific for human blood group antigens from a phage display library. *Bio/technology (Nature Publishing Company)* 11:1145-1149.
73. Garrard, L. J., and D. J. Henner. 1993. Selection of an anti-IGF-1 Fab from a Fab phage library created by mutagenesis of multiple CDR loops. *Gene* 128:103-109.
74. Akamatsu, Y., M. S. Cole, J. Y. Tso, and N. Tsurushita. 1993. Construction of a human Ig combinatorial library from genomic V segments and synthetic CDR3 fragments. *J Immunol* 151:4651-4659.
75. Baeuerle, P. A., and C. Reinhardt. 2009. Bispecific T-cell engaging antibodies for cancer therapy. *Cancer research* 69:4941-4944.
76. Bratkovic, T. 2010. Progress in phage display: evolution of the technique and its application. *Cell Mol Life Sci* 67:749-767.
77. Kourilov, V., and M. Steinitz. 2002. Magnetic-bead enzyme-linked immunosorbent assay verifies adsorption of ligand and epitope accessibility. *Analytical biochemistry* 311:166-170.

78. Ooi, D. J., A. Dzulkurnain, R. Y. Othman, S. H. Lim, and J. A. Harikrishna. 2006. Use of superparamagnetic beads for the isolation of a peptide with specificity to cymbidium mosaic virus. *Journal of virological methods* 136:160-165.
79. Oyama, T., I. T. Rombel, K. N. Samli, X. Zhou, and K. C. Brown. 2006. Isolation of multiple cell-binding ligands from different phage displayed-peptide libraries. *Biosensors & bioelectronics* 21:1867-1875.
80. Siegel, D. L., T. Y. Chang, S. L. Russell, and V. Y. Bunya. 1997. Isolation of cell surface-specific human monoclonal antibodies using phage display and magnetically-activated cell sorting: applications in immunohematology. *Journal of immunological methods* 206:73-85.
81. Krumpe, L. R., and T. Mori. 2006. The Use of Phage-Displayed Peptide Libraries to Develop Tumor-Targeting Drugs. *International journal of peptide research and therapeutics* 12:79-91.
82. Allison, J. P., and L. L. Lanier. 1987. Structure, function, and serology of the T-cell antigen receptor complex. *Annual review of immunology* 5:503-540.
83. Clevers, H., B. Alarcon, T. Wileman, and C. Terhorst. 1988. The T cell receptor/CD3 complex: a dynamic protein ensemble. *Annual review of immunology* 6:629-662.
84. Weiss, A. 1991. Molecular and genetic insights into T cell antigen receptor structure and function. *Annual review of genetics* 25:487-510.
85. Samelson, L. E. 2002. Signal transduction mediated by the T cell antigen receptor: the role of adapter proteins. *Annual review of immunology* 20:371-394.
86. Allison, J. P., B. W. McIntyre, and D. Bloch. 1982. Tumor-specific antigen of murine T-lymphoma defined with monoclonal antibody. *J Immunol* 129:2293-2300.
87. Haskins, K., R. Kubo, J. White, M. Pigeon, J. Kappler, and P. Murrack. 1983. The major histocompatibility complex-restricted antigen receptor on T cells. I. Isolation with a monoclonal antibody. *The Journal of experimental medicine* 157:1149-1169.
88. Kindred, B., and D. C. Shreffler. 1972. H-2 dependence of co-operation between T and B cells in vivo. *J Immunol* 109:940-943.
89. Zinkernagel, R. M., and P. C. Doherty. 1974. Restriction of in vitro T cell-mediated cytotoxicity in lymphocytic choriomeningitis within a syngeneic or semiallogeneic system. *Nature* 248:701-702.
90. Borst, J., J. E. Coligan, H. Oettgen, S. Pessano, R. Malin, and C. Terhorst. 1984. The delta- and epsilon-chains of the human T3/T-cell receptor complex are distinct polypeptides. *Nature* 312:455-458.
91. Oettgen, H. C., J. Kappler, W. J. Tax, and C. Terhorst. 1984. Characterization of the two heavy chains of the T3 complex on the surface of human T lymphocytes. *The Journal of biological chemistry* 259:12039-12048.
92. Meuer, S. C., S. F. Schlossman, and E. L. Reinherz. 1982. Clonal analysis of human cytotoxic T lymphocytes: T4+ and T8+ effector T cells recognize products of different major histocompatibility complex regions. *Proceedings of the National Academy of Sciences of the United States of America* 79:4395-4399.



93. Abraham, N., M. C. Miceli, J. R. Parnes, and A. Veillette. 1991. Enhancement of T-cell responsiveness by the lymphocyte-specific tyrosine protein kinase p56lck. *Nature* 350:62-66.
94. Straus, D. B., and A. Weiss. 1992. Genetic evidence for the involvement of the lck tyrosine kinase in signal transduction through the T cell antigen receptor. *Cell* 70:585-593.
95. Zhang, W., J. Sloan-Lancaster, J. Kitchen, R. P. Tribble, and L. E. Samelson. 1998. LAT: the ZAP-70 tyrosine kinase substrate that links T cell receptor to cellular activation. *Cell* 92:83-92.
96. Williams, B. L., B. J. Irvin, S. L. Sutor, C. C. Chini, E. Yacyshyn, J. Bubeck Wardenburg, M. Dalton, A. C. Chan, and R. T. Abraham. 1999. Phosphorylation of Tyr319 in ZAP-70 is required for T-cell antigen receptor-dependent phospholipase C-gamma1 and Ras activation. *The EMBO journal* 18:1832-1844.
97. Bubeck Wardenburg, J., C. Fu, J. K. Jackman, H. Flotow, S. E. Wilkinson, D. H. Williams, R. Johnson, G. Kong, A. C. Chan, and P. R. Findell. 1996. Phosphorylation of SLP-76 by the ZAP-70 protein-tyrosine kinase is required for T-cell receptor function. *The Journal of biological chemistry* 271:19641-19644.
98. Franklin, R. A., A. Tordai, H. Patel, A. M. Gardner, G. L. Johnson, and E. W. Gelfand. 1994. Ligation of the T cell receptor complex results in activation of the Ras/Raf-1/MEK/MAPK cascade in human T lymphocytes. *The Journal of clinical investigation* 93:2134-2140.
99. Penninger, J. M., J. Irie-Sasaki, T. Sasaki, and A. J. Oliveira-dos-Santos. 2001. CD45: new jobs for an old acquaintance. *Nature immunology* 2:389-396.
100. Mustelin, T., and A. Altman. 1990. Dephosphorylation and activation of the T cell tyrosine kinase pp56lck by the leukocyte common antigen (CD45). *Oncogene* 5:809-813.
101. Mustelin, T., K. M. Coggeshall, and A. Altman. 1989. Rapid activation of the T-cell tyrosine protein kinase pp56lck by the CD45 phosphotyrosine phosphatase. *Proceedings of the National Academy of Sciences of the United States of America* 86:6302-6306.
102. D'Oro, U., and J. D. Ashwell. 1999. Cutting edge: the CD45 tyrosine phosphatase is an inhibitor of Lck activity in thymocytes. *J Immunol* 162:1879-1883.
103. Johnson, K. G., S. K. Bromley, M. L. Dustin, and M. L. Thomas. 2000. A supramolecular basis for CD45 tyrosine phosphatase regulation in sustained T cell activation. *Proceedings of the National Academy of Sciences of the United States of America* 97:10138-10143.
104. Ledbetter, J. A., C. H. June, L. S. Grosmaire, and P. S. Rabinovitch. 1987. Crosslinking of surface antigens causes mobilization of intracellular ionized calcium in T lymphocytes. *Proceedings of the National Academy of Sciences of the United States of America* 84:1384-1388.
105. Moretta, A., A. Poggi, D. Olive, C. Bottino, C. Fortis, G. Pantaleo, and L. Moretta. 1987. Selection and characterization of T-cell variants lacking molecules involved in T-cell activation (T3 T-cell receptor, T44, and T11): analysis of the functional relationship among different pathways of activation. *Proceedings of the National Academy of Sciences of the United States of America* 84:1654-1658.

106. Frauwirth, K. A., and C. B. Thompson. 2002. Activation and inhibition of lymphocytes by costimulation. *The Journal of clinical investigation* 109:295-299.
107. Michel, F., G. Attal-Bonnefoy, G. Mangino, S. Mise-Omata, and O. Acuto. 2001. CD28 as a molecular amplifier extending TCR ligation and signaling capabilities. *Immunity* 15:935-945.
108. Michel, F., G. Mangino, G. Attal-Bonnefoy, L. Tuosto, A. Alcover, A. Roumier, D. Olive, and O. Acuto. 2000. CD28 utilizes Vav-1 to enhance TCR-proximal signaling and NF-AT activation. *J Immunol* 165:3820-3829.
109. Myers, L. M., and A. T. Vella. 2005. Interfacing T-cell effector and regulatory function through CD137 (4-1BB) co-stimulation. *Trends in immunology* 26:440-446.
110. Richter, G., and S. Burdach. 2004. ICOS: a new costimulatory ligand/receptor pair and its role in T-cell activation. *Onkologie* 27:91-95.
111. Sugamura, K., N. Ishii, and A. D. Weinberg. 2004. Therapeutic targeting of the effector T-cell co-stimulatory molecule OX40. *Nat Rev Immunol* 4:420-431.
112. Brunet, J. F., F. Denizot, M. F. Luciani, M. Roux-Dosseto, M. Suzan, M. G. Mattei, and P. Golstein. 1987. A new member of the immunoglobulin superfamily--CTLA-4. *Nature* 328:267-270.
113. Linsley, P. S., W. Brady, M. Urnes, L. S. Grosmaire, N. K. Damle, and J. A. Ledbetter. 1991. CTLA-4 is a second receptor for the B cell activation antigen B7. *The Journal of experimental medicine* 174:561-569.
114. Perkins, D., Z. Wang, C. Donovan, H. He, D. Mark, G. Guan, Y. Wang, T. Walunas, J. Bluestone, J. Listman, and P. W. Finn. 1996. Regulation of CTLA-4 expression during T cell activation. *J Immunol* 156:4154-4159.
115. Walunas, T. L., C. Y. Bakker, and J. A. Bluestone. 1996. CTLA-4 ligation blocks CD28-dependent T cell activation. *The Journal of experimental medicine* 183:2541-2550.
116. Walunas, T. L., D. J. Lenschow, C. Y. Bakker, P. S. Linsley, G. J. Freeman, J. M. Green, C. B. Thompson, and J. A. Bluestone. 1994. CTLA-4 can function as a negative regulator of T cell activation. *Immunity* 1:405-413.
117. Agata, Y., A. Kawasaki, H. Nishimura, Y. Ishida, T. Tsubata, H. Yagita, and T. Honjo. 1996. Expression of the PD-1 antigen on the surface of stimulated mouse T and B lymphocytes. *International immunology* 8:765-772.
118. Wang, J., T. Yoshida, F. Nakaki, H. Hiai, T. Okazaki, and T. Honjo. 2005. Establishment of NOD-Pdcd1<sup>-/-</sup> mice as an efficient animal model of type I diabetes. *Proceedings of the National Academy of Sciences of the United States of America* 102:11823-11828.
119. Nishimura, H., T. Okazaki, Y. Tanaka, K. Nakatani, M. Hara, A. Matsumori, S. Sasayama, A. Mizoguchi, H. Hiai, N. Minato, and T. Honjo. 2001. Autoimmune dilated cardiomyopathy in PD-1 receptor-deficient mice. *Science (New York, N.Y)* 291:319-322.
120. Riddell, S. R., K. S. Watanabe, J. M. Goodrich, C. R. Li, M. E. Agha, and P. D. Greenberg. 1992. Restoration of viral immunity in immunodeficient humans by the adoptive transfer of T cell clones. *Science (New York, N.Y)* 257:238-241.
121. Papadopoulos, E. B., M. Ladanyi, D. Emanuel, S. Mackinnon, F. Boulad, M. H. Carabasi, H. Castro-Malaspina, B. H. Childs, A. P. Gillio, T. N. Small, and et al.

1994. Infusions of donor leukocytes to treat Epstein-Barr virus-associated lymphoproliferative disorders after allogeneic bone marrow transplantation. *The New England journal of medicine* 330:1185-1191.
122. Louis, C. U., K. Straathof, C. M. Bollard, C. Gerken, M. H. Huls, M. V. Gresik, M. F. Wu, H. L. Weiss, A. P. Gee, M. K. Brenner, C. M. Rooney, H. E. Heslop, and S. Gottschalk. 2009. Enhancing the in vivo expansion of adoptively transferred EBV-specific CTL with lymphodepleting CD45 monoclonal antibodies in NPC patients. *Blood* 113:2442-2450.
123. Bollard, C. M., L. Aguilar, K. C. Straathof, B. Gahn, M. H. Huls, A. Rousseau, J. Sixbey, M. V. Gresik, G. Carrum, M. Hudson, D. Dilloo, A. Gee, M. K. Brenner, C. M. Rooney, and H. E. Heslop. 2004. Cytotoxic T lymphocyte therapy for Epstein-Barr virus+ Hodgkin's disease. *The Journal of experimental medicine* 200:1623-1633.
124. Rosenberg, S. A., B. S. Packard, P. M. Aebersold, D. Solomon, S. L. Topalian, S. T. Toy, P. Simon, M. T. Lotze, J. C. Yang, C. A. Seipp, and et al. 1988. Use of tumor-infiltrating lymphocytes and interleukin-2 in the immunotherapy of patients with metastatic melanoma. A preliminary report. *The New England journal of medicine* 319:1676-1680.
125. Kolb, H. J., J. Mittermuller, C. Clemm, E. Holler, G. Ledderose, G. Brehm, M. Heim, and W. Wilmanns. 1990. Donor leukocyte transfusions for treatment of recurrent chronic myelogenous leukemia in marrow transplant patients. *Blood* 76:2462-2465.
126. Dudley, M. E., J. R. Wunderlich, P. F. Robbins, J. C. Yang, P. Hwu, D. J. Schwartzentruber, S. L. Topalian, R. Sherry, N. P. Restifo, A. M. Hubicki, M. R. Robinson, M. Raffeld, P. Duray, C. A. Seipp, L. Rogers-Freezer, K. E. Morton, S. A. Mavroukakis, D. E. White, and S. A. Rosenberg. 2002. Cancer regression and autoimmunity in patients after clonal repopulation with antitumor lymphocytes. *Science (New York, N.Y)* 298:850-854.
127. Dudley, M. E., J. R. Wunderlich, J. C. Yang, R. M. Sherry, S. L. Topalian, N. P. Restifo, R. E. Royal, U. Kammula, D. E. White, S. A. Mavroukakis, L. J. Rogers, G. J. Gracia, S. A. Jones, D. P. Mangiameli, M. M. Pelletier, J. Gea-Banacloche, M. R. Robinson, D. M. Berman, A. C. Filie, A. Abati, and S. A. Rosenberg. 2005. Adoptive cell transfer therapy following non-myeloablative but lymphodepleting chemotherapy for the treatment of patients with refractory metastatic melanoma. *J Clin Oncol* 23:2346-2357.
128. Dembic, Z., W. Haas, S. Weiss, J. McCubrey, H. Kiefer, H. von Boehmer, and M. Steinmetz. 1986. Transfer of specificity by murine alpha and beta T-cell receptor genes. *Nature* 320:232-238.
129. Rosenberg, S. A., P. Aebersold, K. Cornetta, A. Kasid, R. A. Morgan, R. Moen, E. M. Karson, M. T. Lotze, J. C. Yang, S. L. Topalian, and et al. 1990. Gene transfer into humans--immunotherapy of patients with advanced melanoma, using tumor-infiltrating lymphocytes modified by retroviral gene transduction. *The New England journal of medicine* 323:570-578.
130. Clay, T. M., M. C. Custer, J. Sachs, P. Hwu, S. A. Rosenberg, and M. I. Nishimura. 1999. Efficient transfer of a tumor antigen-reactive TCR to human

- peripheral blood lymphocytes confers anti-tumor reactivity. *J Immunol* 163:507-513.
131. Stanislawski, T., R. H. Voss, C. Lotz, E. Sadovnikova, R. A. Willemsen, J. Kuball, T. Ruppert, R. L. Bolhuis, C. J. Melief, C. Huber, H. J. Stauss, and M. Theobald. 2001. Circumventing tolerance to a human MDM2-derived tumor antigen by TCR gene transfer. *Nature immunology* 2:962-970.
  132. Xue, S. A., L. Gao, D. Hart, R. Gillmore, W. Qasim, A. Thrasher, J. Apperley, B. Engels, W. Uckert, E. Morris, and H. Stauss. 2005. Elimination of human leukemia cells in NOD/SCID mice by WT1-TCR gene-transduced human T cells. *Blood* 106:3062-3067.
  133. Riviere, I., K. Brose, and R. C. Mulligan. 1995. Effects of retroviral vector design on expression of human adenosine deaminase in murine bone marrow transplant recipients engrafted with genetically modified cells. *Proceedings of the National Academy of Sciences of the United States of America* 92:6733-6737.
  134. Schambach, A., W. P. Swaney, and J. C. van der Loo. 2009. Design and production of retro- and lentiviral vectors for gene expression in hematopoietic cells. *Methods in molecular biology (Clifton, N.J)* 506:191-205.
  135. Hughes, M. S., Y. Y. Yu, M. E. Dudley, Z. Zheng, P. F. Robbins, Y. Li, J. Wunderlich, R. G. Hawley, M. Moayeri, S. A. Rosenberg, and R. A. Morgan. 2005. Transfer of a TCR gene derived from a patient with a marked antitumor response conveys highly active T-cell effector functions. *Human gene therapy* 16:457-472.
  136. Levine, B. L., L. M. Humeau, J. Boyer, R. R. MacGregor, T. Rebello, X. Lu, G. K. Binder, V. Slepishkin, F. Lemiale, J. R. Mascola, F. D. Bushman, B. Dropulic, and C. H. June. 2006. Gene transfer in humans using a conditionally replicating lentiviral vector. *Proceedings of the National Academy of Sciences of the United States of America* 103:17372-17377.
  137. Cavalieri, S., S. Cazzaniga, M. Geuna, Z. Magnani, C. Bordignon, L. Naldini, and C. Bonini. 2003. Human T lymphocytes transduced by lentiviral vectors in the absence of TCR activation maintain an intact immune competence. *Blood* 102:497-505.
  138. Szymczak, A. L., C. J. Workman, Y. Wang, K. M. Vignali, S. Dilioglou, E. F. Vanin, and D. A. Vignali. 2004. Correction of multi-gene deficiency in vivo using a single 'self-cleaving' 2A peptide-based retroviral vector. *Nature biotechnology* 22:589-594.
  139. Wargo, J. A., P. F. Robbins, Y. Li, Y. Zhao, M. El-Gamil, D. Caragacianu, Z. Zheng, J. A. Hong, S. Downey, D. S. Schrupp, S. A. Rosenberg, and R. A. Morgan. 2009. Recognition of NY-ESO-1+ tumor cells by engineered lymphocytes is enhanced by improved vector design and epigenetic modulation of tumor antigen expression. *Cancer Immunol Immunother* 58:383-394.
  140. Cohen, C. J., Y. Zhao, Z. Zheng, S. A. Rosenberg, and R. A. Morgan. 2006. Enhanced antitumor activity of murine-human hybrid T-cell receptor (TCR) in human lymphocytes is associated with improved pairing and TCR/CD3 stability. *Cancer research* 66:8878-8886.

141. Bialer, G., M. Horovitz-Fried, S. Ya'acobi, R. A. Morgan, and C. J. Cohen. 2010. Selected murine residues endow human TCR with enhanced tumor recognition. *J Immunol* 184:6232-6241.
142. Sommermeyer, D., and W. Uckert. 2010. Minimal amino acid exchange in human TCR constant regions fosters improved function of TCR gene-modified T cells. *J Immunol* 184:6223-6231.
143. Davies, D. M., and J. Maher. 2010. Adoptive T-cell immunotherapy of cancer using chimeric antigen receptor-grafted T cells. *Archivum immunologiae et therapeuticae experimentalis* 58:165-178.
144. Irving, B. A., and A. Weiss. 1991. The cytoplasmic domain of the T cell receptor zeta chain is sufficient to couple to receptor-associated signal transduction pathways. *Cell* 64:891-901.
145. Romeo, C., M. Amiot, and B. Seed. 1992. Sequence requirements for induction of cytolysis by the T cell antigen/Fc receptor zeta chain. *Cell* 68:889-897.
146. Eshhar, Z., T. Waks, G. Gross, and D. G. Schindler. 1993. Specific activation and targeting of cytotoxic lymphocytes through chimeric single chains consisting of antibody-binding domains and the gamma or zeta subunits of the immunoglobulin and T-cell receptors. *Proceedings of the National Academy of Sciences of the United States of America* 90:720-724.
147. Weijtens, M. E., R. A. Willemsen, D. Valerio, K. Stam, and R. L. Bolhuis. 1996. Single chain Ig/gamma gene-redirectioned human T lymphocytes produce cytokines, specifically lyse tumor cells, and recycle lytic capacity. *J Immunol* 157:836-843.
148. Gong, M. C., J. B. Latouche, A. Krause, W. D. Heston, N. H. Bander, and M. Sadelain. 1999. Cancer patient T cells genetically targeted to prostate-specific membrane antigen specifically lyse prostate cancer cells and release cytokines in response to prostate-specific membrane antigen. *Neoplasia (New York, N.Y)* 1:123-127.
149. Krause, A., H. F. Guo, J. B. Latouche, C. Tan, N. K. Cheung, and M. Sadelain. 1998. Antigen-dependent CD28 signaling selectively enhances survival and proliferation in genetically modified activated human primary T lymphocytes. *The Journal of experimental medicine* 188:619-626.
150. Haynes, N. M., J. A. Trapani, M. W. Teng, J. T. Jackson, L. Cerruti, S. M. Jane, M. H. Kershaw, M. J. Smyth, and P. K. Darcy. 2002. Single-chain antigen recognition receptors that costimulate potent rejection of established experimental tumors. *Blood* 100:3155-3163.
151. Maher, J., R. J. Brentjens, G. Gunset, I. Riviere, and M. Sadelain. 2002. Human T-lymphocyte cytotoxicity and proliferation directed by a single chimeric TCRzeta /CD28 receptor. *Nature biotechnology* 20:70-75.
152. Wang, J., M. Jensen, Y. Lin, X. Sui, E. Chen, C. G. Lindgren, B. Till, A. Raubitschek, S. J. Forman, X. Qian, S. James, P. Greenberg, S. Riddell, and O. W. Press. 2007. Optimizing adoptive polyclonal T cell immunotherapy of lymphomas, using a chimeric T cell receptor possessing CD28 and CD137 costimulatory domains. *Human gene therapy* 18:712-725.
153. Brentjens, R. J., E. Santos, Y. Nikhamin, R. Yeh, M. Matsushita, K. La Perle, A. Quintas-Cardama, S. M. Larson, and M. Sadelain. 2007. Genetically targeted T

- cells eradicate systemic acute lymphoblastic leukemia xenografts. *Clin Cancer Res* 13:5426-5435.
154. Imai, C., K. Mihara, M. Andreansky, I. C. Nicholson, C. H. Pui, T. L. Geiger, and D. Campana. 2004. Chimeric receptors with 4-1BB signaling capacity provoke potent cytotoxicity against acute lymphoblastic leukemia. *Leukemia* 18:676-684.
  155. Finney, H. M., A. N. Akbar, and A. D. Lawson. 2004. Activation of resting human primary T cells with chimeric receptors: costimulation from CD28, inducible costimulator, CD134, and CD137 in series with signals from the TCR zeta chain. *J Immunol* 172:104-113.
  156. Wilkie, S., G. Picco, J. Foster, D. M. Davies, S. Julien, L. Cooper, S. Arif, S. J. Mather, J. Taylor-Papadimitriou, J. M. Burchell, and J. Maher. 2008. Retargeting of human T cells to tumor-associated MUC1: the evolution of a chimeric antigen receptor. *J Immunol* 180:4901-4909.
  157. Nguyen, P., and T. L. Geiger. 2003. Antigen-specific targeting of CD8+ T cells with receptor-modified T lymphocytes. *Gene therapy* 10:594-604.
  158. Pule, M. A., K. C. Straathof, G. Dotti, H. E. Heslop, C. M. Rooney, and M. K. Brenner. 2005. A chimeric T cell antigen receptor that augments cytokine release and supports clonal expansion of primary human T cells. *Mol Ther* 12:933-941.
  159. Daldrup-Link, H. E., R. Meier, M. Rudelius, G. Piontek, M. Piert, S. Metz, M. Settles, C. Uherek, W. Wels, J. Schlegel, and E. J. Rummeny. 2005. In vivo tracking of genetically engineered, anti-HER2/neu directed natural killer cells to HER2/neu positive mammary tumors with magnetic resonance imaging. *European radiology* 15:4-13.
  160. Imai, C., and D. Campana. 2004. Genetic modification of T cells for cancer therapy. *Journal of biological regulators and homeostatic agents* 18:62-71.
  161. Roberts, M. R., K. S. Cooke, A. C. Tran, K. A. Smith, W. Y. Lin, M. Wang, T. J. Dull, D. Farson, K. M. Zsebo, and M. H. Finer. 1998. Antigen-specific cytolysis by neutrophils and NK cells expressing chimeric immune receptors bearing zeta or gamma signaling domains. *J Immunol* 161:375-384.
  162. Kruschinski, A., A. Moosmann, I. Poschke, H. Norell, M. Chmielewski, B. Seliger, R. Kiessling, T. Blankenstein, H. Abken, and J. Charo. 2008. Engineering antigen-specific primary human NK cells against HER-2 positive carcinomas. *Proceedings of the National Academy of Sciences of the United States of America* 105:17481-17486.
  163. Pegram, H. J., J. T. Jackson, M. J. Smyth, M. H. Kershaw, and P. K. Darcy. 2008. Adoptive transfer of gene-modified primary NK cells can specifically inhibit tumor progression in vivo. *J Immunol* 181:3449-3455.
  164. Teng, M. W., M. H. Kershaw, M. Moeller, M. J. Smyth, and P. K. Darcy. 2004. Immunotherapy of cancer using systemically delivered gene-modified human T lymphocytes. *Human gene therapy* 15:699-708.
  165. Haynes, N. M., J. A. Trapani, M. W. Teng, J. T. Jackson, L. Cerruti, S. M. Jane, M. H. Kershaw, M. J. Smyth, and P. K. Darcy. 2002. Rejection of syngeneic colon carcinoma by CTLs expressing single-chain antibody receptors codelivering CD28 costimulation. *J Immunol* 169:5780-5786.
  166. Kowolik, C. M., M. S. Topp, S. Gonzalez, T. Pfeiffer, S. Olivares, N. Gonzalez, D. D. Smith, S. J. Forman, M. C. Jensen, and L. J. Cooper. 2006. CD28

- costimulation provided through a CD19-specific chimeric antigen receptor enhances in vivo persistence and antitumor efficacy of adoptively transferred T cells. *Cancer research* 66:10995-11004.
167. Loskog, A., V. Giandomenico, C. Rossig, M. Pule, G. Dotti, and M. K. Brenner. 2006. Addition of the CD28 signaling domain to chimeric T-cell receptors enhances chimeric T-cell resistance to T regulatory cells. *Leukemia* 20:1819-1828.
  168. Moeller, M., N. M. Haynes, J. A. Trapani, M. W. Teng, J. T. Jackson, J. E. Tanner, L. Cerutti, S. M. Jane, M. H. Kershaw, M. J. Smyth, and P. K. Darcy. 2004. A functional role for CD28 costimulation in tumor recognition by single-chain receptor-modified T cells. *Cancer gene therapy* 11:371-379.
  169. Vera, J., B. Savoldo, S. Vigouroux, E. Biagi, M. Pule, C. Rossig, J. Wu, H. E. Heslop, C. M. Rooney, M. K. Brenner, and G. Dotti. 2006. T lymphocytes redirected against the kappa light chain of human immunoglobulin efficiently kill mature B lymphocyte-derived malignant cells. *Blood* 108:3890-3897.
  170. Cartellieri, M., M. Bachmann, A. Feldmann, C. Bippes, S. Stamova, R. Wehner, A. Temme, and M. Schmitz. 2010. Chimeric antigen receptor-engineered T cells for immunotherapy of cancer. *Journal of biomedicine & biotechnology* 2010:956304.
  171. Subramanian, C., S. Hasan, M. Rowe, M. Hottiger, R. Orre, and E. S. Robertson. 2002. Epstein-Barr virus nuclear antigen 3C and prothymosin alpha interact with the p300 transcriptional coactivator at the CH1 and CH3/HAT domains and cooperate in regulation of transcription and histone acetylation. *Journal of virology* 76:4699-4708.
  172. Maruo, S., B. Zhao, E. Johannsen, E. Kieff, J. Zou, and K. Takada. 2011. Epstein-Barr virus nuclear antigens 3C and 3A maintain lymphoblastoid cell growth by repressing p16INK4A and p14ARF expression. *Proceedings of the National Academy of Sciences of the United States of America* 108:1919-1924.
  173. Epstein, M. A., G. Henle, B. G. Achong, and Y. M. Barr. 1965. Morphological and Biological Studies on a Virus in Cultured Lymphoblasts from Burkitt's Lymphoma. *The Journal of experimental medicine* 121:761-770.
  174. Henle, G., W. Henle, and V. Diehl. 1968. Relation of Burkitt's tumor-associated herpes-yppe virus to infectious mononucleosis. *Proceedings of the National Academy of Sciences of the United States of America* 59:94-101.
  175. zur Hausen, H., H. Schulte-Holthausen, G. Klein, W. Henle, G. Henle, P. Clifford, and L. Santesson. 1970. EBV DNA in biopsies of Burkitt tumours and anaplastic carcinomas of the nasopharynx. *Nature* 228:1056-1058.
  176. Cohen, J. I. 2000. Epstein-Barr virus infection. *The New England journal of medicine* 343:481-492.
  177. Weiss, L. M., L. A. Movahed, R. A. Warnke, and J. Sklar. 1989. Detection of Epstein-Barr viral genomes in Reed-Sternberg cells of Hodgkin's disease. *The New England journal of medicine* 320:502-506.
  178. Garrido, J. L., S. Maruo, K. Takada, and A. Rosendorff. 2009. EBNA3C interacts with Gadd34 and counteracts the unfolded protein response. *Virology journal* 6:231.

179. Kerr, B. M., N. Kienzle, J. M. Burrows, S. Cross, S. L. Silins, M. Buck, E. M. Benson, B. Coupar, D. J. Moss, and T. B. Sculley. 1996. Identification of type B-specific and cross-reactive cytotoxic T-lymphocyte responses to Epstein-Barr virus. *Journal of virology* 70:8858-8864.
180. Zhao, B., J. C. Mar, S. Maruo, S. Lee, B. E. Gewurz, E. Johannsen, K. Holton, R. Rubio, K. Takada, J. Quackenbush, and E. Kieff. 2010. Epstein-Barr virus nuclear antigen 3C regulated genes in lymphoblastoid cell lines. *Proceedings of the National Academy of Sciences of the United States of America* 108:337-342.
181. Yang, L., Y. Han, F. Suarez Saiz, and M. D. Minden. 2007. A tumor suppressor and oncogene: the WT1 story. *Leukemia* 21:868-876.
182. Sugiyama, H. 2010. WT1 (Wilms' tumor gene 1): biology and cancer immunotherapy. *Japanese journal of clinical oncology* 40:377-387.
183. Englert, C., X. Hou, S. Maheswaran, P. Bennett, C. Ngwu, G. G. Re, A. J. Garvin, M. R. Rosner, and D. A. Haber. 1995. WT1 suppresses synthesis of the epidermal growth factor receptor and induces apoptosis. *The EMBO journal* 14:4662-4675.
184. Coppes, M. J., C. E. Campbell, and B. R. Williams. 1993. The role of WT1 in Wilms tumorigenesis. *Faseb J* 7:886-895.
185. O'Reilly, R. J., T. Dao, G. Koehne, D. Scheinberg, and E. Doubrovina. 2010. Adoptive transfer of unselected or leukemia-reactive T-cells in the treatment of relapse following allogeneic hematopoietic cell transplantation. *Seminars in immunology* 22:162-172.
186. Rezvani, K., J. M. Brenchley, D. A. Price, Y. Kilical, E. Gostick, A. K. Sewell, J. Li, S. Mielke, D. C. Douek, and A. J. Barrett. 2005. T-cell responses directed against multiple HLA-A\*0201-restricted epitopes derived from Wilms' tumor 1 protein in patients with leukemia and healthy donors: identification, quantification, and characterization. *Clin Cancer Res* 11:8799-8807.
187. Borbulevych, O. Y., P. Do, and B. M. Baker. 2010. Structures of native and affinity-enhanced WT1 epitopes bound to HLA-A\*0201: implications for WT1-based cancer therapeutics. *Molecular immunology* 47:2519-2524.
188. Gao, L., I. Bellantuono, A. Elsassser, S. B. Marley, M. Y. Gordon, J. M. Goldman, and H. J. Stauss. 2000. Selective elimination of leukemic CD34(+) progenitor cells by cytotoxic T lymphocytes specific for WT1. *Blood* 95:2198-2203.
189. Mailander, V., C. Scheibenbogen, E. Thiel, A. Letsch, I. W. Blau, and U. Keilholz. 2004. Complete remission in a patient with recurrent acute myeloid leukemia induced by vaccination with WT1 peptide in the absence of hematological or renal toxicity. *Leukemia* 18:165-166.
190. Keilholz, U., A. Letsch, A. Busse, A. M. Asemissen, S. Bauer, I. W. Blau, W. K. Hofmann, L. Uharek, E. Thiel, and C. Scheibenbogen. 2009. A clinical and immunologic phase 2 trial of Wilms tumor gene product 1 (WT1) peptide vaccination in patients with AML and MDS. *Blood* 113:6541-6548.
191. Shu, L., C. F. Qi, J. Schlom, and S. V. Kashmiri. 1993. Secretion of a single-gene-encoded immunoglobulin from myeloma cells. *Proceedings of the National Academy of Sciences of the United States of America* 90:7995-7999.
192. Powers, D. B., P. Amersdorfer, M. Poul, U. B. Nielsen, M. R. Shalaby, G. P. Adams, L. M. Weiner, and J. D. Marks. 2001. Expression of single-chain Fv-Fc fusions in *Pichia pastoris*. *Journal of immunological methods* 251:123-135.



193. Valadon, P., J. D. Garnett, J. E. Testa, M. Bauerle, P. Oh, and J. E. Schnitzer. 2006. Screening phage display libraries for organ-specific vascular immunotargeting in vivo. *Proceedings of the National Academy of Sciences of the United States of America* 103:407-412.
194. Garboczi, D. N., P. Ghosh, U. Utz, Q. R. Fan, W. E. Biddison, and D. C. Wiley. 1996. Structure of the complex between human T-cell receptor, viral peptide and HLA-A2. *Nature* 384:134-141.
195. Garboczi, D. N., U. Utz, P. Ghosh, A. Seth, J. Kim, E. A. VanTienhoven, W. E. Biddison, and D. C. Wiley. 1996. Assembly, specific binding, and crystallization of a human TCR-alpha-beta with an antigenic Tax peptide from human T lymphotropic virus type 1 and the class I MHC molecule HLA-A2. *J Immunol* 157:5403-5410.
196. Altman, J. D., P. A. Moss, P. J. Goulder, D. H. Barouch, M. G. McHeyzer-Williams, J. I. Bell, A. J. McMichael, and M. M. Davis. 1996. Phenotypic analysis of antigen-specific T lymphocytes. *Science (New York, N.Y)* 274:94-96.
197. Busch, D. H., I. M. Pilip, S. Vijh, and E. G. Pamer. 1998. Coordinate regulation of complex T cell populations responding to bacterial infection. *Immunity* 8:353-362.
198. Schatz, P. J. 1993. Use of peptide libraries to map the substrate specificity of a peptide-modifying enzyme: a 13 residue consensus peptide specifies biotinylation in *Escherichia coli*. *Bio/technology (Nature Publishing Company)* 11:1138-1143.
199. de Wildt, R. M., C. R. Mundy, B. D. Gorick, and I. M. Tomlinson. 2000. Antibody arrays for high-throughput screening of antibody-antigen interactions. *Nature biotechnology* 18:989-994.
200. Gould, L. H., J. Sui, H. Foellmer, T. Oliphant, T. Wang, M. Ledizet, A. Murakami, K. Noonan, C. Lambeth, K. Kar, J. F. Anderson, A. M. de Silva, M. S. Diamond, R. A. Koski, W. A. Marasco, and E. Fikrig. 2005. Protective and therapeutic capacity of human single-chain Fv-Fc fusion proteins against West Nile virus. *Journal of virology* 79:14606-14613.
201. Kim, Y. J., S. H. Kim, P. Mantel, and B. S. Kwon. 1998. Human 4-1BB regulates CD28 co-stimulation to promote Th1 cell responses. *European journal of immunology* 28:881-890.
202. Hurtado, J. C., Y. J. Kim, and B. S. Kwon. 1997. Signals through 4-1BB are costimulatory to previously activated splenic T cells and inhibit activation-induced cell death. *J Immunol* 158:2600-2609.
203. Jackson, R. J., M. T. Howell, and A. Kaminski. 1990. The novel mechanism of initiation of picornavirus RNA translation. *Trends in biochemical sciences* 15:477-483.
204. de Haard, H. J., N. van Neer, A. Reurs, S. E. Hufton, R. C. Roovers, P. Henderikx, A. P. de Bruine, J. W. Arends, and H. R. Hoogenboom. 1999. A large non-immunized human Fab fragment phage library that permits rapid isolation and kinetic analysis of high affinity antibodies. *The Journal of biological chemistry* 274:18218-18230.
205. Denkberg, G., A. Lev, L. Eisenbach, I. Benhar, and Y. Reiter. 2003. Selective targeting of melanoma and APCs using a recombinant antibody with TCR-like

- specificity directed toward a melanoma differentiation antigen. *J Immunol* 171:2197-2207.
206. Baas, E. J., H. M. van Santen, M. J. Kleijmeer, H. J. Geuze, P. J. Peters, and H. L. Ploegh. 1992. Peptide-induced stabilization and intracellular localization of empty HLA class I complexes. *The Journal of experimental medicine* 176:147-156.
  207. Koehne, G., K. M. Smith, T. L. Ferguson, R. Y. Williams, G. Heller, E. G. Pamer, B. Dupont, and R. J. O'Reilly. 2002. Quantitation, selection, and functional characterization of Epstein-Barr virus-specific and alloreactive T cells detected by intracellular interferon-gamma production and growth of cytotoxic precursors. *Blood* 99:1730-1740.
  208. van der Merwe, P. A., and S. J. Davis. 2003. Molecular interactions mediating T cell antigen recognition. *Annual review of immunology* 21:659-684.
  209. Sykulev, Y., R. J. Cohen, and H. N. Eisen. 1995. The law of mass action governs antigen-stimulated cytolytic activity of CD8+ cytotoxic T lymphocytes. *Proceedings of the National Academy of Sciences of the United States of America* 92:11990-11992.
  210. Schodin, B. A., T. J. Tsomides, and D. M. Kranz. 1996. Correlation between the number of T cell receptors required for T cell activation and TCR-ligand affinity. *Immunity* 5:137-146.
  211. Cartron, G., L. Dacheux, G. Salles, P. Solal-Celigny, P. Bardos, P. Colombat, and H. Watier. 2002. Therapeutic activity of humanized anti-CD20 monoclonal antibody and polymorphism in IgG Fc receptor FcgammaRIIIa gene. *Blood* 99:754-758.
  212. Weng, W. K., R. S. Negrin, P. Lavori, and S. J. Horning. Immunoglobulin G Fc receptor FcgammaRIIIa 158 V/F polymorphism correlates with rituximab-induced neutropenia after autologous transplantation in patients with non-Hodgkin's lymphoma. *J Clin Oncol* 28:279-284.
  213. Saoulli, K., S. Y. Lee, J. L. Cannons, W. C. Yeh, A. Santana, M. D. Goldstein, N. Bangia, M. A. DeBenedette, T. W. Mak, Y. Choi, and T. H. Watts. 1998. CD28-independent, TRAF2-dependent costimulation of resting T cells by 4-1BB ligand. *The Journal of experimental medicine* 187:1849-1862.
  214. Lee, H. W., S. J. Park, B. K. Choi, H. H. Kim, K. O. Nam, and B. S. Kwon. 2002. 4-1BB promotes the survival of CD8+ T lymphocytes by increasing expression of Bcl-xL and Bfl-1. *J Immunol* 169:4882-4888.
  215. Sabbagh, L., G. Pulle, Y. Liu, E. N. Tsitsikov, and T. H. Watts. 2008. ERK-dependent Bim modulation downstream of the 4-1BB-TRAF1 signaling axis is a critical mediator of CD8 T cell survival in vivo. *J Immunol* 180:8093-8101.
  216. Arch, R. H., and C. B. Thompson. 1998. 4-1BB and Ox40 are members of a tumor necrosis factor (TNF)-nerve growth factor receptor subfamily that bind TNF receptor-associated factors and activate nuclear factor kappaB. *Molecular and cellular biology* 18:558-565.
  217. Cannons, J. L., Y. Choi, and T. H. Watts. 2000. Role of TNF receptor-associated factor 2 and p38 mitogen-activated protein kinase activation during 4-1BB-dependent immune response. *J Immunol* 165:6193-6204.

218. Cannons, J. L., K. P. Hoefflich, J. R. Woodgett, and T. H. Watts. 1999. Role of the stress kinase pathway in signaling via the T cell costimulatory receptor 4-1BB. *J Immunol* 163:2990-2998.
219. Jang, I. K., Z. H. Lee, Y. J. Kim, S. H. Kim, and B. S. Kwon. 1998. Human 4-1BB (CD137) signals are mediated by TRAF2 and activate nuclear factor-kappa B. *Biochemical and biophysical research communications* 242:613-620.
220. Imai, C., S. Iwamoto, and D. Campana. 2005. Genetic modification of primary natural killer cells overcomes inhibitory signals and induces specific killing of leukemic cells. *Blood* 106:376-383.
221. George, A. J., J. Stark, and C. Chan. 2005. Understanding specificity and sensitivity of T-cell recognition. *Trends in immunology* 26:653-659.
222. Betts, M. R., J. M. Brechley, D. A. Price, S. C. De Rosa, D. C. Douek, M. Roederer, and R. A. Koup. 2003. Sensitive and viable identification of antigen-specific CD8+ T cells by a flow cytometric assay for degranulation. *Journal of immunological methods* 281:65-78.
223. Alter, G., J. M. Malenfant, and M. Altfeld. 2004. CD107a as a functional marker for the identification of natural killer cell activity. *Journal of immunological methods* 294:15-22.
224. Weidanz, J. A., T. Nguyen, T. Woodburn, F. A. Neethling, M. Chiriva-Internati, W. H. Hildebrand, and J. Lustgarten. 2006. Levels of specific peptide-HLA class I complex predicts tumor cell susceptibility to CTL killing. *J Immunol* 177:5088-5097.
225. Spinsanti, P., U. de Grazia, A. Faggioni, L. Frati, A. Calogero, and G. Ragona. 2000. Wilms' tumor gene expression by normal and malignant human B lymphocytes. *Leukemia & lymphoma* 38:611-619.
226. Hamilton, T. C., R. C. Young, W. M. McKoy, K. R. Grotzinger, J. A. Green, E. W. Chu, J. Whang-Peng, A. M. Rogan, W. R. Green, and R. F. Ozols. 1983. Characterization of a human ovarian carcinoma cell line (NIH:OVCA-3) with androgen and estrogen receptors. *Cancer research* 43:5379-5389.
227. Viel, A., F. Giannini, E. Capozzi, V. Canzonieri, C. Scarabelli, A. Gloghini, and M. Boiocchi. 1994. Molecular mechanisms possibly affecting WT1 function in human ovarian tumors. *International journal of cancer* 57:515-521.
228. Findley, H. W., Jr., M. D. Cooper, T. H. Kim, C. Alvarado, and A. H. Ragab. 1982. Two new acute lymphoblastic leukemia cell lines with early B-cell phenotypes. *Blood* 60:1305-1309.
229. Krug, L. M., T. Dao, A. B. Brown, P. Maslak, W. Travis, S. Bekele, T. Korontsvit, V. Zakhaleva, J. Wolchok, J. Yuan, H. Li, L. Tyson, and D. A. Scheinberg. 2010. WT1 peptide vaccinations induce CD4 and CD8 T cell immune responses in patients with mesothelioma and non-small cell lung cancer. *Cancer Immunol Immunother* 59:1467-1479.
230. Chaise, C., S. L. Buchan, J. Rice, J. Marquet, H. Rouard, M. Kuentz, G. E. Vites, V. Molinier-Frenkel, J. P. Farcet, H. J. Stauss, M. H. Delfau-Larue, and F. K. Stevenson. 2008. DNA vaccination induces WT1-specific T-cell responses with potential clinical relevance. *Blood* 112:2956-2964.
231. Lamers, C. H., S. C. Langeveld, C. M. Groot-van Ruijven, R. Debets, S. Sleijfer, and J. W. Gratama. 2007. Gene-modified T cells for adoptive immunotherapy of

- renal cell cancer maintain transgene-specific immune functions in vivo. *Cancer Immunol Immunother* 56:1875-1883.
232. Lamers, C. H., S. Sleijfer, A. G. Vulto, W. H. Kruit, M. Kliffen, R. Debets, J. W. Gratama, G. Stoter, and E. Oosterwijk. 2006. Treatment of metastatic renal cell carcinoma with autologous T-lymphocytes genetically retargeted against carbonic anhydrase IX: first clinical experience. *J Clin Oncol* 24:e20-22.
  233. Kershaw, M. H., J. A. Westwood, L. L. Parker, G. Wang, Z. Eshhar, S. A. Mavroukakis, D. E. White, J. R. Wunderlich, S. Canevari, L. Rogers-Freezer, C. C. Chen, J. C. Yang, S. A. Rosenberg, and P. Hwu. 2006. A phase I study on adoptive immunotherapy using gene-modified T cells for ovarian cancer. *Clin Cancer Res* 12:6106-6115.
  234. Till, B. G., M. C. Jensen, J. Wang, E. Y. Chen, B. L. Wood, H. A. Greisman, X. Qian, S. E. James, A. Raubitschek, S. J. Forman, A. K. Gopal, J. M. Pagel, C. G. Lindgren, P. D. Greenberg, S. R. Riddell, and O. W. Press. 2008. Adoptive immunotherapy for indolent non-Hodgkin lymphoma and mantle cell lymphoma using genetically modified autologous CD20-specific T cells. *Blood* 112:2261-2271.
  235. Pule, M. A., B. Savoldo, G. D. Myers, C. Rossig, H. V. Russell, G. Dotti, M. H. Huls, E. Liu, A. P. Gee, Z. Mei, E. Yvon, H. L. Weiss, H. Liu, C. M. Rooney, H. E. Heslop, and M. K. Brenner. 2008. Virus-specific T cells engineered to coexpress tumor-specific receptors: persistence and antitumor activity in individuals with neuroblastoma. *Nature medicine* 14:1264-1270.
  236. Zhang, L., J. R. Conejo-Garcia, D. Katsaros, P. A. Gimotty, M. Massobrio, G. Regnani, A. Makrigiannakis, H. Gray, K. Schlienger, M. N. Liebman, S. C. Rubin, and G. Coukos. 2003. Intratumoral T cells, recurrence, and survival in epithelial ovarian cancer. *The New England journal of medicine* 348:203-213.
  237. Odunsi, K., and L. J. Old. 2007. Tumor infiltrating lymphocytes: indicators of tumor-related immune responses. *Cancer Immun* 7:3.
  238. Sun, J. C., J. N. Beilke, and L. L. Lanier. 2010. Immune memory redefined: characterizing the longevity of natural killer cells. *Immunological reviews* 236:83-94.
  239. Tam, Y. K., B. Miyagawa, V. C. Ho, and H. G. Klingemann. 1999. Immunotherapy of malignant melanoma in a SCID mouse model using the highly cytotoxic natural killer cell line NK-92. *Journal of hematotherapy* 8:281-290.
  240. Korbelik, M., and J. Sun. 2001. Cancer treatment by photodynamic therapy combined with adoptive immunotherapy using genetically altered natural killer cell line. *International journal of cancer* 93:269-274.
  241. Arai, S., R. Meagher, M. Swearingen, H. Myint, E. Rich, J. Martinson, and H. Klingemann. 2008. Infusion of the allogeneic cell line NK-92 in patients with advanced renal cell cancer or melanoma: a phase I trial. *Cytotherapy* 10:625-632.
  242. Tomkinson, B., E. Robertson, and E. Kieff. 1993. Epstein-Barr virus nuclear proteins EBNA-3A and EBNA-3C are essential for B-lymphocyte growth transformation. *Journal of virology* 67:2014-2025.
  243. Bendle, G. M., C. Linnemann, A. I. Hooijkaas, L. Bies, M. A. de Witte, A. Jorritsma, A. D. Kaiser, N. Pouw, R. Debets, E. Kieback, W. Uckert, J. Y. Song, J. B. Haanen, and T. N. Schumacher. 2010. Lethal graft-versus-host disease in

- mouse models of T cell receptor gene therapy. *Nature medicine* 16:565-570, 561p following 570.
244. Singh, R., and Y. Paterson. 2007. Immunoediting sculpts tumor epitopes during immunotherapy. *Cancer research* 67:1887-1892.
  245. Yasukawa, M., H. Ohminami, S. Kaneko, Y. Yakushijin, Y. Nishimura, K. Inokuchi, T. Miyakuni, S. Nakao, K. Kishi, I. Kubonishi, K. Dan, and S. Fujita. 1998. CD4(+) cytotoxic T-cell clones specific for bcr-abl b3a2 fusion peptide augment colony formation by chronic myelogenous leukemia cells in a b3a2-specific and HLA-DR-restricted manner. *Blood* 92:3355-3361.
  246. Chmielewski, M., A. Hombach, C. Heuser, G. P. Adams, and H. Abken. 2004. T cell activation by antibody-like immunoreceptors: increase in affinity of the single-chain fragment domain above threshold does not increase T cell activation against antigen-positive target cells but decreases selectivity. *J Immunol* 173:7647-7653.
  247. Moore, T. V., G. E. Lyons, N. Brasic, J. J. Roszkowski, S. Voelkl, A. Mackensen, W. M. Kast, I. C. Le Poole, and M. I. Nishimura. 2009. Relationship between CD8-dependent antigen recognition, T cell functional avidity, and tumor cell recognition. *Cancer Immunol Immunother* 58:719-728.
  248. Turatti, F., M. Figini, E. Balladore, P. Alberti, P. Casalini, J. D. Marks, S. Canevari, and D. Mezzanzanica. 2007. Redirected activity of human antitumor chimeric immune receptors is governed by antigen and receptor expression levels and affinity of interaction. *J Immunother* 30:684-693.
  249. Guest, R. D., R. E. Hawkins, N. Kirillova, E. J. Cheadle, J. Arnold, A. O'Neill, J. Irlam, K. A. Chester, J. T. Kemshead, D. M. Shaw, M. J. Embleton, P. L. Stern, and D. E. Gilham. 2005. The role of extracellular spacer regions in the optimal design of chimeric immune receptors: evaluation of four different scFvs and antigens. *J Immunother* 28:203-211.
  250. Rossig, C., C. M. Bollard, J. G. Nuchtern, C. M. Rooney, and M. K. Brenner. 2002. Epstein-Barr virus-specific human T lymphocytes expressing antitumor chimeric T-cell receptors: potential for improved immunotherapy. *Blood* 99:2009-2016.
  251. Zakrzewski, J. L., A. A. Kochman, S. X. Lu, T. H. Terwey, T. D. Kim, V. M. Hubbard, S. J. Muriglan, D. Suh, O. M. Smith, J. Grubin, N. Patel, A. Chow, J. Cabrera-Perez, R. Radhakrishnan, A. Diab, M. A. Perales, G. Rizzuto, E. Menet, E. G. Pamer, G. Heller, J. C. Zuniga-Pflucker, O. Alpdogan, and M. R. van den Brink. 2006. Adoptive transfer of T-cell precursors enhances T-cell reconstitution after allogeneic hematopoietic stem cell transplantation. *Nature medicine* 12:1039-1047.
  252. Zakrzewski, J. L., D. Suh, J. C. Markley, O. M. Smith, C. King, G. L. Goldberg, R. Jenq, A. M. Holland, J. Grubin, J. Cabrera-Perez, R. J. Brentjens, S. X. Lu, G. Rizzuto, D. B. Sant'Angelo, I. Riviere, M. Sadelain, G. Heller, J. C. Zuniga-Pflucker, C. Lu, and M. R. van den Brink. 2008. Tumor immunotherapy across MHC barriers using allogeneic T-cell precursors. *Nature biotechnology* 26:453-461.
  253. Papapetrou, E. P., D. Kovalovsky, L. Beloeil, D. Sant'angelo, and M. Sadelain. 2009. Harnessing endogenous miR-181a to segregate transgenic antigen receptor

- expression in developing versus post-thymic T cells in murine hematopoietic chimeras. *The Journal of clinical investigation* 119:157-168.
254. Wang, G., R. K. Chopra, R. E. Royal, J. C. Yang, S. A. Rosenberg, and P. Hwu. 1998. A T cell-independent antitumor response in mice with bone marrow cells retrovirally transduced with an antibody/Fc-gamma chain chimeric receptor gene recognizing a human ovarian cancer antigen. *Nature medicine* 4:168-172.
255. Mulder, A., C. Eijnsink, M. J. Kardol, M. E. Franke-van Dijk, S. H. van der Burg, M. Kester, Doxiadis, II, and F. H. Claas. 2003. Identification, isolation, and culture of HLA-A2-specific B lymphocytes using MHC class I tetramers. *J Immunol* 171:6599-6603.
256. Mulder, A., C. Eijnsink, M. G. Kester, M. E. Franke, M. J. Kardol, M. H. Heemskerk, C. van Kooten, F. A. Verreck, J. W. Drijfhout, F. Koning, Doxiadis, II, and F. H. Claas. 2005. Impact of peptides on the recognition of HLA class I molecules by human HLA antibodies. *J Immunol* 175:5950-5957.
257. Bansal, H., S. Bansal, M. Rao, K. P. Foley, J. Sang, D. A. Proia, R. K. Blackman, W. Ying, J. Barsoum, M. R. Baer, K. Kelly, R. Swords, G. E. Tomlinson, M. Battiwalla, F. J. Giles, K. P. Lee, and S. Padmanabhan. 2010. Heat shock protein 90 regulates the expression of Wilms tumor 1 protein in myeloid leukemias. *Blood* 116:4591-4599.
258. O'Reilly, R. J. 2008. Epstein-Barr virus sustains tumor killers. *Nature medicine* 14:1148-1150.
259. Milner, E., E. Barnea, I. Beer, and A. Admon. 2006. The turnover kinetics of major histocompatibility complex peptides of human cancer cells. *Mol Cell Proteomics* 5:357-365.
260. Vicent, S., R. Chen, L. C. Sayles, C. Lin, R. G. Walker, A. K. Gillespie, A. Subramanian, G. Hinkle, X. Yang, S. Saif, D. E. Root, V. Huff, W. C. Hahn, and E. A. Sweet-Cordero. 2010. Wilms tumor 1 (WT1) regulates KRAS-driven oncogenesis and senescence in mouse and human models. *The Journal of clinical investigation* 120:3940-3952.
261. de Jong, A., J. M. van der Hulst, G. G. Kenter, J. W. Drijfhout, K. L. Franken, P. Vermeij, R. Offringa, S. H. van der Burg, and C. J. Melief. 2005. Rapid enrichment of human papillomavirus (HPV)-specific polyclonal T cell populations for adoptive immunotherapy of cervical cancer. *International journal of cancer* 114:274-282.
262. Trivedi, D., R. Y. Williams, R. J. O'Reilly, and G. Koehne. 2005. Generation of CMV-specific T lymphocytes using protein-spanning pools of pp65-derived overlapping pentadecapeptides for adoptive immunotherapy. *Blood* 105:2793-2801.
263. Lee, S. W., A. T. Vella, B. S. Kwon, and M. Croft. 2005. Enhanced CD4 T cell responsiveness in the absence of 4-1BB. *J Immunol* 174:6803-6808.
264. Lee, S. W., Y. Park, A. Song, H. Cheroutre, B. S. Kwon, and M. Croft. 2006. Functional dichotomy between OX40 and 4-1BB in modulating effector CD8 T cell responses. *J Immunol* 177:4464-4472.
265. Kwon, B. S., J. C. Hurtado, Z. H. Lee, K. B. Kwack, S. K. Seo, B. K. Choi, B. H. Koller, G. Wolisi, H. E. Broxmeyer, and D. S. Vinay. 2002. Immune responses in 4-1BB (CD137)-deficient mice. *J Immunol* 168:5483-5490.

266. Halstead, E. S., Y. M. Mueller, J. D. Altman, and P. D. Katsikis. 2002. In vivo stimulation of CD137 broadens primary antiviral CD8+ T cell responses. *Nature immunology* 3:536-541.
267. Melero, I., W. W. Shuford, S. A. Newby, A. Aruffo, J. A. Ledbetter, K. E. Hellstrom, R. S. Mittler, and L. Chen. 1997. Monoclonal antibodies against the 4-1BB T-cell activation molecule eradicate established tumors. *Nature medicine* 3:682-685.
268. Foell, J., S. Strahotin, S. P. O'Neil, M. M. McCausland, C. Suwyn, M. Haber, P. N. Chander, A. S. Bapat, X. J. Yan, N. Chiorazzi, M. K. Hoffmann, and R. S. Mittler. 2003. CD137 costimulatory T cell receptor engagement reverses acute disease in lupus-prone NZB x NZW F1 mice. *The Journal of clinical investigation* 111:1505-1518.
269. Seo, S. K., J. H. Choi, Y. H. Kim, W. J. Kang, H. Y. Park, J. H. Suh, B. K. Choi, D. S. Vinay, and B. S. Kwon. 2004. 4-1BB-mediated immunotherapy of rheumatoid arthritis. *Nature medicine* 10:1088-1094.
270. Sun, Y., H. M. Chen, S. K. Subudhi, J. Chen, R. Koka, L. Chen, and Y. X. Fu. 2002. Costimulatory molecule-targeted antibody therapy of a spontaneous autoimmune disease. *Nature medicine* 8:1405-1413.
271. Sun, Y., X. Lin, H. M. Chen, Q. Wu, S. K. Subudhi, L. Chen, and Y. X. Fu. 2002. Administration of agonistic anti-4-1BB monoclonal antibody leads to the amelioration of experimental autoimmune encephalomyelitis. *J Immunol* 168:1457-1465.
272. Choi, B. K., Y. H. Kim, C. H. Kim, M. S. Kim, K. H. Kim, H. S. Oh, M. J. Lee, D. K. Lee, D. S. Vinay, and B. S. Kwon. 2010. Peripheral 4-1BB signaling negatively regulates NK cell development through IFN-gamma. *J Immunol* 185:1404-1411.
273. Lanier, L. L. 2008. Up on the tightrope: natural killer cell activation and inhibition. *Nature immunology* 9:495-502.
274. Helene, M., V. Lake-Bullock, J. S. Bryson, C. D. Jennings, and A. M. Kaplan. 1997. Inhibition of graft-versus-host disease. Use of a T cell-controlled suicide gene. *J Immunol* 158:5079-5082.
275. Garrido, F., T. Cabrera, A. Concha, S. Glew, F. Ruiz-Cabello, and P. L. Stern. 1993. Natural history of HLA expression during tumour development. *Immunology today* 14:491-499.
276. Garrido, F., F. Ruiz-Cabello, T. Cabrera, J. J. Perez-Villar, M. Lopez-Botet, M. Duggan-Keen, and P. L. Stern. 1997. Implications for immunosurveillance of altered HLA class I phenotypes in human tumours. *Immunology today* 18:89-95.
277. Marincola, F. M., E. M. Jaffee, D. J. Hicklin, and S. Ferrone. 2000. Escape of human solid tumors from T-cell recognition: molecular mechanisms and functional significance. *Advances in immunology* 74:181-273.
278. Yang, Y., Z. Xiang, H. C. Ertl, and J. M. Wilson. 1995. Upregulation of class I major histocompatibility complex antigens by interferon gamma is necessary for T-cell-mediated elimination of recombinant adenovirus-infected hepatocytes in vivo. *Proceedings of the National Academy of Sciences of the United States of America* 92:7257-7261.

279. Propper, D. J., D. Chao, J. P. Braybrooke, P. Bahl, P. Thavas, F. Balkwill, H. Turley, N. Dobbs, K. Gatter, D. C. Talbot, A. L. Harris, and T. S. Ganesan. 2003. Low-dose IFN-gamma induces tumor MHC expression in metastatic malignant melanoma. *Clin Cancer Res* 9:84-92.
280. Boissel, L. B., M. Van Etten, RA. and Klingemann, HG. 2009. Transfection of NK Cells with mRNA or Lentivirus Expressing Chimeric Antigen Receptors Results in Highly Efficient Killing of Lymphoid Malignancies and Compares Favorably with Monoclonal Antibody-Directed ADCC. In *51st ASH Annual Meeting and Exposition*, Ernest N. Morial Convention Center, New Orleans, LA.